A Competitive Heuristic Algorithm for Vehicle Routing Problems with Drones

Xuan Ren, Aurélien Froger, Ola Jabali, Gongqian Liang

A Competitive Heuristic Algorithm for Vehicle Routing Problems with Drones

Xuan Ren[1], Aurélien Froger[2], Ola Jabali[3], Gongqian Liang[1]

[1] School of Management, Northwestern Polytechnical University, 710129, Xi'an, China
[2] Université de Bordeaux, CNRS, INRIA, Bordeaux INP, IMB, UMR 5251, F-33400 Talence, France
[3] Dipartimento di Elettronica, Informazione e Bioingegneria, Politecnico di Milano, 20133 Milan, Italy

Abstract

We propose a heuristic algorithm capable of handling eight possible versions of the vehicle routing problems with drones (VRPD). These are characterized according to three axes, 1) single or multiple trucks each equipped with a single drone, 2) allowing the drone to land and wait or not, and 3) minimizing the transportation cost or minimizing the makespan. One of our main algorithmic contributions relates to a subproblem of the VRPD, which we refer to as the fixed route drone dispatch problem (FRDDP). Given a sequence of customers being visited by a truck, the FRDDP determines a subset of customers to be visited by the drone. Solving the FRDDP exactly with dynamic programming entails a computational complexity of $\mathcal{O}(n^3)$, where n is the number of customers contained in the route. Considering that the FRDDP is very frequently solved in local search algorithms, we introduce a heuristic dynamic program (HDP) with a computational complexity of $\mathcal{O}(n^2)$ for each of the two FRDDP objectives. We embed HDPs in a hybrid variable neighborhood search algorithm, which we reinforce by developing filtering strategies based on the HDP. We compare via seven benchmarks the performance of our algorithm on four versions of the VRPD that have been studied in the literature. Considering the VRPD with minimizing the transportation cost, our method identifies new best-known solutions for 42 of 112 instances. For the VRPD with minimizing the makespan, our method computes 607 out of 644 optimal solutions and identifies 119 new best-known solutions among the 798 instances.

Keywords— Routing, Heuristics, Drones, Dynamic programming, Variable neighborhood search

1 Introduction

With the rapid growth of B2C e-commerce, the global last-mile delivery market is projected to grow at a compound annual growth rate of 8.16% from 2022 to 2031 (Singh and Mutreja, 2022). To gain competitive advantages, last-mile delivery companies have to actively deal with the increasing demand for quantity and quality of service. Unmanned aerial vehicles (UAVs), generally known as drones, have shown significant market potential in last-mile delivery as an emerging technology (Sah et al., 2021).

Compared to trucks, a major advantage of drones is that they are not restricted by road infrastructure (Poikonen and Campbell, 2021). As traffic congestion is one of the most critical challenges in urban areas, drones may complete delivery tasks faster than trucks, especially in metropolises (Salama and Srinivas, 2022). Furthermore, drones are flexible and easy to operate, which may decrease labor costs (Otto et al., 2018). Besides, since they are battery-powered, drones are relatively energy-efficient (Kirschstein, 2020; Salama and Srinivas, 2020). However, drones still have shortcomings such as a small payload capacity, limited flight range, and susceptibility to interference, so they cannot meet the needs of modern logistics on their own. As a result, the current projected use of drones in last-mile delivery is in collaboration with trucks (Campbell et al., 2017).

Murray and Chu (2015) were the first to investigate the collaboration between a truck and a drone in a logistics context. They proposed a new variant of the traveling salesman problem (TSP) called the flying sidekick traveling salesman problem (FSTSP). In particular, a scenario where a truck delivers goods to customers together with a single drone is considered. The drone may be dispatched to serve a customer while the truck serves other customers simultaneously. Once the drone completes its delivery task, it must return to the truck. The temporal alignment between the drone and the truck along a route can be viewed as a form of *synchronization* between two vehicles (Drexl, 2012). Murray and Chu (2015) considered a makespan minimization objective, that is the maximum arrival time to the depot between the truck and the drone. As such, the makespan includes the time required for serving customers, as well as the potential waiting time induced by the synchronization between the truck and the drone.

The FSTSP has attracted increasing attention in the past years. We refer the reader to the surveys of Macrina et al. (2020); Li et al. (2021); Chung et al. (2020); Moshref-Javadi and Winkenbach (2021). Notably, a number of variants have been proposed. The generalization of the FSTSP to multiple trucks, each equipped with one or more drones, is commonly referred to as the vehicle routing problem with drones (VRPD). This problem, which can be seen as an extension of the vehicle routing problem (VRP), has been studied by several authors (e.g., Poikonen et al., 2017; Wang et al., 2017; Tamke and Buscher, 2021; Schermer et al., 2019a; Zhou et al., 2023). In addition to the objective of minimizing makespan, several authors have considered the VRPD with a cost minimization objective (e.g., Sacramento et al., 2019; Wang and Sheu, 2019). The considered costs typically include those related to both trucks and drones.

Due to the NP-hardness of the FSTSP and its variants (Murray and Chu, 2015), existing exact approaches can only solve small-sized instances (e.g., Tamke and Buscher, 2021; Roberti and Ruthmair, 2021; Zhou et al., 2023). Therefore, a fair amount of the literature on the FSTSP and its variants proposes solution methods based on meta-heuristics, such as adaptive large neighborhood search (ALNS) (Sacramento et al., 2019), genetic algorithm (Ha et al., 2020), and variable neighborhood search (VNS) (de Freitas and Penna, 2020).

The objective of this paper is to propose an efficient solution method for several variants of the VRPD. In particular, we study the VRPD with two different objective functions: minimization of transportation cost and minimization of the makespan. Hereinafter, we refer to these two versions as VRPD-C and VRPD-M. One of our main algorithmic contributions relates to a subproblem of the VRPD, which we refer to as the fixed route drone dispatch problem (FRDDP). Given a sequence of customers being visited by a truck, the FRDDP determines a subset of customers to be served by the drone, assuming that they succeed their launch positions and precede their recovery positions in the sequence. We note that the FRDDP is instrumental to evaluating possible solutions in most local search-based heuristic algorithms

for the VRPD and its variants. Given the vast landscape of such variants, we believe that our algorithmic contribution for the FRDDP may significantly accelerate the solution process of a number of VRPD configurations. We summarize the main contributions of this paper as follows.

(i) We study the FRDDP with two different objective functions, that is minimizing the transportation cost (FRDDP-C) and minimizing the makespan (FRDDP-M), and with the possibility for the drone to land and wait. For each version, we propose a heuristic dynamic program (HDP) with a computational complexity of $\mathcal{O}(n^2)$ (where n is the number of customers contained in a single route). This is in contrast to exact dynamic programs (DPs) for the FRDDP with a computational complexity of $\mathcal{O}(n^3)$ (e.g., Agatz et al. (2018)).

(ii) We propose an efficient hybrid variable neighborhood search (HVNS) algorithm that embeds our HDP to solve the VRPD. The HVNS combines a shaking step, variable neighborhood descent (VND), and a simulated annealing-based acceptance criterion. We introduce two drone-related local search operators. To accelerate the search in the VND, we also develop a sub-heuristic dynamic program (subHDP) procedure to filter non-promising moves. The subHDP utilizes the core of the HDP to approximate objective function savings.

(iii) We demonstrate the effectiveness of our algorithm on a large set of computational experiments. We first compare the performance of the HVNS using our HDP and subHDP with the HVNS using an exact DP. Notably, given the same computational runtime budget, the former outperforms the latter in terms of the objective function on average by 20.13% for the VRPD-C and by 29.73% for the VRPD-M. Furthermore, we compare our method with state-of-the-art algorithms on both versions of the VRPD. For the VRPD-C, out of a total of 112 instances, our algorithm identifies 42 new best-known solutions and matches 55 solutions in comparison with the benchmark results from Sacramento et al. (2019) and Rave et al. (2022). For the VRPD-M, out of a total of 798 instances, our algorithm yields 607 out of 644 optimal solutions and identifies 119 new best-known solutions in comparison with the benchmark results from El-Adle et al. (2021), Tamke and Buscher (2021) and Roberti and Ruthmair (2021).

The remainder of this paper is organized as follows. In Section 2 we review the related literature. We define the treated problems and formulate them in Section 3. We formally introduce the FRDDP and the HDPs for both objective functions in Section 4. In Section 5 we describe the HVNS along with the subHDP, and present its computational results in Section 6. Finally, in Section 7 we draw conclusions and discuss possible future developments of our work.

2 Related Literature

The introduction of the FSTSP by Murray and Chu (2015) has paved the way for subsequent contributions on the collaborative use of trucks and drones for parcel delivery. For a comprehensive survey of models and applications, the reader is referred to Macrina et al. (2020); Li et al. (2021); Chung et al. (2020); Moshref-Javadi and Winkenbach (2021). In this section, we present the research most relevant to this work. In particular, we first discuss the most common characteristics and objective functions in Section 2.1, and then describe the main algorithmic frameworks used in solving the resulting problems in Section 2.2.

2.1 Problem definitions and assumptions

Agatz et al. (2018) present a variant of the FSTSP called the traveling salesman problem with drone (TSPD). Similar to Murray and Chu (2015), the authors assume that the drone has limited capacity and can only serve one customer at each dispatch. However, they also assume that the drone can be launched from the same location multiple times, while the truck remains stationary for the drone to return. This is called a *cyclic* operation (Schermer et al., 2019b) or a *loop* (Roberti and Ruthmair, 2021). We observe that the FSTSP is characterized by a slightly different assumption, as loops are prohibited. In addition, Agatz et al. (2018) and Bouman et al. (2018a) also allow the truck to revisit nodes for drone recovery, which is prohibited in most of the literature (e.g., Murray and Chu, 2015; Sacramento et al., 2019; Roberti and Ruthmair, 2021; Dell'Amico et al., 2021). Roberti and Ruthmair (2021) study several variants of the TSPD, one of which requires that the drone cannot land and wait (NoLW) to be recovered by the truck. Since the limited battery capacity of the drone impacts its flight endurance, this assumption implies that the truck must recover the drone before its battery runs out. Thus, the time between launching and recovering the drone is more constrained. A similar assumption is also used by Murray and Chu (2015); Sacramento et al. (2019); Rave et al. (2022). However, this is not the case in several works (e.g., Agatz et al., 2018; El-Adle et al., 2021; Tamke and Buscher, 2021), where the drone is allowed to land and wait (LW) for recovery.

Murray and Raj (2020) extend the FSTSP to the multiple FSTSP, where a single truck carries a heterogeneous fleet of drones with different travel speeds, payload capacities, service times, and flight endurances. Although the weight or volume capacity of each drone may differ, the drone can only carry one parcel at a time. Wang et al. (2017) and Poikonen et al. (2017) introduce the VRPD by extending the problem from a single truck to multiple trucks. Both works analyze several worst-case scenarios and introduce bounds on the best possible time savings of using trucks and drones, as opposed to using trucks alone. Schermer et al. (2019b) formulate a mixed integer linear program (MILP) model along with valid inequalities for the VRPD, where cyclic operations are allowed, i.e., drones can be launched and recovered at the same node.

As one of the main advantages of using drones is their higher speed when compared to trucks, most of the aforementioned studies considered makespan minimization as an objective function. However, as operational costs also play an important role in logistics, several authors considered optimizing them in VRPDs. Ha et al. (2018) were the first to consider a cost minimization objective in a TSPD model. The considered costs include the transportation costs (of both the truck and the drone), as well as a waiting time penalty for the truck and for the drone. Sacramento et al. (2019) minimize the transportation cost of trucks and drones for the VRPD. Wang and Sheu (2019) include fixed cost of deploying trucks in the VRPD.

With exception of Ha et al. (2018); Roberti and Ruthmair (2021); Tamke and Buscher (2021), the aforementioned contributions primarily deal with a single problem. Considering non-cyclic operations, our method may handle eight versions of the problem, characterized by the following three axes, each referring to two alternative assumptions for the problem: 1) single or multiple trucks each equipped with a single drone, 2) allowing the drone to land and wait (i.e., LW) or not (i.e., NoLW), and 3) objective functions of minimizing the transportation cost or minimizing the makespan. Considering these eight versions, four versions have been extensively studied in the literature. We compare the performance of our algorithm on those four problems in Section 6.

2.2 Solutions methods

Compact MILP models for the FSTSP and its variants are capable of solving very small instances typically not exceeding 12 customers (e.g., Murray and Chu, 2015; Sacramento et al., 2019). Bouman et al. (2018a) develop a dynamic program with three steps for the TSPD, which solves instances with up to 20 nodes to optimality. El-Adle et al. (2021) propose a mixed integer program (MIP) model for the TSPD, which is enhanced by a series of bound improvement strategies. The authors are able to solve instances with 32 customers. Several authors focused on developing exact methods for the FSTSP and its variants, such as branch-and-bound algorithm (Poikonen et al., 2019), branch-and-price algorithm (Roberti and Ruthmair, 2021; Zhou et al., 2023), and branch-and-cut algorithm (Tamke and Buscher, 2021). Among these works, notably, Roberti and Ruthmair (2021) solve instances with up to 40 nodes to optimality.

To solve instances with a larger number of customers, several works propose metaheuristic approaches. Ha et al. (2020) develop a hybrid genetic algorithm (HGA) to solve two versions of the TSPD with minimizing cost and minimizing makespan objective functions. The authors test their HGA on three benchmark sets (Murray and Chu, 2015; Ha et al., 2018; de Freitas and Penna, 2020), showing that the HGA can handle instances with up to 100 customers and it outperforms other methods in the literature in terms of solution quality. Moshref-Javadi et al. (2020) present a hybrid tabu search-simulated annealing algorithm for the case of a single truck equipped with multiple drones. The authors solve real-world-size problem instances with up to 159 customers. Sacramento et al. (2019) propose an ALNS with several destroy operators and repair operators for the VRPD. The authors test their ALNS on instances with up to 200 customers considering realistic values for the used parameters.

The heuristics in the aforementioned works generally employ local search operators that do not alter the given assignment of each customer to the truck or to the drone. However, there are a series of works that reoptimize these assignments for each evaluated solution. Murray and Chu (2015) propose a route and re-assign heuristic. The route step constructs a TSP tour containing all the customers served by the truck. Then the re-assign step assigns a subset of customers to be served by the drone by evaluating the achievable time saving of the drone insertion. When the drone is assigned to a customer, it may be launched at a node positioned after this customer or be recovered at a node positioned before this customer. It just must be recovered at a node positioned after the launch node in the initial tour. Such a re-assign step is slightly restricted by Agatz et al. (2018), who consider a potential visit of a customer by the drone to be such that the drone can only be launched at a node preceding the customer and recovered at a node succeeding the customer. The re-assign step proposed by Agatz et al. (2018) is the case of what we refer to as the FRDDP, i.e., determining a subset of customers to be served by the drone, assuming that they succeed their launch positions and precede their recovery positions in the sequence. The authors propose a greedy heuristic and an exact method based on a DP for the FRDDP. Ha et al. (2018) introduce a greedy randomized adaptive search procedure (GRASP) that embeds an exact DP to solve both the FRDDP-C and the FRDDP-M. The FRDDP is only solved once in each iteration of the GRASP to obtain a starting solution, and is not considered during the improvement phase. Najy et al. (2022) consider a FRDDP in an inventory-routing problem with a single truck and a single drone. In particular, they solve the FRDDP as a shortest path problem in a network that defines arcs between customers that are possibly served by the drone. Schermer et al. (2019b) decompose the VRPD into two subproblems. The first subproblem consists of allocating customers to routes and sequencing these customers within each route, while the second subproblem consists of an independent FRDDP for each route. The authors solve the first subproblem

with a classical heuristic for VRPs and the second subproblem through a MILP model.

The existing heuristics for the FSTSP and its variants can be broadly classified into two main categories. The first includes methods purely applying local search operators on the truck and drone solutions (e.g., Ha et al., 2020; Sacramento et al., 2019; de Freitas and Penna, 2020), whereas the second applies local search operators to truck routes, and evaluates those truck routes by inserting drone visits (i.e., solving an appropriately defined version of the FRDDP). The methods in the latter category have been shown to be promising. However, exactly solving the FRDDP at every evaluation of a local search move is computationally expensive. To handle this issue, our method uses a heuristic DP during the local search in combination with filtering procedures on non-promising moves. These features dramatically improve the local search.

3 Problem Definition

We first describe the VRPD-C and present its MILP model introduced by Sacramento et al. (2019) using our notation. We then describe the modifications required for modeling the VRPD-M.

The VRPD-C is defined on a directed graph $\mathcal{G} = (\mathcal{N}, \mathcal{A})$, where $\mathcal{N} = \{0, 1, ..., n+1\}$ is the set of nodes, nodes 0 and $n+1$ represent the departure and arrival depot, and $\mathcal{C} = \{1, 2, ..., n\}$ is the set of nodes representing customers. The set of arcs is denoted by $\mathcal{A} = \{(i, j) : i \in \mathcal{N}\backslash\{n+1\}, j \in \mathcal{N}\backslash\{0\}\}$. We consider a set of homogeneous trucks $\mathcal{H}$. Each truck $h \in \mathcal{H}$ has a capacity of Q and carries a single drone. Each drone has a capacity of Q' and a flight endurance T' time units. Each customer $i \in \mathcal{C}$ has a demand q_i that must be served in a single visit (i.e., split deliveries are not allowed). If $q_i \leqslant Q'$, then customer i may be served either by a truck or by a drone, otherwise customer i can only be served by a truck. We define $\mathcal{C}' \subseteq \mathcal{C}$ as the set of customers that may be served by a truck or a drone.

Each arc $(i, j) \in \mathcal{A}$ is associated with two non-negative transportation costs, c_{ij} for a truck and c'_{ij} for a drone. Considering that trucks and drones have different speeds, the travel times for a truck and for a drone in arc $(i, j) \in \mathcal{A}$ are denoted by τ_{ij} and τ'_{ij}. In general, drones travel faster than trucks, thus we assume $\tau_{ij} = \alpha\tau'_{ij}$, where $\alpha \geqslant 1$. The service times of a truck and of a drone at node $i \in \mathcal{N}$ are s_i and s'_i. The drone needs $\hat{\tau}$ and $\check{\tau}$ time to be launched and recovered. Furthermore, we assume NoLW, thus if the drone waits to be recovered by the truck, it waits while flying in the air (i.e., consuming its battery) until the truck arrives at the recovery location. Therefore, the time between when a drone is prepared to be launched and when it is recovered after landing should not exceed its flight endurance T'. This time includes $\hat{\tau}$ and $\check{\tau}$. Note that one can always convert an instance where $\hat{\tau}$ and $\check{\tau}$ should not be counted in the flight endurance into an instance where they should be included in it by simply increasing T' by $\hat{\tau} + \check{\tau}$.

The truck and the drone must depart from and return to the depot. The drone can only be launched from a node $i \in \mathcal{N}\backslash\{n+1\}$ and recovered at a node $k \in \mathcal{N}\backslash\{0\}$ which is different from i. We define $\Delta = \{\langle i, j, k\rangle : i \in \mathcal{N}\backslash\{n+1\} \wedge j \in \mathcal{C}' \wedge k \in \mathcal{N}\backslash\{0\} \wedge i \neq j \wedge j \neq k \wedge k \neq i \wedge \hat{\tau} + \tau'_{ij} + s'_j + \tau'_{jk} + \check{\tau} \leqslant T'\}$ as the set of all possible drone sorties. A drone sortie $\langle i, j, k\rangle$ entails that a drone may serve customer $j \in \mathcal{C}'$ if it takes off from a truck at node i and is recovered at node k by the same truck. In such cases, we refer to node i and node k as a *launch node* and a *recovery node*. A drone sortie is deemed possible (and inserted in Δ) if the flight endurance of the drone is respected. Similar to the assumptions presented in Sacramento et al. (2019) and Roberti and Ruthmair (2021), we assume that if the drone should be launched by the truck at a customer, it must be launched before the truck serves this customer. Furthermore, if the truck

Notation	Type	Description
x_{ij}^h	Binary	1, if truck $h \in \mathcal{H}$ travels from node $i \in \mathcal{N}\backslash\{n+1\}$ to node $j \in \mathcal{N}\backslash\{0\}$; 0, otherwise
y_{ijk}^h	Binary	1, if the drone on truck $h \in \mathcal{H}$ performs the sortie $\langle i,j,k\rangle \in \Delta$; 0, otherwise
p_i^h	Continuous	the position of node $i \in \mathcal{N}$ in the route of truck $h \in \mathcal{H}$
w_{ij}^h	Binary	1, if node $j \in \mathcal{N}\backslash\{0\}$ is visited after node $i \in \mathcal{N}\backslash\{n+1\}$ in the route of truck $h \in \mathcal{H}$; 0, otherwise
t_i^h	Continuous	ready time of truck $h \in \mathcal{H}$ at node $i \in \mathcal{N}$ to launch a drone, serve a customer or arrive at the depot
$t_i'^h$	Continuous	ready time of the drone on truck $h \in \mathcal{H}$ to start serving customer $i \in \mathcal{C}'$, the time at which it starts being launched from $i \in \mathcal{N}\backslash\{n+1\}$, the time at which it terminates being recovered at $i \in \mathcal{N}\backslash\{0\}$.

Table 1: Decision variables for the VRPD-C

should recover the drone at a customer, it must do so before serving this customer, even if it arrives at this customer earlier than the drone. As customers can only be visited once, the truck cannot revisit a customer that has already been served to recover the drone. If a drone does not have any delivery task, it remains on its truck. The duration of each route is defined as the maximum between the time the truck returns to the depot and the time its drone is recovered at the depot. The maximum working duration of each route is T.

The decision variables are listed in Table 1. The continuous variable t_i^h indicates the earliest time at which the truck h can launch its drone at i or serve the customer if no drone launch is performed. If the drone is recovered by the truck at i, then t_i^h is the time when the recovery is complete. Otherwise, it is the arrival time of the truck at i. The drone's corresponding ready time $t_i'^h$ is equal to t_i^h if the drone is either launched or recovered by the truck h at customer i. Otherwise, $t_i'^h$ is the earliest time at which the drone can serve customer i.

$$\text{(VRPD-C)} \quad \min f^{\text{cost}} = \sum_{h\in\mathcal{H}} \sum_{(i,j)\in\mathcal{A}} c_{ij} x_{ij}^h + \sum_{h\in\mathcal{H}} \sum_{\langle i,j,k\rangle\in\Delta} (c'_{ij} + c'_{jk}) y_{ijk}^h \tag{1}$$

subject to

$$\sum_{h\in\mathcal{H}} \Big(\sum_{i:(i,j)\in\mathcal{A}} x_{ij}^h + \sum_{i,k:\langle i,j,k\rangle\in\Delta} y_{ijk}^h \Big) = 1 \qquad \forall j \in \mathcal{C} \tag{2}$$

$$\sum_{j\in\mathcal{N}\backslash\{0\}} x_{0j}^h \leqslant 1 \qquad \forall h \in \mathcal{H} \tag{3}$$

$$\sum_{i\in\mathcal{N}\backslash\{n+1\}} x_{i,n+1}^h \leqslant 1 \qquad \forall h \in \mathcal{H} \tag{4}$$

$$x_{0,n+1}^h = 0 \qquad \forall h \in \mathcal{H} \tag{5}$$

$$\sum_{i:(i,j)\in\mathcal{A}} x_{ij}^h = \sum_{k:(j,k)\in\mathcal{A}} x_{jk}^h \qquad \forall h \in \mathcal{H}, j \in \mathcal{C} \tag{6}$$

$$p_i^h + 1 \leqslant p_j^h + |\mathcal{N}|(1 - x_{ij}^h) \qquad \forall h \in \mathcal{H}, (i,j) \in \mathcal{A} \tag{7}$$

$$p_j^h \leqslant |\mathcal{N}| \sum_{i:(i,j)\in\mathcal{A}} x_{ij}^h \qquad \forall h \in \mathcal{H}, j \in \mathcal{N}\backslash\{0\} \tag{8}$$

$$\sum_{j\in\mathcal{C}} q_j \Big(\sum_{i:(j,i)\in\mathcal{A}} x_{ji}^h + \sum_{i,k:\langle i,j,k\rangle\in\Delta} y_{ijk}^h \Big) \leqslant Q \qquad \forall h \in \mathcal{H} \tag{9}$$

$$\sum_{j,k:\langle i,j,k\rangle\in\Delta} y_{ijk}^h \leqslant 1 \qquad \forall h \in \mathcal{H}, i \in \mathcal{N}\backslash\{n+1\} \tag{10}$$

$$\sum_{i,j:\langle i,j,k\rangle\in\Delta} y^h_{ijk} \leqslant 1 \qquad \forall h\in\mathcal{H}, k\in\mathcal{N}\backslash\{0\} \tag{11}$$

$$2y^h_{ijk} \leqslant \sum_{l:(i,l)\in\mathcal{A}} x^h_{il} + \sum_{l:(l,k)\in\mathcal{A}} x^h_{lk} \qquad \forall h\in\mathcal{H}, \langle i,j,k\rangle\in\Delta \tag{12}$$

$$t^h_0 = 0 \qquad \forall h\in\mathcal{H} \tag{13}$$

$$t'^h_0 = 0 \qquad \forall h\in\mathcal{H} \tag{14}$$

$$t^h_{n+1} \leqslant T \sum_{i\in\mathcal{N}\backslash\{n+1\}} x^h_{i,n+1} \qquad \forall h\in\mathcal{H} \tag{15}$$

$$t'^h_{n+1} \leqslant T \sum_{i,j:\langle i,j,n+1\rangle\in\Delta} y^h_{i,j,n+1} \qquad \forall h\in\mathcal{H} \tag{16}$$

$$t^h_i + \widehat{\tau} \sum_{j,l:\langle i,j,l\rangle\in\Delta} y^h_{ijl} + s_i + \tau_{ik} + \breve{\tau} \sum_{l,j:\langle l,j,k\rangle\in\Delta} y^h_{ljk} \leqslant t^h_k + T(1-x^h_{ik}) \qquad \forall h\in\mathcal{H}, (i,k)\in\mathcal{A} \tag{17}$$

$$t'^h_i + \widehat{\tau} + \tau'_{ij} \leqslant t'^h_j + T(1 - \sum_{k:\langle i,j,k\rangle\in\Delta} y^h_{ijk}) \qquad \forall h\in\mathcal{H}, i\in\mathcal{N}\backslash\{n+1\}, j\in\mathcal{C}'\backslash\{i\} \tag{18}$$

$$t'^h_j + s'_j + \tau'_{jk} + \breve{\tau} \leqslant t'^h_k + T(1 - \sum_{i:\langle i,j,k\rangle\in\Delta} y^h_{ijk}) \qquad \forall h\in\mathcal{H}, j\in\mathcal{C}', k\in\mathcal{N}\backslash\{0\}\cup\{j\} \tag{19}$$

$$t^h_i - T(1 - \sum_{j,k:\langle i,j,k\rangle\in\Delta} y^h_{ijk}) \leqslant t'^h_i \qquad \forall h\in\mathcal{H}, i\in\mathcal{N}\backslash\{n+1\} \tag{20}$$

$$t^h_i + T(1 - \sum_{j,k:\langle i,j,k\rangle\in\Delta} y^h_{ijk}) \geqslant t'^h_i \qquad \forall h\in\mathcal{H}, i\in\mathcal{N}\backslash\{n+1\} \tag{21}$$

$$t^h_k - T(1 - \sum_{i,j:\langle i,j,k\rangle\in\Delta} y^h_{ijk}) \leqslant t'^h_k \qquad \forall h\in\mathcal{H}, k\in\mathcal{C} \tag{22}$$

$$t^h_k + T(1 - \sum_{i,j:\langle i,j,k\rangle\in\Delta} y^h_{ijk}) \geqslant t'^h_k \qquad \forall h\in\mathcal{H}, k\in\mathcal{C} \tag{23}$$

$$T' + T(1 - \sum_{j:\langle i,j,k\rangle\in\Delta} y^h_{ijk}) \geqslant t'^h_k - t'^h_i \qquad \forall h\in\mathcal{H}, i\in\mathcal{N}\backslash\{n+1\}, k\in\mathcal{N}\backslash\{0\}\cup\{i\} \tag{24}$$

$$p^h_j - p^h_i \leqslant |\mathcal{N}| w^h_{ij} \qquad \forall h\in\mathcal{H}, i\in\mathcal{N}\backslash\{n+1\}, j\in\mathcal{C}\backslash\{i\} \tag{25}$$

$$p^h_j - p^h_i \geqslant |\mathcal{N}|(w^h_{ij}-1)+1 \qquad \forall h\in\mathcal{H}, i\in\mathcal{N}\backslash\{n+1\}, j\in\mathcal{C}\backslash\{i\} \tag{26}$$

$$t^h_k - T\big(3 - \sum_{j:\langle i,j,k\rangle\in\Delta} y^h_{ijk} - \sum_{l,g:\langle f,l,g\rangle\in\Delta} y^h_{flg} - w^h_{if}\big) \leqslant t'^h_f \qquad \forall h\in\mathcal{H}, i\in\mathcal{N}\backslash\{n+1\}, k\in\mathcal{N}\backslash\{0\}, f\in\mathcal{C}\backslash\{i\} \tag{27}$$

$$x^h_{ij}\in\{0,1\} \qquad \forall h\in\mathcal{H}, (i,j)\in\mathcal{A} \tag{28}$$

$$y^h_{ijk}\in\{0,1\} \qquad \forall h\in\mathcal{H}, \langle i,j,k\rangle\in\Delta \tag{29}$$

$$w^h_{ij}\in\{0,1\} \qquad \forall h\in\mathcal{H}, i\in\mathcal{N}\backslash\{n+1\}, j\in\mathcal{N}\backslash\{0\} \tag{30}$$

$$p^h_i, t^h_i, t'^h_i \geqslant 0 \qquad \forall h\in\mathcal{H}, i\in\mathcal{N} \tag{31}$$

The objective function (1) minimizes the total transportation cost of both trucks and drones. Constraints (2) ensure that each customer is served exactly once by a truck or a drone. Constraints (3) and (4) guarantee that all trucks must depart from and return to the depot at most once. Constraints (5) prohibit traveling between depots. Constraints (6) enforce the flow conservation for a truck tour. Constraints (7) and (8) eliminate subtours for the truck. Constraints (9) state that the total demand served by the truck and its carried drone cannot exceed the capacity of the truck. Constraints (10) and (11) make sure that the drone can be launched and recovered at most once at a node. Constraints (12) ensure that if a drone is launched at node $i\in\mathcal{N}\backslash\{n+1\}$ and recovered $k\in\mathcal{N}\backslash\{0\}$, then its truck must visits nodes i and k. Note that a truck h may visit several nodes between the launch of the drone at a node i and its recovery

at a node k. Constraints (13) and (14) initialize the time for trucks and drones at the beginning of each route. Constraints (15) and (16) enforce the maximum route duration for trucks and drones. Constraints (17) describe the truck movement together with a drone sortie. Correspondingly, constraints (18) and (19) enforce the ready time of the drones. Constraints (20) – (23) ensure the synchronization between the truck and its carried drone. Constraints (24) limit the time between the launch of the drone and its recovery according to the flight endurance T'. Constraints (25) and (26) ensure the customer order of each truck. Constraints (27) enforce that the drone can only serve another customer after being recovered. Finally, constraints (28)–(31) define the domain of decision variables.

We now derive a model for the VRPD-M from the one introduced for the VRPD-C. For this purpose, we introduce an additional variable t equal to the makespan, i.e., the maximum duration of all routes. We obtain a formulation for the VRPD-M by replacing the objective function (1) by (32) and adding constraints (33) and (34).

$$\begin{aligned}
\text{(VRPD-M)} \quad & \min f^{\text{makespan}} = t && (32)\\
\text{s.t.} \quad & (2) - (31) && \\
& t \geqslant t^h_{n+1} \qquad \forall h \in \mathcal{H} && (33)\\
& t \geqslant t'^h_{n+1} \qquad \forall h \in \mathcal{H} && (34)
\end{aligned}$$

4 Fixed Route Drone Dispatch Problem

In this section, we first describe the FRDDP, which we treat under the two objective functions. We present two exact dynamic programs for both considered objectives of the problem in Section 4.1. We then develop heuristics for solving the FRDDP with both objectives in Section 4.2. These dynamic programs will be used in our algorithm for the VRPD-C and the VRPD-M (Section 5). In what follows, we present common definitions and notations for all treated problems in this section.

Let $\mathcal{R} = (v_0, v_1, ..., v_{\bar{n}-1}, v_{\bar{n}})$ denote the sequence of nodes visited by a truck, where v_0 and $v_{\bar{n}}$ represent the departure and arrival depot (i.e., $v_0 = 0$ and $v_{\bar{n}} = n + 1$) and v_e for $e \in \{1, ..., \bar{n} - 1\}$ is a customer node (i.e., $v_e \in \mathcal{C}$). We refer to $\mathcal{R}$ as a *truck route*. Given a truck route, the FRDDP establishes a subset of customers to be visited by the drone. Such customers, must succeed the drone's launch position and precede the drone's recovery position in the truck route. Assuming that $\mathcal{R}$ respects the maximum duration limit T, when introducing the dynamic programs, we disregard this duration limit. This is justified by the fact that drones travel faster than trucks, thus any drone insertions in $\mathcal{R}$ would shorten its duration.

Given a truck route $\mathcal{R}$, we define a directed acyclic graph $\mathcal{G}_\mathcal{R} = (\mathcal{N}_\mathcal{R}, \mathcal{A}_\mathcal{R})$ for the dynamic programs. The node set $\mathcal{N}_\mathcal{R} = \{v_e \in \mathcal{R} \cup \mathcal{R}'\}$ includes not only all nodes (hereafter called *truck-visited nodes*) in route $\mathcal{R}$, but also a new set of nodes $\mathcal{R}'$ (hereafter called *drone-served customers*) corresponding to customers in $\mathcal{R}$ that could be served by a drone. To distinguish between the customers in $\mathcal{R}$ and $\mathcal{R}'$, we use $v'_f \in \mathcal{R}'$ when referring to the possibility of customer v_f being served by the drone. Specifically, $\mathcal{R}' = \{v'_f \in \mathcal{R} : \exists \langle v_e, v_f, v_g \rangle \in \Delta\}$. Thus, v'_f is possibly neither launched nor recovered from a node in $\mathcal{R}$.

The set of arcs $\mathcal{A}_{\mathcal{R}}$ is defined as follows:

$$\mathcal{A}_{\mathcal{R}} = \left\{ \begin{array}{ll} (v_e, v_{e+1}) : v_e \in \mathcal{R} \backslash \{n+1\} & \text{(35a)} \\ (v_e, v'_f) : 0 \leqslant e < f < \bar{n}, \exists k \in \mathcal{N} \backslash \{0\} \text{ with } \langle v_e, v_f, k \rangle \in \Delta & \text{(35b)} \\ (v'_f, v_g) : 0 < f < g \leqslant \bar{n}, \exists i \in \mathcal{N} \backslash \{n+1\} \text{ with } \langle i, v_f, v_g \rangle \in \Delta & \text{(35c)} \\ (v_e, v_{e+2}) : v_e \in \mathcal{R} \backslash \{n+1, v_{\bar{n}-1}\} \wedge v'_{e+1} \in \mathcal{R}' & \text{(35d)} \end{array} \right\}$$

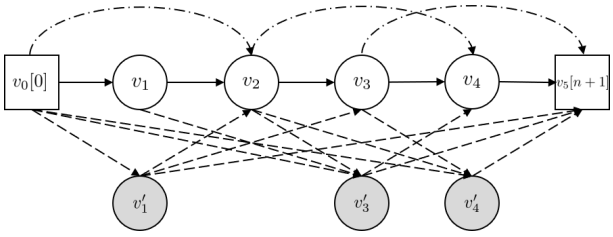

Figure 1: Illustration of $\mathcal{G}_{\mathcal{R}}$ for a truck route $\mathcal{R}$ serving four customers

We provide an example of $\mathcal{G}_{\mathcal{R}}$ in Figure 1. The truck-visited nodes in route $\mathcal{R} = (v_0 = 0, v_1, v_2, v_3, v_4, v_5 = n+1)$ are marked with white circles (customers) or white squares (the departure and arrival depot) and all possible drone-served customers of set $\mathcal{R}' = (v'_1, v'_3, v'_4)$ are marked with gray circles. Arcs are defined according to conditions (35). The *truck-arcs* between adjacent truck-visited nodes in $\mathcal{R}$, as described in conditions (35a), are marked with solid arrows. The *drone-arcs*, described in conditions (35b)–(35c) and marked with dashed arrows, are between a truck-visited node v_e and a drone-served customer v'_f, and between a drone-served customer v'_f and a truck-visited node v_g. As previously mentioned, under conditions (35b)–(35c) nodes k and i may not be in route $\mathcal{R}$. However, the combination of conditions (35b)–(35c) ensures that drone arcs represent feasible launch and recovery arcs. The *truck bypass arcs* (v_e, v_{e+2}), described in condition (35d) and marked with dot-dash arrows, model the situations where the truck traverses directly from node v_e to node v_{e+2} when customer v'_{e+1} is served by the drone. This is due to the fact that the drone can only serve one customer at each dispatch. Note that if customer v'_{e+1} cannot be served by the drone, there is no truck bypass arc between node v_e and v_{e+2}. Therefore, since customer v_2 cannot be served by a drone, there is no arc between customer v_1 and v_3 in Figure 1.

We define an FRDDP solution as a *complete route* and denote it by $\overline{\mathcal{R}} = (\mathcal{R}^t, \mathcal{R}^d)$, where $\mathcal{R}^t$ is a sequence of nodes starting at 0 and ending at $n+1$, containing all the customers of $\mathcal{R}$ that are served by the truck, and $\mathcal{R}^d$ contains a sequence of drone sorties. Figure 2 shows a complete route for the truck route $\mathcal{R}$ given in Figure 1. The drone serves customer v_1 after being launched at the depot. The truck departs from the depot to serve customer v_2, bypassing customer v_1. Then, the drone is recovered by the truck at customer v_3 and launched again to serve customer v_4 before being recovered at the depot, while the truck returns to the depot after serving customer v_3 bypassing customer v_4. Accordingly, we have $\mathcal{R}^t = (0, v_2, v_3, n+1)$ and $\mathcal{R}^d = (\langle 0, v_1, v_3 \rangle, \langle v_3, v_4, n+1 \rangle)$.

For notational convenience, in this section, we denote by c_{ef} and c'_{ef} the cost of the truck and the drone traveling from v_e to v_f in truck route $\mathcal{R}$. We then define C_{ef} as the total truck cost incurred if the truck visits the nodes of subsequence $(v_e, v_{e+1}, ..., v_f)$. The value C_{ef} is computed as follows.

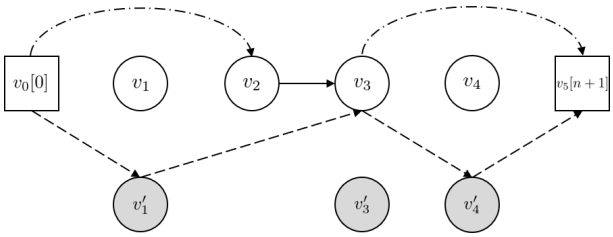

Figure 2: An example of a complete route

$$C_{ef} = \begin{cases} 0 & e = f \\ c_{ef} & f = e+1 \\ C_{e,f-1} + c_{f-1,f} & f > e+1 \end{cases} \tag{36}$$

Let τ_{ef} and τ'_{ef} be the travel time of the truck and the drone from v_e to v_f in truck route $\mathcal{R}$, and let s_e and s'_e be the service time of the truck and the drone serving customer v_e in $\mathcal{R}$. We then define T_{ef} as the sum of the truck's travel and service time for a subsequence $(v_e, v_{e+1}, ..., v_f)$ as follows.

$$T_{ef} = \begin{cases} 0 & e = f \\ s_e + \tau_{ef} & f = e+1 \\ T_{e,f-1} + s_{f-1} + \tau_{f-1,f} & f > e+1 \end{cases} \tag{37}$$

Given a truck route $\mathcal{R}$, we define $\langle v_e, v_f, v_g \rangle$ with $v_e, v_f, v_g \in \mathcal{R}$ as a possible drone sortie if it satisfies the following conditions:

$$(v_e, v'_f) \in \mathcal{A}_{\mathcal{R}} \tag{38a}$$

$$(v'_f, v_g) \in \mathcal{A}_{\mathcal{R}} \tag{38b}$$

$$\langle v_e, v_f, v_g \rangle \in \Delta \tag{38c}$$

$$\widehat{\tau} + \sum_{l=e}^{g-1} (\tau_{l,l+1} + s_l) + \breve{\tau} \leqslant T' \tag{38d}$$

Condition (38d) ensures the NoLW assumption where the drone must be recovered by the truck within the drone endurance T'. In the case of the LW assumption, we remove condition (38d).

4.1 Exact dynamic programs

In this section, we first introduce an EDP for the FRDDP-C, and then present an EDP for FRDDP-M. Let $\omega^{\mathsf{E}}_{\mathsf{C}}(v_g)$ and $\omega^{\mathsf{E}}_{\mathsf{M}}(v_g)$ denote the minimum cost and minimum makespan up to node v_g when visited by a truck while the drone is either on the truck or has just been recovered at v_g.

The EDP for the FRDDP-C is formulated in equation (39). Two cases are considered when computing $\omega^{\mathsf{E}}_{\mathsf{C}}(v_g)$ (where $g \geqslant 2$). In the first case, the truck arrives from node v_{g-1} while carrying the drone. In the second case, the drone is recovered by the truck at node v_g, having served one of the previous nodes of the route. This case is illustrated in Figure 3, where unvisited customers and untraveled arcs are marked in gray. The computation considers every possible couple of nodes (v_e, v'_f) in $\mathcal{G}_{\mathcal{R}}$ that can form a feasible drone sortie $\langle v_e, v_f, v_g \rangle$ (i.e., a drone sortie satisfying conditions (38a)–(38d)), and includes the minimum cost up to node v_e, the cost of the drone $c'_{ef} + c'_{fg}$, and the cost of the truck $C_{e,f-1} + c_{f-1,f+1} + C_{f+1,g}$ bypassing customer v_f. The computational complexity of this EDP is $\mathcal{O}(\bar{n}^3)$.

$$\omega_{\mathsf{C}}^{\mathsf{E}}(v_g) = \begin{cases} 0 & g = 0 \\ c_{01} & g = 1 \\ \min\Big\{\omega_{\mathsf{C}}^{\mathsf{E}}(v_{g-1}) + c_{g-1,g}, \min\limits_{v_e, v'_f : \langle v_e, v_f, v_g \rangle \text{ satisfies (38a)–(38d)}} \Big\{\omega_{\mathsf{C}}^{\mathsf{E}}(v_e) \\ \quad + c'_{ef} + c'_{fg} + C_{e,f-1} + c_{f-1,f+1} + C_{f+1,g}\Big\}\Big\} & g \in \{2, ..., \bar{n}\} \end{cases} \tag{39}$$

An EDP for the FRDDP-M is proposed by Agatz et al. (2018). We describe it by using our notation in equation (40). Slightly different from the FRDDP-C, truck and drone time synchronization is explicitly handled in the FRDDP-M. Specifically, the minimum makespan at node v_g is the maximum between the arrival time of the truck and the arrival time of the drone at that node. The computational complexity of this EDP is $\mathcal{O}(\bar{n}^3)$.

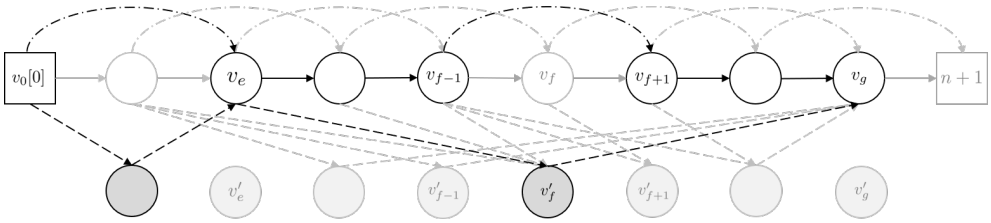

Figure 3: Illustration of the computation performed in the EDP

$$\omega_{\mathsf{M}}^{\mathsf{E}}(v_g) = \begin{cases} 0 & g = 0 \\ \tau_{01} & g = 1 \\ \min\Big\{\omega_{\mathsf{M}}^{\mathsf{E}}(v_{g-1}) + T_{g-1,g}, \min\limits_{v_e, v'_f : \langle v_e, v_f, v_g \rangle \text{ satisfies (38a)–(38d)}} \Big\{\omega_{\mathsf{M}}^{\mathsf{E}}(v_e) + \widehat{\tau} \\ \quad + \max\{\tau'_{ef} + s'_f + \tau'_{fg}, T_{e,f-1} + s_{f-1} + \tau_{f-1,f+1} + T_{f+1,g}\} + \breve{\tau}\Big\}\Big\} & g \in \{2, ..., \bar{n}\} \end{cases} \tag{40}$$

4.2 Heuristic dynamic programs

In this section, we develop novel heuristic dynamic programs for both versions of the FRDDP. In Section 4.2.1, we introduce the HDP for the FRDDP-C, and in Section 4.2.2, we introduce the HDP for the FRDDP-M.

4.2.1 FRDDP-C

We define $\omega_{\mathsf{C}}^{\mathsf{H}}(v_g)$ as the minimum cost up to node v_g when visited by a truck while the drone is either on the truck or has just been recovered at v_g. We define $\omega_{\mathsf{C}}^{\mathsf{H}}(v'_f)$ as the minimum cost up to the drone-served customer v'_f, where the cost for the truck up to v_{f-1} is included. The values $\omega_{\mathsf{C}}^{\mathsf{H}}(v_g)$ and $\omega_{\mathsf{C}}^{\mathsf{H}}(v'_f)$ are computed recursively by equations (41) and (42). We denote by $p_{\mathsf{C}}(v'_f)$ the index of the launch node leading to the minimum cost when computing $\omega_{\mathsf{C}}^{\mathsf{H}}(v_g)$.

$$\omega_{\mathsf{C}}^{\mathsf{H}}(v_g) = \begin{cases} 0 & g = 0 \\ c_{01} & g = 1 \\ \min\Big\{\omega_{\mathsf{C}}^{\mathsf{H}}(v_{g-1}) + c_{g-1,g}, \min\limits_{v'_f:\langle v_{p_{\mathsf{C}}(v'_f)}, v_f, v_g\rangle \text{ satisfies (38b)}-\text{(38d)}} \Big\{\omega_{\mathsf{C}}^{\mathsf{H}}(v'_f) \\ \qquad +c'_{fg} + c_{f-1,f+1} + C_{f+1,g}\Big\}\Big\} & g \in \{2, ..., \bar{n}\} \end{cases} \tag{41}$$

$$\omega_{\mathsf{C}}^{\mathsf{H}}(v'_f) = \min_{v_e:(v_e,v'_f)\in\mathcal{A}_{\mathcal{R}}} \Big\{\omega_{\mathsf{C}}^{\mathsf{H}}(v_e) + c'_{ef} + C_{e,f-1}\Big\} \qquad v'_f \in \mathcal{R}' \tag{42}$$

$$\text{where,} \quad p_{\mathsf{C}}(v'_f) = \arg\min_{e:(v_e,v'_f)\in\mathcal{A}_{\mathcal{R}}} \Big\{\omega_{\mathsf{C}}^{\mathsf{H}}(v_e) + c'_{ef} + C_{e,f-1}\Big\} \qquad v'_f \in \mathcal{R}' \tag{43}$$

Figure 4 illustrates how the HDP functions. Similar to Figure 3, the unvisited customers and untraveled arcs are shown in grey. Instead of considering each possible drone sortie preceding v_g like in the EDP, the HDP decomposes this computation into two components. The first component, computed in equation (42), accounts for each feasible launch node v_e for serving v'_f with a drone, i.e., $(v_e, v'_f) \in \mathcal{A}_{\mathcal{R}}$ (as shown in Figure 4 (a)). The cost $\omega_{\mathsf{C}}^{\mathsf{H}}(v'_f)$ is set as the minimum cost of launching the drone from a node v_e and the cost of serving all customers between v_e and v_{f-1} by the truck. Based on this computation, the launch node of v'_f is fixed in equation (43). The second component is computed in equation (41). Similar to the EDP, we consider that the truck may arrive at v_g while carrying the drone or recovers the drone at v_g. However, the computation of the latter case in the HDP is different. Each possible previous drone-served customer v'_f and its fixed launch node $v_{p_{\mathsf{C}}(v'_f)}$ (according to equation (43) and connected by dashed blue arrows in Figure 4 (b)) are considered. Specifically, we check if $\langle v_{p_{\mathsf{C}}(v'_f)}, v_f, v_g\rangle$ satisfies conditions (38b)–(38d). To compute the minimum cost at customer v_g in the case there is a recovery of the drone, we add c'_{fg} (the cost of the drone traveling from v'_f to v_g), and $c_{f-1,f+1} + C_{f+1,g}$ (the cost of the truck traversing from v_{f-1} to v_{f+1} bypassing customer v_f and visiting all the customers between v_{f+1} and v_g) to $\omega_{\mathsf{C}}^{\mathsf{H}}(v'_f)$ (see equation (41)). Since the launch node $v_{p_{\mathsf{C}}(v'_f)}$ is fixed in equation (43), the computational complexity of the HDP is $\mathcal{O}(\bar{n}^2)$.

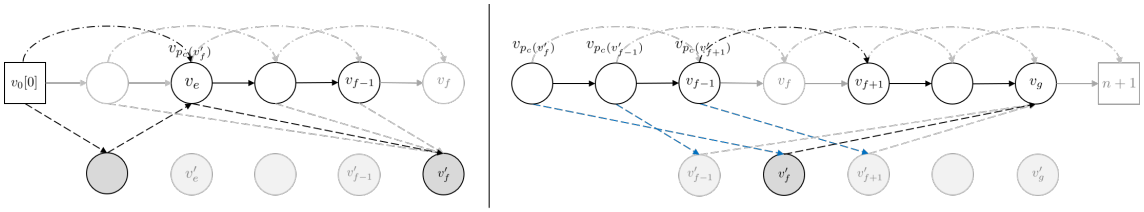

(a) Customer v'_f served by the drone

(b) Customer v_g served by the truck (as the recovery node for the drone)

Figure 4: Illustration of the computation performed in the HDP

The reduced complexity of the HDP, when compared to the EDP, comes at the expense of compromising optimally. There are two main reasons for this. First, a sortie $\langle v_{p_{\mathsf{C}}(v'_f)}, v_f, v_g\rangle$ may not be feasible, thus would be discarded when checking the conditions (38b)–(38d) in equation (41). However, there may exist a feasible drone sortie $\langle v_l, v_f, v_g\rangle$ with $v_l \neq v_{p_{\mathsf{C}}(v'_f)}$, which was eliminated in the computation of $\omega_{\mathsf{C}}^{\mathsf{H}}(v'_f)$ in equation (42). The second reason for the HDP not finding an optimal solution is due to the fact that while $\langle v_{p_{\mathsf{C}}(v'_f)}, v_f, v_g\rangle$ may be feasible, there may exist an alternative drone sortie $\langle v_l, v_f, v_g\rangle$ with $v_l \neq v_{p_{\mathsf{C}}(v'_f)}$

with a lower cost. This comes from the fact that $\omega^{\mathsf{H}}_{\mathsf{C}}(v'_f)$ is computed without knowing where the drone will be recovered.

4.2.2 FRDDP-M

In this section, we formulate an HDP for the FRDDP-M in equations (44) and (45) that share similar ideas with the ones introduced in Section 4.2.1. We define $\omega^{\mathsf{H}}_{\mathsf{M}}(v_g)$ as the minimum makespan up to node v_g when visited by a truck and the drone is either on the truck when arriving at v_g or has just been recovered at v_g, and denote by $p_{\mathsf{M}}(v'_f)$ the index of the launch node leading to the minimum makespan at v'_f.

Different from the HDP for the FRDDP-C, the estimation of the minimum makespan at node v'_f is computed by considering each possible previous node v_e in $\mathcal{R}$ to find the one that minimizes the maximum between the arrival time of the drone at customer v'_f and the arrival time of the truck at node v_{f-1}. This computation is only performed to fix the launch node $v_{p_{\mathsf{M}}(v'_f)}$ of the drone when it serves customer v_f (in equation (45)). When computing $\omega^{\mathsf{H}}_{\mathsf{M}}(v_g)$ for the case where the drone is recovered at v_g after serving customer v'_f, we add to $\omega^{\mathsf{H}}_{\mathsf{M}}(v_{p_{\mathsf{M}}(v'_f)})$ the maximum between the travel time of the truck and the travel time of the drone between the launch node $v_{p_{\mathsf{M}}(v'_f)}$ and v_g, along with the launch time and the recovery time. The computational complexity of this HDP is $\mathcal{O}(\bar{n}^2)$. Its heuristic nature stems from the same reasons discussed in Section 4.2.1.

$$\omega^{\mathsf{H}}_{\mathsf{M}}(v_g) = \begin{cases} 0 & g = 0 \\ \tau_{01} & g = 1 \\ \min\Big\{\omega^{\mathsf{H}}_{\mathsf{M}}(v_{g-1}) + T_{g-1,g},\ \min\limits_{v'_f:\langle v_{p_{\mathsf{M}}(v'_f)}, v_f, v_g\rangle \text{ satisfies (38b)–(38d)}} \Big\{\omega^{\mathsf{H}}_{\mathsf{M}}(v_{p_{\mathsf{M}}(v'_f)}) + \\ \quad \widehat{\tau} + \max\{\tau'_{p_{\mathsf{M}}(v'_f),f} + s'_f + \tau'_{fg}, T_{p_{\mathsf{M}}(v'_f),f-1} + s_{f-1} + \tau_{f-1,f+1} + T_{f+1,g}\} + \breve{\tau}\Big\}\Big\} & g \in \{2,...,\bar{n}\} \end{cases} \tag{44}$$

$$\text{where} \quad p_{\mathsf{M}}(v'_f) = \underset{e:(v_e,v'_f)\in\mathcal{A}_{\mathcal{R}}}{\arg\min} \Big\{\omega^{\mathsf{H}}_{\mathsf{M}}(v_e) + \widehat{\tau} + \max\Big\{\tau'_{ef}, T_{e,f-1}\Big\}\Big\} \qquad v'_f \in \mathcal{R}' \tag{45}$$

5 Solution Method

We propose an HVNS heuristic to solve different versions of the VRPD. The general scheme of the algorithm is described in Section 5.1. The basic structure of our HVNS is a VNS, which combines diversification by a perturbation procedure (usually known as shaking) and intensification by a local search mechanism (Mladenović and Hansen, 1997). Our shaking phase (Section 5.2) is performed through the use of destroy and repair operators. Our local search (Section 5.3) is a VND method with seven neighborhoods. Throughout the algorithm, we evaluate solutions via the HDP described in Section 4. To further accelerate the algorithm, we introduce a subHDP procedure that is used to filter non-promising moves (Section 5.4). Furthermore, to avoid being trapped in a local optimum, we use a simulated annealing acceptance criterion (in the supplementary material).

In the HVNS, we represent a VRPD solution using the concept of truck routes and complete routes introduced in Section 4. Specifically, we define a *truck solution* and a *complete solution* of the VRPD as $\mathcal{S} = \{\mathcal{R}_1, \mathcal{R}_2, ..., \mathcal{R}_{|\mathcal{H}|}\}$ and $\overline{\mathcal{S}} = \{\overline{\mathcal{R}}_1, \overline{\mathcal{R}}_2, ..., \overline{\mathcal{R}}_{|\mathcal{H}|}\}$ where $\mathcal{R}_l$ and $\overline{\mathcal{R}}_l$ are respectively the l-th truck route and complete route.

5.1 HVNS framework

Algorithm 1 outlines the general framework of the HVNS. The algorithm is initialized with a nearest neighborhood heuristic to generate a truck solution $\mathcal{S}$ (line 2). We build each truck route $\mathcal{R} \in \mathcal{S}$ by first selecting the nearest unvisited customer to the depot, and by then iteratively inserting the nearest unvisited customer as long as neither the working duration nor the capacity of the truck is violated. After $\mathcal{S}$ is generated, we initialize λ, a parameter in the VND to determine whether we should consider a move or not (see details in Section 5.3). We solve the FRDDP using the HDP for each truck route in $\mathcal{S}$ to obtain the initial complete solution $\overline{\mathcal{S}}$ (line 3). In the first iteration of the algorithm (line 6–7), the HVNS calls the VND to improve the complete solution $\overline{\mathcal{S}}$ and obtains the value of λ^{avg} and λ^{max}, which determine the range of λ. In the remaining iterations, the HVNS first perturbs the incumbent complete solution $\overline{\mathcal{S}}$ with a `Shaking` procedure that generates a new truck solution $\mathcal{S}^{\mathsf{SH}}$ (line 9). Then, it obtains a new complete solution $\overline{\mathcal{S}}^{\mathsf{SH}}$ by running the `HDP` procedure to insert drone dispatches in $\mathcal{S}^{\mathsf{SH}}$ (line 10). From this solution, the algorithm gets a new local optimal truck solution $\mathcal{S}^{\mathsf{VND}}$ using the VND (line 11). The `EDP` procedure uses the EDP to optimally insert drone dispatches and get a complete solution $\overline{\mathcal{S}}^{\mathsf{VND}}$ (line 12). To increase diversification, we use an acceptance criterion based on simulated annealing (SA) with a parameter κ representing the non-improved times of iteration, which is also used to update the parameter λ (line 13). The algorithm iterates until the maximum time limit $\mathsf{T}^{\mathsf{max}}$ is reached, or the maximum iteration number $\mathsf{I}^{\mathsf{max}}$ is reached. In the entire algorithm, we denote the current computational time by T, which is initialized at the beginning of the HVNS.

Algorithm 1: The framework of the HVNS algorithm

Data: Maximum time limit $\mathsf{T}^{\mathsf{max}}$, maximum iteration number $\mathsf{I}^{\mathsf{max}}$

1 $\mathsf{T} \leftarrow 0, \mathsf{I} \leftarrow 0, \overline{\mathcal{S}}^{*} \leftarrow \varnothing$;
2 Generate an initial truck solution $\mathcal{S}$ with a nearest neighborhood heuristic, initialize λ ;
3 $\overline{\mathcal{S}} \leftarrow$ `HDP` $(\mathcal{S})$;
4 $\kappa \leftarrow 0, \overline{\mathcal{S}}^{*} \leftarrow \overline{\mathcal{S}}$;
5 **while** $\mathsf{T} \leqslant \mathsf{T}^{\mathsf{max}}$ *or* $\mathsf{I} \leqslant \mathsf{I}^{\mathsf{max}}$ **do**
6 **if** $\mathsf{I} = 0$ **then**
7 $(\mathcal{S}^{\mathsf{VND}}, \lambda^{\mathsf{avg}}, \lambda^{\mathsf{max}}) \leftarrow$ `VariableNeighborhoodDescent`$(\mathcal{S}, \overline{\mathcal{S}}, \lambda, \mathsf{I}, \mathsf{T})$; ▷ see Section 5.3, Algorithm 2
8 **else**
9 $\mathcal{S}^{\mathsf{SH}} \leftarrow$ `Shaking`$(\overline{\mathcal{S}})$; ▷ see Section 5.2
10 $\overline{\mathcal{S}}^{\mathsf{SH}} \leftarrow$ `HDP` $(\mathcal{S}^{\mathsf{SH}})$;
11 $(\mathcal{S}^{\mathsf{VND}}, \lambda^{\mathsf{avg}}, \lambda^{\mathsf{max}}) \leftarrow$ `VariableNeighborhoodDescent`$(\mathcal{S}^{\mathsf{SH}}, \overline{\mathcal{S}}^{\mathsf{SH}}, \lambda, \mathsf{I}, \mathsf{T})$; ▷ see Section 5.3, Algorithm 2
12 $\overline{\mathcal{S}}^{\mathsf{VND}} \leftarrow$ `EDP` $(\mathcal{S}^{\mathsf{VND}})$;
13 $(\overline{\mathcal{S}}, \overline{\mathcal{S}}^{*}, \lambda, \kappa) \leftarrow$ `SA AcceptanceCriterion`$(\overline{\mathcal{S}}, \overline{\mathcal{S}}^{*}, \overline{\mathcal{S}}^{\mathsf{VND}}, \lambda, \lambda^{\mathsf{avg}}, \lambda^{\mathsf{max}}, \kappa)$; ▷ see Algorithm 4 in the supplementary material
14 $\mathsf{I} \leftarrow \mathsf{I} + 1$;

Result: $\overline{\mathcal{S}}^{*}$

5.2 Shaking

The shaking phase borrows the ideas of destroying and repairing solutions from the LNS literature. We define six destroy operators to remove customers from the given incumbent complete solution $\overline{\mathcal{S}}$ and three repair operators to insert those customers to form a new truck solution $\mathcal{S}^{\mathsf{SH}}$. We also use an operator to

split one route into two.

Among the six destroy operators in our algorithm, the first four are widely used in the VRP literature (e.g., Demir et al. (2012); Macrina et al. (2019); Chen et al. (2021)), whereas the last two are specific for the VRPD and are adapted from Kitjacharoenchai et al. (2020). Each time the HVNS calls `Shaking` (Algorithm 1, line 9), a destroy operator is randomly chosen with an equal probability. The destroy phase takes a complete solution as input and returns a partial truck solution by removing customers from the incumbent complete solution and storing them in a removal list $\mathcal{L}$.

We define two types of destroy operators. The first type removes β customers according to a certain predefined order. If a removed customer is a launch node or a recovery node in a drone sortie, then the corresponding drone-served customer in this sortie is also removed. The second type removes all customers that meet a predefined criterion. The six destroy operators are as follows.

1. **Random destroy** This operator randomly removes customers from $\mathcal{S}$ until β customers have been removed.

2. **Worst travel time destroy** This operator aims at removing customers that incur high truck travel times given their current position in a route. For this purpose, we sort all truck travel arcs in $\overline{\mathcal{S}}$ in descending order with respect to their travel time. We then iterate through these arcs and delete customers at their head and tail until β customers have been removed.

3. **Cluster destroy** This operator randomly selects a seed customer, removes it first, and then removes the $\beta - 1$ customers that can be reached from the seed customer with the least truck travel time.

4. **One route destroy** This operator removes all the customers of the truck route with the fewest customers in solution $\overline{\mathcal{S}}$.

5. **Drone destroy** This operator removes all drone-served customers in the complete solution $\overline{\mathcal{S}}$.

6. **Worst waiting-time destroy** Since the truck and the drone may wait for each other at a recovery node, this operator focuses on drone sorties that result in the longest waiting times. For this purpose, we sort all drone sorties in $\overline{\mathcal{S}}$ in descending order of their waiting time. We then iterate through these drone sorties and delete customers until β customers have been deleted. For a chosen drone sortie $\langle i, j, k \rangle$ where $i, k \in \mathcal{C}$, this operator removes not only the nodes i, j, and k, but also all customers served by the truck between i and k.

After the destroy phase removes a set $\mathcal{L}$ of customers, the repair phase inserts these customers into the partial truck solution $\mathcal{S}$ to form a new truck solution $\mathcal{S}^{\mathsf{SH}}$. We define three repair operators. The `Shaking` procedure randomly selects one of them with an equal probability. As long as $\mathcal{L}$ is not empty, the repair operator randomly removes one customer i from $\mathcal{L}$ and then inserts it to a specific position in the partial truck solution $\mathcal{S}$. The three repair operators are as follows.

1. **Random repair** This operator inserts i at a random position in $\mathcal{S}$.

2. **Least travel time repair** This operator inserts i in a position with the least increase in travel time, i.e., $\tau_{ji} + \tau_{ik} - \tau_{jk}$ for every arc (j, k) in $\mathcal{S}$.

3. **Nearest polar angle repair** Let a_l be the polar angle of a customer l. This operator inserts i after customer $j = \arg\min_{l \in \mathcal{C} \setminus \mathcal{L}} \{|a_i - a_l|\}$ in $\mathcal{S}$.

In some cases, creating an additional route lowers the value of the objective function. The split operator randomly selects one truck route, then splits it into two truck routes in a random position. If the incumbent best solution in the HVNS has not been improved during the last κ iterations, the `Shaking` procedure calls the split operator after the repair operators have built a new truck solution.

5.3 Variable neighborhood descent

The VND relies on a list of neighborhoods $(\mathcal{K}_\vartheta)_{\vartheta=1,\dots,\vartheta_{max}}$. Its general scheme is presented in Algorithm 2. At each iteration, a new solution is generated by calling the procedure `Search` (line 4) considering the ϑ-th neighborhood. As soon as an improved neighboring solution (with respect to $\mathcal{S}^{\mathsf{inc}}$) is found, the procedure `Search` stops searching the current neighborhood and restarts the search with $\mathcal{K}_1$ (line 6). Otherwise, the VND moves to the next neighborhood $\mathcal{K}_{\vartheta+1}$ (line 9). A local optimum is reached when the last neighborhood fails to improve the incumbent solution. During the VND, we may accept an improving infeasible solution (i.e., a complete solution having at least one complete route whose total working duration exceeds the maximum working duration). For this reason, we store every improving feasible (truck) solution returned by the procedure `Search` (line 7).

Algorithm 2: VariableNeighborhoodDescent$(\mathcal{S}^{\mathsf{inc}}, \overline{\mathcal{S}}^{\mathsf{inc}}, \lambda, \mathsf{I}, \mathsf{T})$

Data: An incumbent truck solution $\mathcal{S}^{\mathsf{inc}}$, its corresponding complete solution $\overline{\mathcal{S}}^{\mathsf{inc}}$, a working duration variation threshold λ, the HVNS iteration number I, the current computational time T, the maximum time limit $\mathsf{T}^{\mathsf{max}}$, the list of neighborhoods $(\mathcal{K}_\vartheta)_{\vartheta=1,\dots,\vartheta_{max}}$

1 $\vartheta \leftarrow 1, \mathcal{S}^{\mathsf{feas}} \leftarrow \mathcal{S}^{\mathsf{inc}}$;
2 **if** $\mathsf{I} = 0$ **then** $\lambda^{\mathsf{avg}} \leftarrow 0, \lambda^{\mathsf{max}} \leftarrow 0$;
3 **while** $\vartheta \leqslant |\mathcal{K}|$ *or* $\mathsf{T} \leqslant \mathsf{T}^{\mathsf{max}}$ **do**
4 $\quad (\mathcal{S}^{\mathsf{new}}, \overline{\mathcal{S}}^{\mathsf{new}}, \lambda^{\mathsf{avg}}, \lambda^{\mathsf{max}}, \mathit{improved}) \leftarrow$ `Search`$(\mathcal{S}^{\mathsf{inc}}, \overline{\mathcal{S}}^{\mathsf{inc}}, \lambda, \lambda^{\mathsf{avg}}, \lambda^{\mathsf{max}}, \mathsf{I}, \mathcal{K}_\vartheta)$; ▷ see Algorithm 3
5 $\quad$ **if** *improved* **then**
6 $\quad\quad \mathcal{S}^{\mathsf{inc}} \leftarrow \mathcal{S}^{\mathsf{new}}, \overline{\mathcal{S}}^{\mathsf{inc}} \leftarrow \overline{\mathcal{S}}^{\mathsf{new}}, \vartheta \leftarrow 1$;
7 $\quad\quad$ **if** $\overline{\mathcal{S}}^{\mathsf{new}}$ *is feasible* **then** $\mathcal{S}^{\mathsf{feas}} \leftarrow \mathcal{S}^{\mathsf{new}}$;
8 $\quad$ **else**
9 $\quad\quad \vartheta \leftarrow \vartheta + 1$;

Result: $\mathcal{S}^{\mathsf{feas}}, \lambda^{\mathsf{avg}}, \lambda^{\mathsf{max}}$

We use seven local search operators that are based either on intra-route moves or on inter-route moves. The moves are defined for solutions represented as truck solutions. Five of them are well-known for solving VRPs (e.g., (Vidal, 2022)), and include the inter-route and intra-route versions of 1-1 swap (exchanging two nodes) and 2-opt (exchanging two arcs in the route, which corresponds to reverse a section of the sequence), and the intra-route version of 1-0 relocate (removing a node and reinserting it in a different position). The remaining two neighborhoods are drone-related: 3-1 swap and 3-0 relocate. Rather than moving a single node, they move together three consecutive nodes i, j and k of a truck route with the condition that $\langle i, j, k \rangle$ is a drone sortie in the incumbent complete solution. The 3-1 swap neighborhood exchanges a single node and a drone sortie that belongs to the same route. Similarly, the 3-0 relocate neighborhood moves a drone sortie to another position in the same route.

We present our `Search` procedure in Algorithm 3. Specifically, we differentiate between inter-route moves (line 2–13) and intra-route moves (line 14–24). The general scheme is the same for both types of moves, except that for an inter-route move the total customer demand within each route is checked first (line 4). Given an incumbent solution $\mathcal{S}^{\mathsf{inc}}$, we define a *neighboring truck route* as a truck route resulting from a move an incumbent route $\mathcal{R}^{\mathsf{inc}} \in \mathcal{S}^{\mathsf{inc}}$. We refer to every inter-route move as a pair of neighboring truck routes $(\mathcal{R}_1^{\mathsf{new}}, \mathcal{R}_2^{\mathsf{new}})$ generated from a pair of truck routes $(\mathcal{R}_1^{\mathsf{inc}}, \mathcal{R}_2^{\mathsf{inc}})$ in $\mathcal{S}^{\mathsf{inc}}$. Similarly, we refer to every intra-route move as a single neighboring truck route $\mathcal{R}^{\mathsf{new}}$ generated from a truck route $\mathcal{R}^{\mathsf{inc}}$ in $\mathcal{S}^{\mathsf{inc}}$.

Given an intra-route move, for each neighboring truck route $\mathcal{R}^{\mathsf{new}}$ from $\mathcal{R}^{\mathsf{inc}}$, we compute the total

working duration $T_{\mathcal{R}^{\text{new}}}$ required by the truck to serve all customers as $T_{\mathcal{R}^{\text{new}}} = \sum_{(i,j)\in\mathcal{R}^{\text{new}}}(s_i + \tau_{ij})$. Truck routes are likely to have drone sorties in the complete solution. Since $\widehat{\tau}$ and $\breve{\tau}$ are usually negligible compared to the travel times and as serving a customer by a drone is generally faster than serving it by the truck, adding drone sorties generally reduces the total working duration. For this reason, we allow the working duration of each route to become greater than T, but not greater than μT, with $\mu \geqslant 1$ (lines 5 and 16). However, we limit the working duration variation $T_{\mathcal{R}^{\text{new}}} - T_{\mathcal{R}^{\text{inc}}}$ by λ (lines 6 and 17). This parameter is initialized in Algorithm 1 (line 2). Specifically, λ is initialized by multiplying the longest route working duration in $\mathcal{S}$ by λ_0. In $\mathsf{I} = 0$ (Algorithm 1, line 7), we store the maximum working duration variation λ^{max} and an average working duration variation λ^{avg} by accounting for all working duration variations associated with improving moves in Algorithm 3 (lines 11 and 22). We use ς to count the number of improving solutions computed in the VND. Each time an improving solution is found, `Search` stops and returns it.

Algorithm 3: Search$(\mathcal{S}^{\text{inc}}, \overline{\mathcal{S}}^{\text{inc}}, \lambda, \lambda^{\text{avg}}, \lambda^{\text{max}}, \mathsf{I}, \mathcal{K}_\vartheta)$

Data: Incumbent truck solution $\mathcal{S}^{\text{inc}}$, its complete solution $\overline{\mathcal{S}}^{\text{inc}}$, duration threshold μ, duration variation threshold λ, the average duration variation threshold λ^{avg}, the maximum duration variation threshold λ^{max}, the current iteration number I, a neighborhood $\mathcal{K}_\vartheta$, a search counter ς

1 $improved \leftarrow \mathsf{false}, \varsigma \leftarrow 0, \mathcal{S}^{\text{new}} \leftarrow \mathcal{S}^{\text{inc}}, \overline{\mathcal{S}}^{\text{new}} \leftarrow \overline{\mathcal{S}}^{\text{inc}}$;
2 **if** $\mathcal{K}_\vartheta$ *defines inter-route moves* **then**
3 **for** *each pair of neighborhood truck route* $(\mathcal{R}_1^{\text{new}}, \mathcal{R}_2^{\text{new}})$ *generated from* $(\mathcal{R}_1^{\text{inc}}, \mathcal{R}_2^{\text{inc}}) \in \mathcal{S}^{\text{inc}}$ **do**
4 **if** $\sum_{i\in\mathcal{R}_1^{\text{new}}} q_i \leqslant Q$ *and* $\sum_{i\in\mathcal{R}_2^{\text{new}}} q_i \leqslant Q$ **then**
5 **if** $T_{\mathcal{R}_1^{\text{new}}} \leqslant \mu T$ *and* $T_{\mathcal{R}_2^{\text{new}}} \leqslant \mu T$ **then**
6 **if** $T_{\mathcal{R}_1^{\text{new}}} - T_{\mathcal{R}_1^{\text{inc}}} \leqslant \lambda$ *or* $T_{\mathcal{R}_2^{\text{new}}} - T_{\mathcal{R}_2^{\text{inc}}} \leqslant \lambda$ **then**
7 **if** `subHDP` $(\mathcal{R}_1^{\text{new}}, \mathcal{R}_1^{\text{inc}})$+`subHDP` $(\mathcal{R}_2^{\text{new}}, \mathcal{R}_2^{\text{inc}}) < 0$ **then**
8 $\overline{\mathcal{R}}_1^{\text{new}} \leftarrow$ `HDP`$(\mathcal{R}_1^{\text{new}}), \overline{\mathcal{R}}_2^{\text{new}} \leftarrow$ `HDP`$(\mathcal{R}_2^{\text{new}})$;
9 **if** $f(\overline{\mathcal{R}}_1^{\text{new}}) + f(\overline{\mathcal{R}}_2^{\text{new}}) < f(\overline{\mathcal{R}}_1^{\text{inc}}) + f(\overline{\mathcal{R}}_2^{\text{inc}})$ **then**
10 $\overline{\mathcal{S}}^{\text{new}} \leftarrow \overline{\mathcal{R}}_1^{\text{new}} \cup \overline{\mathcal{R}}_2^{\text{new}} \cup \overline{\mathcal{S}}^{\text{inc}} \backslash \{\overline{\mathcal{R}}_1^{\text{inc}}, \overline{\mathcal{R}}_2^{\text{inc}}\}, \mathcal{S}^{\text{new}} \leftarrow \mathcal{R}_1^{\text{new}} \cup \mathcal{R}_2^{\text{new}} \cup \mathcal{S}^{\text{inc}} \backslash \{\mathcal{R}_1^{\text{inc}}, \mathcal{R}_2^{\text{inc}}\}$;
11 **if** $\mathsf{I} = 0$ **then** update λ^{max}, $\lambda^{\text{avg}} \leftarrow \big(\lambda^{\text{avg}}\varsigma + (T_{\mathcal{R}_1^{\text{new}}} - T_{\mathcal{R}_1^{\text{inc}}}) + (T_{\mathcal{R}_2^{\text{new}}} - T_{\mathcal{R}_2^{\text{inc}}})\big)/(\varsigma + 2), \varsigma \leftarrow \varsigma + 2$;
12 **else** $\lambda^{\text{avg}} \leftarrow \lambda$;
13 $improved \leftarrow \mathsf{true}$; **break**;
14 **else if** $\mathcal{K}_\vartheta$ *defines intra-route moves* **then**
15 **for** *each neighborhood truck route* $\mathcal{R}^{\text{new}}$ *generated from* $\mathcal{R}^{\text{inc}} \in \mathcal{S}^{\text{inc}}$ **do**
16 **if** $T_{\mathcal{R}^{\text{new}}} \leqslant \mu T$ **then**
17 **if** $T_{\mathcal{R}^{\text{new}}} - T_{\mathcal{R}^{\text{inc}}} \leqslant \lambda$ **then**
18 **if** `subHDP` $(\mathcal{R}^{\text{new}}, \mathcal{R}^{\text{inc}}) < 0$ **then**
19 $\overline{\mathcal{R}}^{\text{new}} \leftarrow$ `HDP` $(\mathcal{R}^{\text{new}})$;
20 **if** $f(\overline{\mathcal{R}}^{\text{new}}) < f(\overline{\mathcal{R}}^{\text{inc}})$ **then**
21 $\overline{\mathcal{S}}^{\text{new}} \leftarrow \overline{\mathcal{R}}^{\text{new}} \cup \overline{\mathcal{S}}^{\text{inc}} \backslash \{\overline{\mathcal{R}}^{\text{inc}}\}; \mathcal{S}^{\text{new}} \leftarrow \mathcal{R}^{\text{new}} \cup \mathcal{S}^{\text{inc}} \backslash \{\mathcal{R}^{\text{inc}}\}$;
22 **if** $\mathsf{I} = 0$ **then** update λ^{max}, $\lambda^{\text{avg}} \leftarrow \big(\lambda^{\text{avg}}\varsigma + (T_{\mathcal{R}^{\text{new}}} - T_{\mathcal{R}^{\text{inc}}})\big)/(\varsigma + 1), \varsigma \leftarrow \varsigma + 1$;
23 **else** $\lambda^{\text{avg}} \leftarrow \lambda$;
24 $improved \leftarrow \mathsf{true}$; **break**;

Result: $\mathcal{S}^{\text{new}}, \overline{\mathcal{S}}^{\text{new}}, \lambda^{\text{avg}}, \lambda^{\text{max}}, improved$

5.4 Filtering moves with a sub-heuristic dynamic program

Although our HDP is an order of magnitude faster than the EDP, calling the HDP at each search move, where λ is respected, is computationally expensive. In this section, we develop a more time-efficient subHDP based on the HDP to approximate the potential objective function value savings of a move. If the value of savings is negative, we reevaluate the move using the HDP.

Given a neighboring truck route $\mathcal{R}^{\mathsf{new}}$ of $\mathcal{R}^{\mathsf{inc}} \in \mathcal{S}^{\mathsf{inc}}$, we extract a number of consecutive nodes from $\mathcal{R}^{\mathsf{new}}$, which we refer to as a *subroute*. The subHDP calculates an approximation of the objective function value savings induced by the subroute. The general scheme of the subHDP is as follows: for an inter-route (resp. intra-route) move: 1) Create one subroute (resp. one or two subroutes) for each of the two neighboring truck routes (resp. for the single neighboring truck route); 2) Calculate the objective function value for each created subroute; 3) Calculate the approximate savings induced by the move.

As the extracted number of consecutive nodes from $\mathcal{R}^{\mathsf{new}}$ may lead to overlaps, we distinguish between two cases. The case where a move results in inconsecutive node changes in a route, and the case where a move results in consecutive node changes in a route. In the first case, two subroutes are created, whereas in the second case, a single subroute is created. The former is always the case for inter-route operators. Figure 5 shows two different examples of an intra-route 3-1 swap move: three consecutive nodes that form a drone sortie in the incumbent complete route $\overline{\mathcal{R}}^{\mathsf{inc}}$ (marked with dark gray) and a node (marked with light gray), where the index of each customer is in the brackets. In Figure 5 (a), the move results in node changes with two components because the node 1 and nodes $3, 5, 11$ are not consecutive in the new truck route $\mathcal{R}^{\mathsf{new}}$. But in Figure 5 (b), despite that the move changes two groups of nodes, the node 13 and nodes $3, 5, 11$ are consecutive, merging the two components into one.

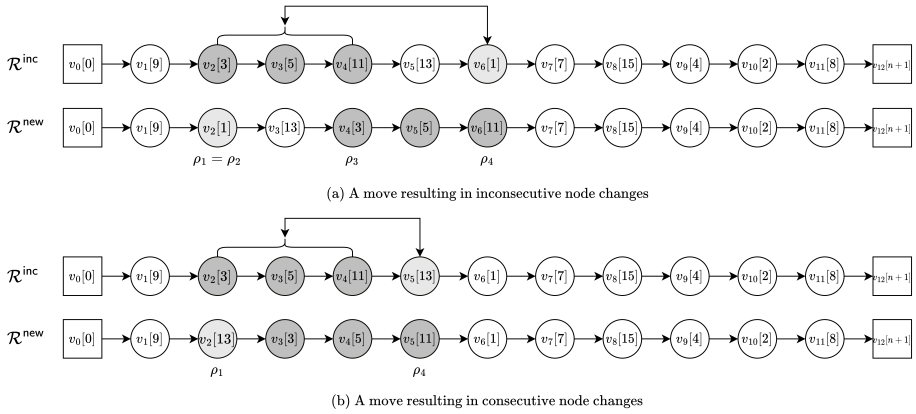

(a) A move resulting in inconsecutive node changes

(b) A move resulting in consecutive node changes

Figure 5: Move component illustration

To create subroutes from a neighboring truck route $\mathcal{R}^{\mathsf{new}}$, we define ρ_1 (resp. ρ_3) and ρ_2 (resp. ρ_4) as the starting position and the ending position of the first component (resp. second component) in $\mathcal{R}^{\mathsf{new}}$ when the move results in inconsecutive node changes. If there is only one node included in a component, then $\rho_1 = \rho_2, \rho_3 = \rho_4$. For example, in Figure 5 (a), $\rho_1 = \rho_2 = 2, \rho_3 = 4, \rho_4 = 6$. If the move results in consecutive node changes, we discard ρ_2 and ρ_3. In Figure 5 (b), $\rho_1 = 2, \rho_4 = 5$. In addition, we define $\underline{\varepsilon}$ as the number of nodes to be considered after ρ_2 (or ρ_4) in the subroute of $\mathcal{R}^{\mathsf{new}}$.

We first present the case where we generate a single subroute SR from a neighboring truck route $\mathcal{R}^{\mathsf{new}}$.

Let n^{new} be the number of customers in $\mathcal{R}^{\mathsf{new}}$. We define the subroute $\mathsf{SR} = (v_{\rho_1-\eta_1}, ..., v_{\rho_1}, ..., v_{\rho_4}, ..., v_{\rho_4+\eta_4})$ from $\mathcal{R}^{\mathsf{new}}$, where $\eta_1 = \max\{\rho_1, \overline{\varepsilon}\}$ with $\overline{\varepsilon}$ the number of consecutive customers before position $\max\{0, \rho_1\}$ that cannot be reached by a drone, and $\eta_4 = \min\{\underline{\varepsilon}, n^{\mathsf{new}} + 1 - \rho_4\}$. More precisely, if there are not enough $\overline{\varepsilon}$ (resp. $\underline{\varepsilon}$) customers before ρ_1 (resp. after ρ_4), then we include all of them in SR. For the particular move in Figure 6, assume that $\overline{\varepsilon} = 1$, and $\underline{\varepsilon} = 3$, we have $\mathsf{SR} = (9, 1, 13, 3, 5, 11, 7, 15, 4)$.

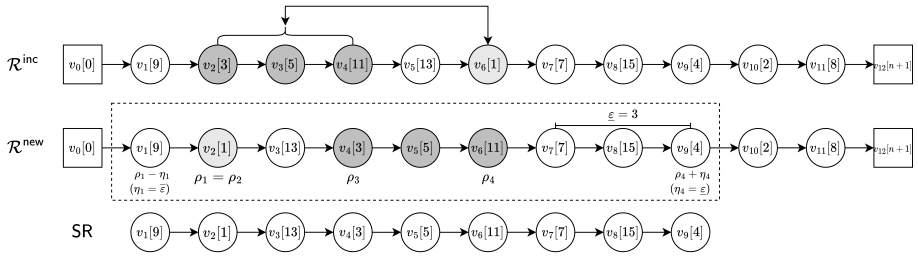

Figure 6: An example of creating a subroute

We generate two subroutes $\mathsf{SR}_1 = (v_{\rho_1-\eta_1}, ..., v_{\rho_1}, ..., v_{\rho_2}, ..., v_{\rho_2+\eta_2})$ and $\mathsf{SR}_2 = (v_{\rho_3-\eta_3}, ..., v_{\rho_3}, ..., v_{\rho_4}, ..., v_{\rho_4+\eta_4})$ for $\mathcal{R}^{\mathsf{new}}$ if the two components are very distanced. To do so, we define Ψ as a parameter to determine whether to split the subroute into two and check if the following condition $\rho_2 + \eta_2 + \Psi < \rho_3 - \eta_3$ is satisfied. Figure 7 shows an example of creating two subroutes when $\Psi = 1$ (the values of other parameters are the same as in Figure 6.)

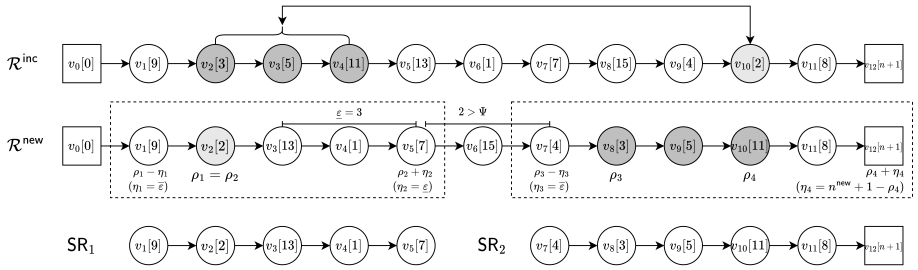

Figure 7: An example of creating two subroutes

To calculate the objective function value of a subroute $(v_{\rho-\eta}, ..., v_{\rho}, ..., v_{\rho'}, ..., v_{\rho'+\eta'})$ in $\mathcal{R}^{\mathsf{new}}$ with $(\rho, \eta, \rho', \eta') \in \{(\rho_1, \eta_1, \rho_4, \eta_4), (\rho_1, \eta_1, \rho_2, \eta_2), (\rho_3, \eta_3, \rho_4, \eta_4)\}$, we adapt the computation performed for the HDP, which is the core of the subHDP, as shown in equations (46)–(50). We denote by $\mathcal{R}^{\mathsf{new}'}$ the set of customers that can be served by the drone in $\mathcal{R}^{\mathsf{new}}$, and denote by $\mathcal{A}_{\mathcal{R}^{\mathsf{new}}}$ the arc set in $\mathcal{G}_{\mathcal{R}^{\mathsf{new}}}$. In (46)–(48) for the FRDDP-C, $\widetilde{\omega}_{\mathsf{C}}(v_g)$ is the approximate minimum cost up to the truck-visited node v_g, $\widetilde{\omega}_{\mathsf{C}}(v'_f)$ is the approximate minimum cost up to the drone-served customer v'_f taking into account that the truck is traveling to v_{f-1}, and $\widetilde{p}_{\mathsf{C}}(v'_f)$ the index of the node that leads to the minimum cost when computing $\widetilde{\omega}_{\mathsf{C}}(v'_f)$. In equations (49) and (50) for the FRDDP-M, $\widetilde{\omega}_{\mathsf{M}}(v_g)$ is the approximate minimum makespan up to the truck-visited node v_g, and $\widetilde{p}_{\mathsf{M}}(v'_f)$ is the index of the launch node that leads to the approximate minimum makespan at the drone-served customer v'_f. It is important to note that the values $\omega^{\mathsf{H}}_{\mathsf{C}}(v_g)$, $\omega^{\mathsf{H}}_{\mathsf{C}}(v'_f)$, $p_{\mathsf{C}}(v'_f)$, $\omega^{\mathsf{H}}_{\mathsf{M}}(v_g)$, and $p_{\mathsf{M}}(v'_f)$ come from the incumbent truck route $\mathcal{R}^{\mathsf{inc}}$. The computations for a subroute of $\mathcal{R}^{\mathsf{new}}$ are the following.

$$\widetilde{\omega}_{\mathsf{C}}(v_g) = \begin{cases} \omega^{\mathsf{H}}_{\mathsf{C}}(v_g) & g = \rho - \eta \\ \min\Big\{\widetilde{\omega}_{\mathsf{C}}(v_{g-1}) + c_{g-1,g}, & \\ \quad \min\limits_{v'_f : f \geqslant \rho-\eta \wedge \langle v_{\widetilde{p}_{\mathsf{C}}(v'_f)}, v_f, v_g\rangle \text{ satisfies (38b)–(38d)}} \Big\{\widetilde{\omega}_{\mathsf{C}}(v'_f) & \\ \quad + c'_{fg} + c_{f-1,f+1} + C_{f+1,g}\Big\}\Big\} & g \in \{\rho - \eta + 1, ..., \rho' + \eta'\} \end{cases} \tag{46}$$

$$\widetilde{\omega}_{\mathsf{C}}(v'_f) = \begin{cases} \omega^{\mathsf{H}}_{\mathsf{C}}(v'_f) & f = \rho - \eta \\ \min\limits_{v_e : e \geqslant \rho-\eta \wedge (v_e, v'_f) \in \mathcal{A}_{\mathcal{R}^{\mathsf{new}}}} \Big\{\widetilde{\omega}_{\mathsf{C}}(v_e) + c'_{ef} + C_{e,f-1}\Big\} & v'_f \in \mathcal{R}^{\mathsf{new}'} \wedge f \in \{\rho - \eta + 1, ..., \rho' + \eta'\} \end{cases} \tag{47}$$

$$\text{where} \quad \widetilde{p}_{\mathsf{C}}(v'_f) = \begin{cases} p_{\mathsf{C}}(v'_f) & f = \rho - \eta \\ \arg\min\limits_{e : e \geqslant \rho-\eta \wedge (v_e, v'_f) \in \mathcal{A}_{\mathcal{R}^{\mathsf{new}}}} \Big\{\widetilde{\omega}_{\mathsf{C}}(v_e) + c'_{ef} + C_{e,f-1}\Big\} & v'_f \in \mathcal{R}^{\mathsf{new}'} \wedge f \in \{\rho - \eta + 1, ..., \rho' + \eta'\} \end{cases} \tag{48}$$

$$\widetilde{\omega}_{\mathsf{M}}(v_g) = \begin{cases} \omega^{\mathsf{H}}_{\mathsf{M}}(v_g) & g = \rho - \eta \\ \min\Big\{\widetilde{\omega}_{\mathsf{M}}(v_{g-1}) + T_{g-1,g}, & \\ \quad \min\limits_{v'_f : f \geqslant \rho-\eta \wedge \langle v_{\widetilde{p}_{\mathsf{M}}(v'_f)}, v_f, v_g\rangle \text{ satisfies (38b)–(38d)}} \Big\{\widetilde{\omega}_{\mathsf{M}}(v_{\widetilde{p}_{\mathsf{M}}(v'_f)}) + \hat{\tau} + \max\{\tau'_{\widetilde{p}_{\mathsf{M}}(v'_f),f} & \\ \quad + s'_f + \tau'_{fg}, T_{\widetilde{p}_{\mathsf{M}}(v'_f),f-1} + s_{f-1} + \tau_{f-1,f+1} + T_{f+1,g}\} + \check{\tau}\Big\}\Big\} & g \in \{\rho - \eta + 1, ..., \rho' + \eta'\} \end{cases} \tag{49}$$

where

$$\widetilde{p}_{\mathsf{M}}(v'_f) = \begin{cases} p_{\mathsf{M}}(v'_f) & f = \rho - \eta \\ \arg\min\limits_{e : e \geqslant \rho-\eta \wedge (v_e, v'_f) \in \mathcal{A}_{\mathcal{R}^{\mathsf{new}}}} \Big\{\widetilde{\omega}_{\mathsf{M}}(v_e) + \hat{\tau} + \max\Big\{\tau'_{ef}, T_{e,f-1}\Big\}\Big\} & v'_f \in \mathcal{R}^{\mathsf{new}'} \wedge f \in \{\rho - \eta + 1, ..., \rho' + \eta'\} \end{cases} \tag{50}$$

Finally, we compute the approximate saving induced by the neighboring truck route $\mathcal{R}^{\mathsf{new}}$ generated from $\mathcal{R}^{\mathsf{inc}}$. This saving, denoted by $\mathtt{subHDP}(\mathcal{R}^{\mathsf{new}}, \mathcal{R}^{\mathsf{inc}})$ (Algorithm 3, line 7 and 18), is calculated in formulation (51) when we have one subroute, and in formulation (52) when we have two subroutes.

$$\mathtt{subHDP}(\mathcal{R}^{\mathsf{new}}, \mathcal{R}^{\mathsf{inc}}) = (\widetilde{\omega}_{\mathsf{C}}(v_{\rho_4+\eta_4}) - \widetilde{\omega}_{\mathsf{C}}(v_{\rho_1-\eta_1})) - (\omega^{\mathsf{H}}_{\mathsf{C}}(v_{\rho_4+\eta_4}) - \omega^{\mathsf{H}}_{\mathsf{C}}(v_{\rho_1-\eta_1})) \tag{51}$$

$$\begin{aligned} \mathtt{subHDP}(\mathcal{R}^{\mathsf{new}}, \mathcal{R}^{\mathsf{inc}}) = {} & (\widetilde{\omega}_{\mathsf{C}}(v_{\rho_2+\eta_2}) - \widetilde{\omega}_{\mathsf{C}}(v_{\rho_1-\eta_1})) - (\omega^{\mathsf{H}}_{\mathsf{C}}(v_{\rho_2+\eta_2}) - \omega^{\mathsf{H}}_{\mathsf{C}}(v_{\rho_1-\eta_1})) \\ & + (\widetilde{\omega}_{\mathsf{C}}(v_{\rho_4+\eta_4}) - \widetilde{\omega}_{\mathsf{C}}(v_{\rho_3-\eta_3})) - (\omega^{\mathsf{H}}_{\mathsf{C}}(v_{\rho_4+\eta_4}) - \omega^{\mathsf{H}}_{\mathsf{C}}(v_{\rho_3-\eta_3})) \end{aligned} \tag{52}$$

6 Computational results

We present a series of computational experiments to test the performance of the HVNS algorithm introduced in Section 5. We first introduce all the data sets we use in Section 6.1. We then compare different configurations of the HVNS to assess the added value of its main algorithmic components in Section 6.2. In Section 6.3, we compare our HVNS with CPLEX on small-sized instances for the VRPD-C, and compare the results obtained by our HVNS with the best-known solutions (BKSs) from the literature.

We coded our HVNS using Java version 18.0.2 and we conducted all experiments on a Linux machine equipped with an Intel Xeon(R) Gold 6226R CPU clocked at 2.90 GHz. We used CPLEX version 12.8

through its Python API to solve the mathematical model presented in Section 3. Table 2 presents the value of the parameters used in our HVNS.

$\mathsf{I}^{\max}$	$\mathsf{T}^{\max}$	μ	β	λ_0	$\underline{\varepsilon}$	Ψ	t^{init}	$\mathsf{N}^{\max}$
10,000	300s	1.3	$U(0.2, 0.3)n$	0.2	5	5	0.004	10

Table 2: Parameters of the HVNS

6.1 Data sets and benchmarks

In this section, we introduce all the data sets that we use in our computational experiments. We also present the benchmarks from the literature against which we compare the results of our HVNS.

There are two data sets we use in Section 6.2 to evaluate different configurations of the HVNS, each corresponding to a different objective. For the VRPD-C, we use the data set introduced by Sacramento et al. (2019). In this data set, there are four sets of 12 instances, each with 6, 10, 12, and 20 customers, and four sets of 16 instances, each with 50, 100, 150, and 200 customers. The problem parameters are as follows: the launch time $\hat{\tau}$ and the recovery time $\check{\tau}$ are both 1 minute. The customer service time of the truck and the drone are 2 minutes and 1 minutes. The speed of the trucks and the drones are 35 mph and 50 mph. The drone flight endurance is 30 minutes. The maximum working duration of each route is 480 minutes. Additionally, the fuel price and consumption of the truck are set to 1.13 €/l and 0.07 l/km. The authors assume that the unit cost of drones is 10% of that of trucks. For the VRPD-M, we use the data set introduced by Bouman et al. (2018b), which contains instances with 4 to 499 customers. In these instances, the drone is twice as fast as the truck on all arcs, i.e., $\alpha = 2$. Similarly to El-Adle et al. (2021) who used this data set, we set the drone flight endurance to 30 minutes. The rest of the parameters are set as 0.

We compare the performance of our HVNS against seven benchmarks from the literature in Section 6.3 (see Table 3 for an overview). For the VRPD-C, we use two benchmarks from Sacramento et al. (2019) and Rave et al. (2022), which we refer to as `SPR` and `RFK`. Both works consider multiple trucks and assume NoLW. Both papers presented an ALNS algorithm and performed computational experiments using the data set introduced by Sacramento et al. (2019). Each instance was run 10 times for 5 minutes.

For the VRPD-M, the first benchmark we compare with is from El-Adle et al. (2021), which we refer to as `EGH`. This work consider a problem with a single truck and a single drone and assumes LW. The problem is formulated with a MIP model enhanced by a series of bound improvement strategies and solved by Gurobi with a time limit of 11,000 seconds (approximately 3.1 hours). The authors generate five groups of 30 instances based on the Bouman et al. (2018b) instances. Specifically, two groups of instances are built by selecting the first 15 and 19 customers of the 19-customer instances, and three groups are built by selecting the first 23, 27, and 31 customers of the 49-customer instances. The next two benchmarks come from Tamke and Buscher (2021), who considered 1 or 2 trucks ($m = 1, 2$), 1 or 2 drones attached to each truck, and the LW assumption. These authors solved the VRPD-M with a branch-and-cut algorithm imposing a time limit of 43,200 seconds (12 hours). For their computational experiments, they took three TSPLIB (Reinelt, 1997) instances: kroA100, kroA200 and kroA300 and selected the first 14, 19, 24, 29 customers to vary the instance size. Since our HVNS cannot handle multiple drones attached to one truck,

we only compare the results they obtained with a single drone attached to each truck. We refer to their benchmarks with one truck and two trucks as `TB1` and `TB2`. The last two benchmarks, denoted `RR-RANGE30` and `RR-MHD`, are two variants of the TSPD tackled by Roberti and Ruthmair (2021), assuming LW and NoLW. The authors proposed a branch-and-price algorithm and imposed a time limit of 3,600 seconds (1 hour) to solve each instance. They used the data set introduced by Poikonen et al. (2019), with 9, 19, 29, and 39 customers (with 75 instances for each customer size). We note that, when solving the VRPD with the LW assumption, condition (38d) is disregarded.

Problem		Benchmark				
		Name	Reference	Method	Time limit	Data set
VRPD-C	NoLW	`SPR` ($m > 1$)	Sacramento et al. (2019)	ALNS	5 minutes (10 runs)	Sacramento et al. (2019)
		`RFK` ($m > 1$)	Rave et al. (2022)			
VRPD-M	LW	`EGH` ($m = 1$)	El-Adle et al. (2021)	MIP model	3.1 hours	Bouman et al. (2018b)
		`TB1` ($m = 1$)	Tamke and Buscher (2021)	Branch-and-cut	12 hours	Reinelt (1997)
		`TB2` ($m = 2$)				
		`RR-RANGE30` ($m = 1$)	Roberti and Ruthmair (2021)	Branch-and-price	1 hour	Poikonen et al. (2019)
	NoLW	`RR-MHD` ($m = 1$)	Roberti and Ruthmair (2021)	Branch-and-price	1 hour	Poikonen et al. (2019)

Table 3: Summary of data sets and benchmarks

In the following sections, for each of our computational experiments, we only present results aggregated according to the number of customers. Detailed results for every single instance are available in the supplementary material.

6.2 Algorithm configuration

In this section, we evaluate the added value of the algorithmic components HDP and subHDP. To this end, we compare the results of our HVNS with two other configurations of the algorithm. In the configuration we call HVNS-NosubHDP we remove filtering moves using the subHDP in Algorithm 3 (lines 7 and 18). In the configuration we call HVNS-EDP we remove filtering moves using the subHDP in Algorithm 3 (lines 7 and 18), and replace all calls to the HDP by a call to the EDP (i.e., we replace the `HDP` by the `EDP` in Algorithms 1 and 3).

To have data sets with a comparable number of customers, we choose instances with 20, 50, 100, 150, and 200 customers from Sacramento et al. (2019) for the VRPD-C, and five sets containing 19, 49, 74, 99, and 174 customers from Bouman et al. (2018b) for the VRPD-M. We run all instances five times, with a time limit $\mathsf{T}^{\max}$ of five minutes and a maximum number of iterations $\mathsf{I}^{\max}$ of 10,000 for each run.

Table 4 and Table 5 compare the three algorithmic configurations for the VRPD-C and VRPD-M. For each algorithm configuration, given the number of customers and the associated number of instances, these two tables report the average objective values ($\overline{\text{Obj}}$), the average number of iterations (Ite), and the average computational times (Time (s)) computed over the five runs. The column Obj* shows the best average objective values among the three configurations, that is the minimum one among the three $\overline{\text{Obj}}$. For each configuration, the column $\overline{\text{Gap}}$ (%) shows the gap between average objective values and the best average values from three configurations. Specifically, given an instance for which obj and obj* are the average objective value for five runs and the best average objective value for five runs obtained among the three configurations, we compute the gap as $100(\text{obj} - \text{obj}^*)/\text{obj}^*$. Then, the values reported in columns $\overline{\text{Gap}}$ (%) are the average of the gap over all instances with the same number of customers. The last two

lines Avg. and Total show the average values over all instances and the number of times each configuration obtains the best solution in the total number of instances.

Tables 4 and 5 show that our HVNS (which includes both HDP and subHDP) significantly outperforms the other two configurations of the algorithm. Overall, the HVNS improves the objective value computed with the HVNS-EDP on average by 20.13% for the VRPD-C and by 29.73% for the VRPD-M. Furthermore, all the best objective values for the VRPD-C are obtained by the HVNS.

Considering the VRPD-M, there are 111 best average objective values obtained from the HVNS among 150 instances. The average gap of HVNS is always within 0.14%. Considering small instances with up to 49 customers, the quality of the solutions obtained by the three configurations are relatively similar, with the HVNS-EDP and the HVNS-NosubHDP giving slightly better results than HVNS on 19 out of the 60 instances. However, the average gaps of HVNS-EDP and the HVNS-NosubHDP become substantially larger with the increase in the size of the instances, up to 77.13% and 43.05% for the instances with 174 customers.

As expected, the number of iterations decreases and the computational time increases for larger instances. Notably, the HVNS runs the fastest or performs the highest number of iterations. The average number of iterations of the HVNS to solve the VRPD-C and the VRPD-M reaches 3,470.69 and 4,027.66, which is almost twice that of the HVNS-EDP. Due to the computational complexity of the EDP, the HVNS-EDP fails to handle instances containing more than 150 customers within the five-minute time limit, with its number of iterations being only 1. Despite that the HVNS-NosubHDP uses the HDP that has a lower complexity than the EDP, it performs 5 to 10 times fewer iterations without the subHDP move filter.

Overall, this computational study clearly demonstrates that when defining local search operators for solutions represented as sequences of customer visits without specifying whether the service will be performed by the truck or the drone (we called each sequence a truck route), the efficiency of move evaluation (performed solving FRDDPs) is essential. Our algorithmic components including the use of the HDP for a fast and good approximation of each route objective function value and the filter based on an approximate move evaluation (subHDP) are critical for our method to work.

n	#Ins.	Obj*	HVNS-EDP				HVNS-NosubHDP				HVNS			
			$\overline{\text{Obj}}$	$\overline{\text{Gap}}$ (%)	Ite	Time (s)	$\overline{\text{Obj}}$	$\overline{\text{Gap}}$ (%)	Ite	Time (s)	$\overline{\text{Obj}}$	$\overline{\text{Gap}}$ (%)	Ite	Time (s)
20	12	4.09	4.09	0.00	9,901.08	198.62	4.09	0.00	10,000.00	75.36	4.09	0.00	10,000.00	39.37
50	16	13.41	13.49	0.59	327.66	300.00	13.42	0.08	1,810.04	300.00	13.41	0.00	7,676.31	279.51
100	16	18.09	20.13	15.55	28.99	300.00	18.30	1.32	137.53	300.00	18.09	0.00	960.93	300.00
150	16	21.86	29.19	36.21	1.00	300.00	23.37	10.47	20.05	300.00	21.86	0.00	236.71	300.00
200	16	26.16	36.95	43.26	1.00	300.00	29.28	16.63	10.09	300.00	26.16	0.00	111.81	300.00
Avg.			21.65	20.13	1,638.83	287.65	18.41	6.00	1,995.31	264.72	17.39	0.00	3,470.69	254.54
Total	76		13				21				76			

Table 4: Results of algorithm configurations for the VRPD-C

6.3 Comparison with state-of-the-art results

In this section, we first compare our HVNS with CPLEX on small-sized instances for the VRPD-C. Then, we compare the solutions computed by our HVNS with the solutions reported in the literature for the VRPD-C (see Section 6.3.1) and the VRPD-M (see Section 6.3.2).

n	#Ins.	Obj*	HVNS-EDP				HVNS-NosubHDP				HVNS			
			$\overline{\text{Obj}}$	$\overline{\text{Gap}}$ (%)	Ite	Time (s)	$\overline{\text{Obj}}$	$\overline{\text{Gap}}$ (%)	Ite	Time (s)	$\overline{\text{Obj}}$	$\overline{\text{Gap}}$ (%)	Ite	Time (s)
19	30	400.95	400.96	0.00	10,000.00	43.47	400.97	0.01	10,000.00	25.15	401.00	0.02	10,000.00	16.10
49	30	458.31	459.19	0.21	577.25	300.00	458.46	0.04	2,630.95	300.00	458.59	0.08	7,655.79	279.40
74	30	528.80	586.80	11.07	41.55	300.00	529.70	0.20	326.67	300.00	529.60	0.14	1,751.63	300.00
99	30	586.24	932.48	60.52	1.47	300.00	592.64	1.07	89.58	300.00	586.45	0.05	652.90	300.00
174	30	734.45	1,275.74	77.13	1.00	300.00	1,042.50	43.05	1.00	300.00	734.45	0.00	77.95	300.00
Avg.			731.03	29.79	2,124.26	250.26	604.85	8.87	2,609.64	245.13	542.02	0.06	4,027.66	239.10
Total	150		32				68				111			

Table 5: Results of algorithm configurations for the VRPD-M

6.3.1 Results for the VRPD-C

We first compare the results of our HVNS algorithm with the results obtained solving the MILP formulation (see Section 3) with CPLEX with a two-hour CPU time limit for all instances with 6, 10, and 12 customers in the data set introduced by Sacramento et al. (2019). We set the number of trucks $|\mathcal{H}|$ to the same value as the number of customers n. In Table 6, we report the objective values and computational times for the two methods, along with the optimality gap (Gap^{milp} (%)) reported by CPLEX and the number of obtained optimal solutions (#Opt). For the HVNS, we report the number of instances where the computed solution has the same value as the best solution computed by CPLEX (#Mat), the number of instances where the computed solution has a strictly better value than the one computed by CPLEX (#Imp) within its time limit, and the gap between HVNS and CPLEX. For each instance, let $\text{obj}^{\text{CPLEX}}$ and obj be the objective value obtained by CPLEX and by our HVNS. We then calculate the gap as $100(\text{obj} - \text{obj}^{\text{CPLEX}})/\text{obj}^{\text{CPLEX}}$. The values in column Gap (%) report the average gaps for the instances with the same number of customers.

We observe that CPLEX can solve 16 out of 36 instances to optimality within the two-hour time limit. As the size of instances becomes larger, CPLEX solves fewer instances and reports a larger optimality gap. In contrast, our HVNS finds the optimal solution for the instances with 6 customers within 10 seconds and improves or matches all solutions computed by CPLEX for the instances with 10 and 12 customers.

n	#Ins.	CPLEX				HVNS				
		$\overline{\text{Obj}}$	Time (s)	Gap^{milp} (%)	#Opt	$\overline{\text{Obj}}$	Time (s)	#Mat	#Imp	Gap (%)
6	12	2.12	32.87	0.00	12	2.12	1.82	12	L	0.00
10	12	3.15	6,068.23	0.23	3	3.15	3.79	11	1	0.00
12	12	3.45	7,182.82	0.36	1	3.36	8.41	5	7	-0.02
Total	36				16			28	8	

Table 6: Comparison of results obtained by CPLEX with results of HVNS

We compare the solutions obtained by our HVNS (run five times) with the benchmarks SPR and RFK in Table 7 and Table 8. For each instance size, Table 7 reports the average objective values of the 10 ALNS runs of SPR and RFK, the average objective values of five runs of our HVNS, and the average gap between the average values obtained by our HVNS and both of their ALNSs. Given an instance, let $\overline{\text{obj}}^{\text{SPR}}$ and $\overline{\text{obj}}$ be the average objective value obtained by SPR and by our HVNS. We then calculate the gap as $100(\overline{\text{obj}} - \overline{\text{obj}}^{\text{SPR}})/\overline{\text{obj}}^{\text{SPR}}$. We report the average of the gap over all instances with the same number of customers in column $\overline{\text{Gap}}^{\text{SPR}}$ (%). The values in column $\overline{\text{Gap}}^{\text{RFK}}$ (%) are calculated in a similar fashion. In the last two columns of the table, we report the average number of iterations and the average

computational times of our HVNS. In addition, for each instance size, Table 8 reports the average best objective values obtained by each approach, the average gap between the average best objective values obtained by our HVNS and those of the two benchmarks, along with the number of matched and improved solutions compared with SPR, RFK and the BKSs from the two benchmarks. Finally, the line Avg. / Total shows overall average gaps, the total number of instances, the total number of matched solutions, and the new best solutions we found compared with SPR, RFK, and the BKSs from the latter two.

n	SPR	RFK	HVNS				
	$\overline{\text{Obj}}^{10}$	$\overline{\text{Obj}}^{10}$	$\overline{\text{Obj}}^{5}$	$\overline{\text{Gap}}^{\text{SPR}}$ (%)	$\overline{\text{Gap}}^{\text{RFK}}$ (%)	Ite	Time (s)
6	2.1210	2.1210	2.1210	0.00	0.00	10,000.00	1.80
10	3.1469	3.1480	3.1469	0.00	-0.02	10,000.00	3.78
12	3.3606	3.3606	3.3649	0.07	0.07	10,000.00	8.40
20	4.1152	4.0905	4.0890	-0.96	-0.02	10,000.00	39.37
50	13.6293	13.6678	13.4114	-1.53	-2.14	7,676.31	279.51
100	18.6604	18.6450	18.0925	-2.76	-2.83	960.93	300.00
150	22.5680	22.2623	21.8632	-3.09	-1.81	236.71	300.00
200	26.9347	26.4741	26.1641	-2.90	-0.86	111.81	300.00
Avg.				-1.56	-1.09	5,569.39	174.22

Table 7: Average results of HVNS and results reported by Sacramento et al. (2019) and Rave et al. (2022) for the VRPD-C

We observe from Table 7 that our HVNS outperforms the two ALNS algorithms proposed by Sacramento et al. (2019) and Rave et al. (2022), reducing the average cost by 1.56% and 1.09%. Moreover, there are significant improvements for larger instances starting from 50 customers, where the cost has been reduced by from 2.14% to 3.09% compared with the two ALNSs. In addition, due to the fact that we impose the iteration limit, despite the difference in computational power, our average computational time is 174.22 seconds (about 2.9 minutes), which is approximately 40% faster than theirs. As reported in Table 8, our HVNS matches the BKSs on all instances with 6, 10, 12, and 20 customers. Considering the 64 instances with 50 customers and more, we obtained 42 new BKSs. This again demonstrates the superiority of our HVNS on large-sized instances.

n	#Ins	SPR	RFK	HVNS					
		Obj^{best}	Obj^{best}	Obj^{best}	Gap^{SPR} (%)	Gap^{RFK} (%)	$\#\text{Mat}(\#\text{Imp})^{\text{SPR}}$	$\#\text{Mat}(\#\text{Imp})^{\text{RFK}}$	$\#\text{Mat}(\#\text{Imp})^{\text{BKS}}$
6	12	2.1210	2.1210	2.1210	0.00	0.00	12(0)	12(0)	12(0)
10	12	3.1469	3.1469	3.1469	0.00	0.00	12(0)	12(0)	12(0)
12	12	3.3606	3.3606	3.3606	0.00	0.00	12(0)	12(0)	12(0)
20	12	4.1112	4.0890	4.0890	-0.87	0.00	9(3)	12(0)	12(0)
50	16	13.4792	13.4845	13.4031	-0.55	-0.67	7(8)	4(9)	7(6)
100	16	18.3439	18.4121	18.0394	-1.46	-1.84	0(15)	0(15)	0(14)
150	16	21.7796	21.8360	21.6346	-0.76	-1.03	0(13)	0(14)	0(12)
200	16	26.3185	25.9569	25.8297	-1.95	-0.60	0(13)	0(10)	0(10)
Avg. / Total	112				-0.77	-0.59	52(52)	52(48)	55(42)

Table 8: Best results of HVNS and results reported by Sacramento et al. (2019) and Rave et al. (2022) for the VRPD-C

6.3.2 Results for the VRPD-M

We evaluate the quality of the solutions computed by our HVNS for the VRPD-M by performing a comparison of the benchmarks EGH, TB1, TB2, RR-RANGE30, and RR-MHD (see Table 3). Similar to our previous experiments, we ran five replications of our HVNS on each instance, each of which with a maximum run time of five minutes and a maximum number of iterations of 10,000. The results are shown in Table 9. The columns $\overline{\text{Gap}}$ (%) and Gap (%) are computed in a similar way as in Table 7 and 8. Since the five benchmarks correspond to solutions computed by exact algorithms, we present the number of optimal solutions (#Opt) from each benchmark and the number of optimal solutions computed by our HVNS ($\#\text{Mat}^{\text{OPT}}$). We also report the number of matched and improved BKSs ($\#\text{Mat}(\#\text{Imp})^{\text{BKS}}$) compared with the BKSs from each benchmark. Despite that these benchmarks only have small and medium-sized instances, we still observe several advantages of our HVNS. Among the 798 instances considered in Table 9, our HVNS obtains 607 out of 644 optimal solutions, matches 647 BKSs and identifies 119 new BKSs. As the instance size becomes larger, our HVNS finds more new BKSs. Specifically, it identifies 50 new BKSs for the 75 instances with 39 customers compared to RR-RANGE30, achieving a significant improvement with a gap of -31.89%. Besides, it identifies 22 new BKSs for the 30 instances with 31 customers compared to EGH and 11 new BKSs for the 75 instances with 39 customers compared to RR-MHD, with a gap of -3.65% and -5.23%. In addition, the differences between the values of the columns $\overline{\text{Gap}}$ (%) and Gap (%) are very small, which means our HVNS is relatively stable. We finally note that the HVNS is relatively fast, with a maximum average computational time equal to 203.25 seconds (around 3 minutes).

Name	m	n	#Ins	Benchmark			HVNS							
				#Opt	BKS	Time (s)	Obj	Gap (%)	$\overline{\text{Obj}}$	$\overline{\text{Gap}}$ (%)	$\#\text{Mat}^{\text{OPT}}$	$\#\text{Mat}(\#\text{Imp})^{\text{BKS}}$	Ite	Time (s)
EGH	1	15	30	30	515.92	64.85	515.92	0.00	515.92	0.00	27	27 (3)	10,000.00	5.38
		19	30	28	549.59	1,979.28	549.59	0.00	549.61	0.00	26	28 (2)	10,000.00	11.22
		23	30	17	550.32	8,241.03	549.55	-0.21	549.55	-0.21	17	24 (6)	10,000.00	26.32
		27	30	5	581.54	10,071.10	578.61	-0.65	578.61	-0.65	5	14 (16)	10,000.00	38.30
		31	30	2	632.08	10,794.95	611.76	-3.65	611.76	-3.65	1	7 (22)	10,000.00	67.00
Avg. / Total			150	82		6,230.24		-0.90		-0.90	76	100 (49)	10,000.00	29.64
TB1	1	14	6	6	6,785.28	137.53	6,785.28	0.00	6785.28	0.00	6	6 (0)	10,000.00	11.86
		19	6	6	7,680.69	15,252.30	7,680.69	0.00	7,680.69	0.00	6	6 (0)	10,000.00	28.03
		24	6	3	8,764.17	23,632.88	8,764.17	0.00	8,764.17	0.00	3	6 (0)	10,000.00	34.74
		29	6	2	9,532.61	33,966.54	9,532.62	0.00	9,532.62	0.00	1	5 (0)	10,000.00	47.09
Avg. / Total			24	17		15,843.90		0.00		0.00	16	23 (0)	10,000.00	30.43
TB2	2	14	6	6	4,380.72	24.68	4,452.38	1.55	4452.38	1.55	5	5 (0)	10,000.00	18.39
		19	6	5	4,840.82	779.07	4,840.81	0.00	4,841.25	0.01	5	6 (0)	10,000.00	47.85
		24	6	4	6,066.45	5,972.25	6,046.80	-0.31	6,046.80	-0.31	3	4 (1)	10,000.00	67.16
		29	6	1	6,444.68	12,668.54	6,423.84	-0.31	6,423.84	-0.31	1	3 (3)	10,000.00	97.19
Avg. / Total			24	16		7,057.68		0.23		0.23	14	18 (4)	10,000.00	57.65
RR-RANGE30	1	9	75	75	121.09	0.25	121.09	0.00	121.09	0.00	75	75 (0)	10,000.00	2.29
		19	75	75	151.49	20.24	151.51	0.01	151.54	0.04	74	74 (0)	10,000.00	23.07
		29	75	68	175.65	755.20	168.68	-2.15	168.82	-2.06	62	64 (5)	10,000.00	82.34
		39	75	25	307.27	2,896.68	187.24	-31.89	187.58	-31.76	24	24 (50)	9,921.78	203.25
Avg. / Total			300	243		2,146.01		-8.51		-8.45	235	237 (55)	9,980.44	77.74
RR-MHD	1	9	75	75	152.37	0.13	152.37	0.00	152.37	0.00	75	75 (0)	10,000.00	1.21
		19	75	75	188.15	3.18	188.21	0.04	188.36	0.12	71	71 (0)	10,000.00	10.21
		29	75	75	210.24	92.29	210.45	0.12	210.62	0.21	68	68 (0)	10,000.00	43.75
		39	75	61	256.72	1475.88	236.29	-5.23	236.47	-5.16	52	55 (11)	10,000.00	109.94
Avg. / Total			300	286		743.50		-1.27		-1.21	266	269 (11)	10,000.00	41.28
Summary			798	644							607	647 (119)		

Table 9: Comparison of the HVNS results against five benchmarks from the literature for the VRPD-M

Problem		Name	Reference	Method	Time limit	Data set	#Mat^{OPT}	#Mat^{BKS}	#Imp^{BKS}
VRPD-C	NoLW	SPR ($m > 1$)	Sacramento et al. (2019)	ALNS	5 minutes (10 runs)	Sacramento et al. (2019)		52/112	52/112
		RFK ($m > 1$)	Rave et al. (2022)					52/112	48/112
VRPD-M	LW	EGH ($m = 1$)	El-Adle et al. (2021)	MIP model	3.1 hours	Bouman et al. (2018b)	76/82	100/150	49/150
		TB1 ($m = 1$)	Tamke and Buscher (2021)	Branch-and-cut	12 hours	Reinelt (1997)	16/17	23/24	0/24
		TB2 ($m = 2$)					14/16	18/24	4/24
		RR-RANGE30 ($m = 1$)	Roberti and Ruthmair (2021)	Branch-and-price	1 hour	Poikonen et al. (2019)	235/243	237/300	55/300
	NoLW	RR-MHD ($m = 1$)	Roberti and Ruthmair (2021)	Branch-and-price	1 hour	Poikonen et al. (2019)	266/286	269/300	11/300

Table 10: Summary of computational results compared with all benchmarks

7 Conclusions

In this work, we consider several versions of the VRPD depending on whether the objective function is related to minimizing the total transportation cost or the makespan, and on whether the drone can land and wait or not. In particular, we study a subproblem of the VRPD called the fixed route drone dispatch problem (FRDDP). Given a truck route, the FRDDP assigns a subset of customers to the drone, assuming that they succeed their launch nodes and precede their recovery nodes in the route. For each version of the FRDDP, we develop a heuristic dynamic program (i.e, HDP) with a computational complexity of $\mathcal{O}(n^2)$, where n is the number of customers contained in the route, achieving a lower computational complexity than exact dynamic programs ($\mathcal{O}(n^3)$) proposed in the literature. We embed the HDP in a hybrid variable neighborhood search (HVNS) to solve the VRPD. To accelerate the search, we present a mechanism to filter unpromising moves based on the core of the HDP. Numerous experiments conducted on two data sets for both objective functions demonstrate the important role of these components to reduce the computational time and to perform a larger exploration of the search space within the time limit. The comparison of the solutions computed by the HVNS on several variants of the problem against seven benchmarks from the literature shows its high-quality results which are reflected in the identification of a large number of new BKSs, as shown in Table 10.

We believe that the algorithmic components proposed in this work can be adapted to tackle more complex variants of the VRPD. For example, considering time windows, or cyclic operations, where the truck can wait for the drone at the same location. Furthermore, the concepts of the heuristic dynamic programs that slightly compromise optimality while achieving significant computational savings, may be instrumental for a variety of synchronization problems involving multiple modes.

Acknowledgements

This work was partially supported by the Innovation Foundation for Doctor Dissertation of Northwestern Polytechnical University (CX2021090). The first author thanks the support of the China Scholarship Council. The second author thanks the financial support of the Department of Elettronica, Informazione e Bioingeneria of Politecnico di Milano that made this collaboration possible.

References

Agatz, N., Bouman, P., and Schmidt, M. (2018). Optimization approaches for the traveling salesman problem with drone. *Transportation Science*, 52(4):965–981.

Bouman, P., Agatz, N., and Schmidt, M. (2018a). Dynamic programming approaches for the traveling salesman problem with drone. *Networks*, 72(4):528–542.

Bouman, P., Agatz, N., and Schmidt, M. (2018b). Instances for the tsp with drone (and some solutions). https://doi.org/10.5281/zenodo.1204676. Accessed: 2023-1-9.

Campbell, J. F., Sweeney, D., and Zhang, J. (2017). Strategic design for delivery with trucks and drones. *Supply Chain Analytics Report SCMA (04 2017)*, pages 47–55.

Chen, C., Demir, E., and Huang, Y. (2021). An adaptive large neighborhood search heuristic for the vehicle routing problem with time windows and delivery robots. *European Journal of Operational Research*, 294(3):1164–1180.

Chung, S. H., Sah, B., and Lee, J. (2020). Optimization for drone and drone-truck combined operations: A review of the state of the art and future directions. *Computers & Operations Research*, 123:105004.

de Freitas, J. C. and Penna, P. H. V. (2020). A variable neighborhood search for flying sidekick traveling salesman problem. *International Transactions in Operational Research*, 27(1):267–290.

Dell'Amico, M., Montemanni, R., and Novellani, S. (2021). Algorithms based on branch and bound for the flying sidekick traveling salesman problem. *Omega*, 104:102493.

Demir, E., Bektaş, T., and Laporte, G. (2012). An adaptive large neighborhood search heuristic for the pollution-routing problem. *European journal of operational research*, 223(2):346–359.

Drexl, M. (2012). Synchronization in vehicle routing—a survey of VRPs with multiple synchronization constraints. *Transportation Science*, 46(3):297–316.

El-Adle, A. M., Ghoniem, A., and Haouari, M. (2021). Parcel delivery by vehicle and drone. *Journal of the Operational Research Society*, 72(2):398–416.

Ha, Q. M., Deville, Y., Pham, Q. D., and Hà, M. H. (2018). On the min-cost traveling salesman problem with drone. *Transportation Research Part C: Emerging Technologies*, 86:597–621.

Ha, Q. M., Deville, Y., Pham, Q. D., and Hà, M. H. (2020). A hybrid genetic algorithm for the traveling salesman problem with drone. *Journal of Heuristics*, 26(2):219–247.

Kirschstein, T. (2020). Comparison of energy demands of drone-based and ground-based parcel delivery services. *Transportation Research Part D: Transport and Environment*, 78:102209.

Kitjacharoenchai, P., Min, B.-C., and Lee, S. (2020). Two echelon vehicle routing problem with drones in last mile delivery. *International Journal of Production Economics*, 225:107598.

Li, H., Chen, J., Wang, F., and Bai, M. (2021). Ground-vehicle and unmanned-aerial-vehicle routing problems from two-echelon scheme perspective: A review. *European Journal of Operational Research*, 294(3):1078–1095.

Macrina, G., Laporte, G., Guerriero, F., and Pugliese, L. D. P. (2019). An energy-efficient green-vehicle routing problem with mixed vehicle fleet, partial battery recharging and time windows. *European Journal of Operational Research*, 276(3):971–982.

Macrina, G., Pugliese, L. D. P., Guerriero, F., and Laporte, G. (2020). Drone-aided routing: A literature review. *Transportation Research Part C: Emerging Technologies*, 120:102762.

Mladenović, N. and Hansen, P. (1997). Variable neighborhood search. *Computers & operations research*, 24(11):1097–1100.

Moshref-Javadi, M., Hemmati, A., and Winkenbach, M. (2020). A truck and drones model for last-mile delivery: A mathematical model and heuristic approach. *Applied Mathematical Modelling*, 80:290–318.

Moshref-Javadi, M. and Winkenbach, M. (2021). Applications and research avenues for drone-based models in logistics: A classification and review. *Expert Systems with Applications*, 177:114854.

Murray, C. C. and Chu, A. G. (2015). The flying sidekick traveling salesman problem: Optimization of

drone-assisted parcel delivery. *Transportation Research Part C: Emerging Technologies*, 54:86–109.

Murray, C. C. and Raj, R. (2020). The multiple flying sidekicks traveling salesman problem: Parcel delivery with multiple drones. *Transportation Research Part C: Emerging Technologies*, 110:368–398.

Najy, W., Archetti, C., and Diabat, A. (2022). Collaborative truck-and-drone delivery for inventory-routing problems. *Transportation Research Part C: Emerging Technologies*, page 103791.

Otto, A., Agatz, N., Campbell, J., Golden, B., and Pesch, E. (2018). Optimization approaches for civil applications of unmanned aerial vehicles (UAVs) or aerial drones: A survey. *Networks*, 72(4):411–458.

Poikonen, S. and Campbell, J. F. (2021). Future directions in drone routing research. *Networks*, 77(1):116–126.

Poikonen, S., Golden, B., and Wasil, E. A. (2019). A branch-and-bound approach to the traveling salesman problem with a drone. *INFORMS Journal on Computing*, 31(2):335–346.

Poikonen, S., Wang, X., and Golden, B. (2017). The vehicle routing problem with drones: Extended models and connections. *Networks*, 70(1):34–43.

Rave, A., Fontaine, P., and Kuhn, H. (2022). Drone location and vehicle fleet planning with trucks and aerial drones. *European Journal of Operational Research*.

Reinelt, G. (1997). Tsplib. https://elib.zib.de/pub/mp-testdata/tsp/tsplib/tsplib.html. Accessed: 2022-10-11.

Roberti, R. and Ruthmair, M. (2021). Exact methods for the traveling salesman problem with drone. *Transportation Science*, 55(2):315–335.

Sacramento, D., Pisinger, D., and Ropke, S. (2019). An adaptive large neighborhood search metaheuristic for the vehicle routing problem with drones. *Transportation Research Part C: Emerging Technologies*, 102:289–315.

Sah, B., Gupta, R., and Bani-Hani, D. (2021). Analysis of barriers to implement drone logistics. *International Journal of Logistics Research and Applications*, 24(6):531–550.

Salama, M. and Srinivas, S. (2020). Joint optimization of customer location clustering and drone-based routing for last-mile deliveries. *Transportation Research Part C: Emerging Technologies*, 114:620–642.

Salama, M. R. and Srinivas, S. (2022). Collaborative truck multi-drone routing and scheduling problem: Package delivery with flexible launch and recovery sites. *Transportation Research Part E: Logistics and Transportation Review*, 164:102788.

Schermer, D., Moeini, M., and Wendt, O. (2019a). A hybrid VNS/tabu search algorithm for solving the vehicle routing problem with drones and en route operations. *Computers & Operations Research*, 109:134–158.

Schermer, D., Moeini, M., and Wendt, O. (2019b). A matheuristic for the vehicle routing problem with drones and its variants. *Transportation Research Part C: Emerging Technologies*, 106:166–204.

Singh, A. and Mutreja, S. (2022). Last mile delivery market. https://www.alliedmarketresearch.com/last-mile-delivery-market. Accessed: 2022-09-27.

Tamke, F. and Buscher, U. (2021). A branch-and-cut algorithm for the vehicle routing problem with drones. *Transportation Research Part B: Methodological*, 144:174–203.

Vidal, T. (2022). Hybrid genetic search for the CVRP: Open-source implementation and swap* neighborhood. *Computers & Operations Research*, 140:105643.

Wang, X., Poikonen, S., and Golden, B. (2017). The vehicle routing problem with drones: several worst-case results. *Optimization Letters*, 11(4):679–697.

Wang, Z. and Sheu, J.-B. (2019). Vehicle routing problem with drones. *Transportation research part B: methodological*, 122:350–364.

Zhou, H., Qin, H., Cheng, C., and Rousseau, L.-M. (2023). An exact algorithm for the two-echelon vehicle routing problem with drones. *Transportation Research Part B: Methodological*, 168:124–150.

Supplementary material

1. Acceptance criterion of the HVNS

To avoid being trapped in a local optimum, in addition to the shaking phase we use an SA-based solution acceptance criterion (see Algorithm 4). If the new solution $\overline{\mathcal{S}}^{\mathsf{new}}$ has an improved objective function value than the incumbent solution $\overline{\mathcal{S}}^{\mathsf{inc}}$, we always accept it. Otherwise, it is accepted with a probability $e^{\frac{f(\overline{\mathcal{S}}^{\mathsf{inc}})-f(\overline{\mathcal{S}}^{\mathsf{new}})}{t^c}}$, where $f(\overline{\mathcal{S}}^{\mathsf{inc}})$ and $f(\overline{\mathcal{S}}^{\mathsf{new}})$ denote the objective function value of $\overline{\mathcal{S}}^{\mathsf{inc}}$ and $\overline{\mathcal{S}}^{\mathsf{new}}$, and t^c controls the acceptance probability. The value of t^c, initially set to t^{init}, decreases linearly towards zero. Let T be the current computational time, we update t^c using the formula $t^c = t^{\text{init}} \left(1 - \frac{\mathsf{T}}{\mathsf{T}^{\mathsf{max}}}\right)$, where $\mathsf{T}^{\mathsf{max}}$ is the computational time limit that is one of the stopping criteria of the HVNS.

Algorithm 4: SA AcceptanceCriterion($\overline{\mathcal{S}}^{\mathsf{inc}}, \overline{\mathcal{S}}^{*}, \overline{\mathcal{S}}^{\mathsf{new}}, \lambda, \lambda^{\mathsf{avg}}, \lambda^{\mathsf{max}}, \kappa$)

Data: The incumbent complete solution $\overline{\mathcal{S}}^{\mathsf{inc}}$, the current best complete solution $\overline{\mathcal{S}}^{*}$ computed so far by the HVNS, a new complete solution $\overline{\mathcal{S}}^{\mathsf{new}}$, a working duration threshold λ, the average working duration variation threshold λ^{avg}, the maximum working duration variation threshold λ^{max}, the current number of iterations without improvement κ

1 $t^c = t^{\text{init}}(1 - \mathsf{T}/\mathsf{T}^{\mathsf{max}})$;
2 **if** $\texttt{Random}(0,1) < exp((f(\overline{\mathcal{S}}^{\mathsf{inc}}) - f(\overline{\mathcal{S}}^{\mathsf{new}}))/t^c)$ **then** $\overline{\mathcal{S}}^{\mathsf{inc}} \leftarrow \overline{\mathcal{S}}^{\mathsf{new}}$;
3 **if** $f(\overline{\mathcal{S}}^{\mathsf{inc}}) < f(\overline{\mathcal{S}}^{*})$ **then** $\overline{\mathcal{S}}^{*} \leftarrow \overline{\mathcal{S}}^{\mathsf{inc}}$, $\kappa \leftarrow 0$, $\lambda \leftarrow \lambda^{\mathsf{avg}}$;
4 **else**
5 $\quad \kappa \leftarrow \kappa + 1$;
6 $\quad$ **if** $\kappa > \mathsf{N}^{\mathsf{max}}$ **then** $\overline{\mathcal{S}}^{\mathsf{inc}} \leftarrow \overline{\mathcal{S}}^{*}$, $\kappa \leftarrow 0$, $\lambda \leftarrow \lambda^{\mathsf{avg}}$;
7 $\quad$ **else** $\lambda \leftarrow \lambda + \kappa\texttt{Random}(0,1)$;

Result: $\overline{\mathcal{S}}^{\mathsf{inc}}, \overline{\mathcal{S}}^{*}, \lambda, \kappa$

The best solution $\overline{\mathcal{S}}^{*}$ computed so far by the HVNS is restored if κ iterations have passed without any improvement (line 6). If an improved solution is found (line 3) or no improvement happens in a certain number of iterations (line 6), the adaptive threshold λ used in the procedure `Search` is set to λ^{avg}. Otherwise, λ is increased based on the number of iterations without improvement κ (line 7).

2. Detailed results of algorithm configurations in Section 6.2

Table 11 and 12 present detailed results of different algorithm configurations in five runs. The notations in both tables are defined as follows.

Instance: The name of the instance.

n: The number of customers in the instance.

Obj*: The best average objective function value of five runs from three algorithm configurations.

Obj: The best objective function value from five runs of each algorithm configuration.

$\overline{\text{Obj}}$: The average objective function value from five runs of each algorithm configuration.

$\overline{\text{Gap}}$ (%): The gap between $\overline{\text{Obj}}$ and Obj* computed by $100(\overline{\text{Obj}} - \text{Obj}^*)/\text{Obj}^*$ of each algorithm configuration.

Ite: The average number of iterations of five runs of each algorithm configuration.

Time (s): The average computational time of five runs of each algorithm configuration.

Table 11: Detailed results of three configurations for the VRPD-C

Instance	n	Obj*	HVNS-EDP					HVNS-NosubHDP					HVNS				
			Obj	$\overline{\text{Obj}}$	$\overline{\text{Gap}}$ (%)	Ite	Time (s)	Obj	$\overline{\text{Obj}}$	$\overline{\text{Gap}}$ (%)	Ite	Time (s)	Obj	$\overline{\text{Obj}}$	$\overline{\text{Gap}}$ (%)	Ite	Time (s)
6.5.1	6	1.10	1.10	1.10	0.00	10000.00	2.76	1.10	1.10	0.00	10000.00	2.76	1.10	1.10	0.00	10000.00	2.71
6.5.2	6	0.84	0.84	0.84	0.00	10000.00	2.57	0.84	0.84	0.00	10000.00	2.58	0.84	0.84	0.00	10000.00	2.28
6.5.3	6	1.21	1.21	1.21	0.00	10000.00	0.98	1.21	1.21	0.00	10000.00	1.04	1.21	1.21	0.00	10000.00	1.15
6.5.4	6	0.95	0.95	0.95	0.00	10000.00	2.50	0.95	0.95	0.00	10000.00	2.29	0.95	0.95	0.00	10000.00	2.30
6.10.1	6	2.41	2.41	2.41	0.00	10000.00	2.28	2.41	2.41	0.00	10000.00	2.17	2.41	2.41	0.00	10000.00	2.20
6.10.2	6	1.68	1.68	1.68	0.00	10000.00	1.57	1.68	1.68	0.00	10000.00	1.61	1.68	1.68	0.00	10000.00	1.69
6.10.3	6	1.33	1.33	1.33	0.00	10000.00	2.25	1.33	1.33	0.00	10000.00	2.28	1.33	1.33	0.00	10000.00	2.44
6.10.4	6	1.44	1.44	1.44	0.00	10000.00	1.60	1.44	1.44	0.00	10000.00	1.61	1.44	1.44	0.00	10000.00	1.70
6.20.1	6	2.68	2.68	2.68	0.00	10000.00	1.38	2.68	2.68	0.00	10000.00	1.88	2.68	2.68	0.00	10000.00	1.80
6.20.2	6	4.32	4.32	4.32	0.00	10000.00	1.13	4.32	4.32	0.00	10000.00	1.02	4.32	4.32	0.00	10000.00	1.12
6.20.3	6	3.82	3.82	3.82	0.00	10000.00	1.11	3.82	3.82	0.00	10000.00	1.16	3.82	3.82	0.00	10000.00	1.11
6.20.4	6	3.68	3.68	3.68	0.00	10000.00	0.85	3.68	3.68	0.00	10000.00	1.07	3.68	3.68	0.00	10000.00	1.06
10.5.1	10	1.66	1.66	1.66	0.00	10000.00	2.05	1.66	1.66	0.00	10000.00	1.75	1.66	1.66	0.00	10000.00	1.76
10.5.2	10	1.45	1.45	1.45	0.00	10000.00	7.45	1.45	1.45	0.00	10000.00	6.05	1.45	1.45	0.00	10000.00	4.91
10.5.3	10	1.47	1.47	1.47	0.00	10000.00	4.85	1.47	1.47	0.00	10000.00	3.77	1.47	1.47	0.00	10000.00	3.61
10.5.4	10	1.28	1.28	1.28	0.00	10000.00	11.16	1.28	1.28	0.00	10000.00	8.00	1.28	1.28	0.00	10000.00	6.91
10.10.1	10	2.33	2.33	2.33	0.00	10000.00	7.38	2.33	2.33	0.00	10000.00	5.60	2.33	2.33	0.00	10000.00	4.87
10.10.2	10	3.16	3.16	3.16	0.00	10000.00	6.14	3.16	3.16	0.00	10000.00	4.75	3.16	3.16	0.00	10000.00	4.15
10.10.3	10	2.55	2.55	2.55	0.00	10000.00	7.62	2.55	2.55	0.00	10000.00	6.79	2.55	2.55	0.00	10000.00	6.03
10.10.4	10	2.54	2.54	2.54	0.00	10000.00	5.41	2.54	2.54	0.00	10000.00	4.04	2.54	2.54	0.00	10000.00	3.56
10.20.1	10	4.45	4.45	4.45	0.00	10000.00	3.22	4.45	4.45	0.00	10000.00	2.16	4.45	4.45	0.00	10000.00	2.06
10.20.2	10	6.17	6.17	6.17	0.00	10000.00	1.82	6.17	6.17	0.00	10000.00	1.42	6.17	6.17	0.00	10000.00	1.41
10.20.3	10	4.55	4.55	4.55	0.00	10000.00	3.22	4.55	4.55	0.00	10000.00	2.34	4.55	4.55	0.00	10000.00	2.19
10.20.4	10	6.15	6.15	6.15	0.00	10000.00	5.98	6.15	6.15	0.00	10000.00	4.72	6.15	6.15	0.00	10000.00	3.90
12.5.1	12	1.37	1.37	1.37	0.00	10000.00	15.68	1.37	1.37	0.00	10000.00	10.76	1.37	1.37	0.00	10000.00	8.24
12.5.2	12	1.06	1.06	1.06	0.00	10000.00	30.38	1.06	1.06	0.00	10000.00	26.04	1.06	1.06	0.00	10000.00	19.27
12.5.3	12	1.45	1.45	1.45	0.00	10000.00	17.49	1.45	1.45	0.00	10000.00	11.29	1.45	1.45	0.00	10000.00	8.25
12.5.4	12	1.58	1.58	1.58	0.00	10000.00	7.82	1.58	1.58	0.00	10000.00	5.28	1.58	1.58	0.00	10000.00	4.29
12.10.1	12	2.68	2.68	2.68	0.00	10000.00	18.20	2.68	2.68	0.00	10000.00	17.53	2.68	2.68	0.00	10000.00	13.79
12.10.2	12	2.68	2.68	2.68	0.00	10000.00	15.34	2.68	2.68	0.00	10000.00	11.44	2.68	2.68	0.00	10000.00	9.31
12.10.3	12	2.88	2.88	2.88	0.00	10000.00	12.71	2.88	2.88	0.00	10000.00	9.23	2.88	2.88	0.00	10000.00	7.36
12.10.4	12	2.31	2.31	2.31	0.00	10000.00	21.58	2.31	2.31	0.00	10000.00	13.81	2.31	2.31	0.00	10000.00	10.87

Table 11 – continued from previous page

Instance	n	Obj*	HVNS-EDP					HVNS-NosubHDP					HVNS				
			Obj	$\overline{\text{Obj}}$	$\overline{\text{Gap}}$ (%)	Ite	Time (s)	Obj	$\overline{\text{Obj}}$	$\overline{\text{Gap}}$ (%)	Ite	Time (s)	Obj	$\overline{\text{Obj}}$	$\overline{\text{Gap}}$ (%)	Ite	Time (s)
12.20.1	12	5.78	5.78	5.78	0.00	10000.00	11.92	5.78	5.78	0.00	10000.00	7.97	5.78	5.78	0.00	10000.00	6.96
12.20.2	12	8.27	8.27	8.27	0.00	10000.00	4.22	8.27	8.27	0.00	10000.00	3.19	8.27	8.27	0.00	10000.00	2.74
12.20.3	12	4.17	4.17	4.17	0.00	10000.00	8.38	4.17	4.17	0.00	10000.00	5.75	4.17	4.17	0.00	10000.00	4.69
12.20.4	12	6.09	6.25	6.25	2.58	10000.00	8.51	6.09	6.09	0.00	10000.00	6.81	6.14	6.14	0.86	10000.00	5.10
20.5.1	20	1.79	1.79	1.79	0.00	10000.00	196.04	1.79	1.79	0.00	10000.00	86.48	1.79	1.79	0.00	10000.00	44.10
20.5.2	20	1.82	1.82	1.82	0.00	10000.00	83.14	1.82	1.82	0.00	10000.00	35.41	1.82	1.82	0.00	10000.00	19.45
20.5.3	20	1.49	1.49	1.49	0.00	10000.00	194.98	1.49	1.49	0.00	10000.00	76.69	1.49	1.49	0.00	10000.00	32.06
20.5.4	20	1.38	1.38	1.38	0.00	9167.00	300.00	1.38	1.38	0.00	10000.00	131.57	1.38	1.38	0.00	10000.00	62.14
20.10.1	20	3.25	3.25	3.25	0.00	10000.00	127.50	3.25	3.25	0.00	10000.00	46.18	3.25	3.25	0.00	10000.00	30.16
20.10.2	20	3.09	3.09	3.09	0.00	9695.20	276.51	3.09	3.09	0.00	10000.00	102.93	3.09	3.09	0.00	10000.00	52.99
20.10.3	20	3.70	3.70	3.70	0.00	9950.80	275.68	3.70	3.70	0.00	10000.00	91.97	3.70	3.70	0.00	10000.00	47.54
20.10.4	20	3.20	3.20	3.20	0.00	10000.00	262.62	3.20	3.20	0.00	10000.00	103.43	3.20	3.20	0.00	10000.00	59.57
20.20.1	20	7.32	7.32	7.32	0.00	10000.00	239.71	7.32	7.32	0.00	10000.00	78.04	7.32	7.32	0.00	10000.00	40.22
20.20.2	20	7.55	7.55	7.55	0.00	10000.00	138.67	7.55	7.55	0.00	10000.00	46.81	7.55	7.55	0.00	10000.00	26.90
20.20.3	20	7.46	7.46	7.46	0.00	10000.00	136.56	7.46	7.46	0.00	10000.00	36.49	7.46	7.46	0.00	10000.00	20.30
20.20.4	20	7.01	7.01	7.01	0.00	10000.00	152.04	7.01	7.01	0.00	10000.00	68.25	7.01	7.01	0.00	10000.00	36.94
50.10.1	50	5.86	5.86	5.86	0.00	136.20	300.01	5.86	5.86	0.00	1086.80	300.00	5.86	5.86	0.00	5905.80	300.00
50.10.2	50	5.58	5.59	5.59	0.01	173.80	300.02	5.58	5.58	0.00	1399.00	300.00	5.58	5.58	0.00	7605.80	300.00
50.10.3	50	5.41	5.49	5.49	1.44	97.80	300.06	5.43	5.43	0.20	740.40	300.00	5.41	5.41	0.00	3905.60	300.00
50.10.4	50	5.14	5.21	5.21	1.44	109.20	300.04	5.14	5.14	0.00	943.40	300.01	5.14	5.14	0.00	5340.60	300.00
50.20.1	50	10.23	10.25	10.25	0.19	130.60	300.03	10.23	10.23	0.00	1168.60	300.00	10.23	10.23	0.00	6139.80	300.00
50.20.2	50	10.06	10.11	10.11	0.51	148.00	300.03	10.06	10.06	0.00	1200.20	300.00	10.06	10.06	0.00	10000.00	279.28
50.20.3	50	10.50	10.52	10.52	0.21	110.60	300.03	10.50	10.50	0.00	1197.00	300.00	10.50	10.50	0.00	6130.60	300.00
50.20.4	50	10.66	10.74	10.74	0.67	107.80	300.04	10.67	10.67	0.06	862.20	300.00	10.66	10.66	0.00	4458.40	300.00
50.30.1	50	15.77	15.80	15.80	0.18	394.80	300.00	15.77	15.77	0.00	2525.20	300.00	15.77	15.77	0.00	10000.00	266.48
50.30.2	50	15.01	15.07	15.07	0.36	548.60	300.03	15.02	15.02	0.00	1248.20	300.00	15.01	15.01	0.00	6099.00	300.00
50.30.3	50	16.39	16.76	16.76	2.29	356.20	300.02	16.39	16.39	0.01	2364.40	300.00	16.39	16.39	0.00	9032.60	300.00
50.30.4	50	18.43	18.55	18.55	0.68	442.00	300.00	18.60	18.60	0.93	2780.20	300.00	18.43	18.43	0.00	10000.00	237.47
50.40.1	50	20.12	20.12	20.12	0.01	778.80	300.01	20.12	20.12	0.00	3872.20	300.00	20.12	20.12	0.00	10000.00	187.15
50.40.2	50	20.42	20.51	20.51	0.43	621.80	300.01	20.43	20.43	0.04	3006.80	300.00	20.42	20.42	0.00	10000.00	245.99
50.40.3	50	22.65	22.65	22.65	0.02	491.00	300.01	22.65	22.65	0.00	1897.20	300.00	22.65	22.65	0.00	8202.80	300.00
50.40.4	50	22.34	22.55	22.55	0.94	595.40	300.02	22.34	22.34	0.00	2668.80	300.00	22.34	22.34	0.00	10000.00	255.82
100.10.1	100	6.72	8.93	8.93	32.80	1.00	303.54	7.02	7.02	4.34	32.60	300.02	6.72	6.72	0.00	291.00	300.01
100.10.2	100	7.50	10.54	10.54	40.61	1.00	305.84	7.67	7.67	2.31	43.00	300.05	7.50	7.50	0.00	686.80	300.00

Table 11 – continued from previous page

Instance	n	Obj*	HVNS-EDP					HVNS-NosubHDP					HVNS				
			Obj	$\overline{\text{Obj}}$	$\overline{\text{Gap}}$ (%)	Ite	Time (s)	Obj	$\overline{\text{Obj}}$	$\overline{\text{Gap}}$ (%)	Ite	Time (s)	Obj	$\overline{\text{Obj}}$	$\overline{\text{Gap}}$ (%)	Ite	Time (s)
100.10.3	100	7.13	8.99	8.99	26.05	1.00	306.57	7.25	7.25	1.64	35.60	300.04	7.13	7.13	0.00	363.40	300.00
100.10.4	100	7.37	8.75	8.75	18.60	1.00	307.46	7.48	7.48	1.43	77.60	300.01	7.37	7.37	0.00	1027.60	300.00
100.20.1	100	13.60	14.66	14.66	7.84	1.00	305.44	13.62	13.62	0.18	89.60	300.01	13.60	13.60	0.00	886.20	300.00
100.20.2	100	14.03	18.11	18.11	29.14	1.00	301.21	14.10	14.10	0.57	62.80	300.02	14.03	14.03	0.00	755.80	300.00
100.20.3	100	13.62	15.45	15.45	13.44	1.00	301.25	13.77	13.77	1.16	62.20	300.02	13.62	13.62	0.00	738.00	300.00
100.20.4	100	13.85	17.08	17.08	23.29	1.00	301.82	13.95	13.95	0.72	60.40	300.02	13.85	13.85	0.00	552.60	300.01
100.30.1	100	21.98	23.36	23.36	6.27	47.40	300.06	22.30	22.30	1.44	178.00	300.00	21.98	21.98	0.00	1037.60	300.00
100.30.2	100	22.23	23.01	23.01	3.50	19.00	300.10	22.60	22.60	1.65	217.00	300.01	22.23	22.23	0.00	1383.80	300.00
100.30.3	100	23.37	25.62	25.62	9.63	1.00	300.73	23.66	23.66	1.25	250.20	300.00	23.37	23.37	0.00	1351.60	300.00
100.30.4	100	22.41	27.01	27.01	20.49	1.00	300.56	22.62	22.62	0.91	178.80	300.00	22.41	22.41	0.00	1417.60	300.00
100.40.1	100	28.76	30.16	30.16	4.87	103.80	300.00	28.95	28.95	0.66	179.00	300.00	28.76	28.76	0.00	957.20	300.00
100.40.2	100	29.86	31.11	31.11	4.19	110.00	300.02	30.34	30.34	1.59	290.00	300.01	29.86	29.86	0.00	1421.40	300.00
100.40.3	100	28.24	30.13	30.13	6.68	93.00	300.00	28.42	28.42	0.65	199.80	300.00	28.24	28.24	0.00	1135.80	300.00
100.40.4	100	28.80	29.20	29.20	1.38	80.60	300.03	28.98	28.98	0.61	243.80	300.00	28.80	28.80	0.00	1368.40	300.00
150.10.1	150	8.74	12.20	12.20	39.64	1.00	314.10	10.95	10.95	25.33	1.00	301.42	8.74	8.74	0.00	148.60	300.01
150.10.2	150	8.24	10.97	10.97	33.17	1.00	306.55	9.53	9.53	15.65	1.00	302.23	8.24	8.24	0.00	151.40	300.01
150.10.3	150	8.44	12.62	12.62	49.51	1.00	314.53	11.22	11.22	32.86	1.00	301.38	8.44	8.44	0.00	174.00	300.02
150.10.4	150	8.85	13.26	13.26	49.93	1.00	311.60	10.64	10.64	20.26	1.00	301.54	8.85	8.85	0.00	93.40	300.04
150.20.1	150	17.34	22.88	22.88	32.00	1.00	301.58	18.09	18.09	4.37	9.60	300.05	17.34	17.34	0.00	157.80	300.01
150.20.2	150	16.84	25.13	25.13	49.23	1.00	305.24	19.41	19.41	15.25	1.00	300.52	16.84	16.84	0.00	192.60	300.00
150.20.3	150	17.72	24.44	24.44	37.87	1.00	302.61	18.80	18.80	6.06	1.00	300.22	17.72	17.72	0.00	130.20	300.01
150.20.4	150	16.88	25.40	25.40	50.46	1.00	304.52	19.90	19.90	17.89	1.00	300.32	16.88	16.88	0.00	136.80	300.01
150.30.1	150	25.53	33.17	33.17	29.94	1.00	301.68	26.75	26.75	4.79	30.20	300.01	25.53	25.53	0.00	234.40	300.00
150.30.2	150	26.30	34.88	34.88	32.62	1.00	301.96	27.52	27.52	4.63	27.00	300.01	26.30	26.30	0.00	353.60	300.00
150.30.3	150	25.58	32.73	32.73	27.94	1.00	302.14	26.36	26.36	3.01	29.60	300.02	25.58	25.58	0.00	302.00	300.00
150.30.4	150	26.27	33.85	33.85	28.86	1.00	304.10	28.30	28.30	7.72	18.20	300.01	26.27	26.27	0.00	303.20	300.00
150.40.1	150	34.23	46.14	46.14	34.81	1.00	301.55	35.10	35.10	2.53	49.00	300.01	34.23	34.23	0.00	336.40	300.00
150.40.2	150	37.30	54.22	54.22	45.36	1.00	300.64	37.73	37.73	1.14	44.20	300.01	37.30	37.30	0.00	326.40	300.00
150.40.3	150	36.54	43.04	43.04	17.80	1.00	300.19	37.73	37.73	3.26	50.80	300.00	36.54	36.54	0.00	393.40	300.00
150.40.4	150	35.01	42.12	42.12	20.29	1.00	300.42	35.96	35.96	2.71	55.20	300.01	35.01	35.01	0.00	353.20	300.00
200.10.1	200	10.07	15.10	15.10	49.94	1.00	311.58	12.00	12.00	19.16	6.80	300.07	10.07	10.07	0.00	108.20	300.01
200.10.2	200	9.88	16.21	16.21	64.11	1.00	320.26	14.00	14.00	41.76	1.00	301.04	9.88	9.88	0.00	49.00	300.01
200.10.3	200	10.04	15.53	15.53	54.67	1.00	336.04	13.73	13.73	36.77	1.00	301.69	10.04	10.04	0.00	53.60	300.01
200.10.4	200	10.27	14.44	14.44	40.59	1.00	303.26	12.31	12.31	19.85	1.00	301.21	10.27	10.27	0.00	72.40	300.01

Table 11 – continued from previous page

Instance	n	Obj*	HVNS-EDP					HVNS-NosubHDP					HVNS				
			Obj	$\overline{\text{Obj}}$	$\overline{\text{Gap}}$ (%)	Ite	Time (s)	Obj	$\overline{\text{Obj}}$	$\overline{\text{Gap}}$ (%)	Ite	Time (s)	Obj	$\overline{\text{Obj}}$	$\overline{\text{Gap}}$ (%)	Ite	Time (s)
200.20.1	200	21.02	29.34	29.34	39.59	1.00	324.63	28.64	28.64	36.28	1.00	300.35	21.02	21.02	0.00	85.00	300.01
200.20.2	200	21.79	30.05	30.05	37.92	1.00	309.94	26.48	26.48	21.55	1.00	301.00	21.79	21.79	0.00	161.80	300.01
200.20.3	200	20.53	27.89	27.89	35.87	1.00	321.43	22.65	22.65	10.32	1.00	300.29	20.53	20.53	0.00	81.80	300.01
200.20.4	200	19.59	27.84	27.84	42.15	1.00	308.41	25.69	25.69	31.14	1.00	300.24	19.59	19.59	0.00	79.60	300.02
200.30.1	200	30.40	43.17	43.17	41.98	1.00	318.69	33.90	33.90	11.51	13.00	300.02	30.40	30.40	0.00	124.20	300.00
200.30.2	200	30.92	44.83	44.83	44.97	1.00	301.84	33.36	33.36	7.89	12.20	300.02	30.92	30.92	0.00	119.40	300.01
200.30.3	200	31.64	47.57	47.57	50.35	1.00	301.23	33.00	33.00	4.31	21.80	300.03	31.64	31.64	0.00	106.80	300.01
200.30.4	200	32.05	44.58	44.58	39.11	1.00	300.72	34.17	34.17	6.62	5.20	300.01	32.05	32.05	0.00	133.80	300.01
200.40.1	200	41.48	57.06	57.06	37.55	1.00	304.25	42.96	42.96	3.56	29.20	300.01	41.48	41.48	0.00	153.00	300.00
200.40.2	200	42.62	62.19	62.19	45.91	1.00	303.78	45.33	45.33	6.35	1.00	300.27	42.62	42.62	0.00	154.80	300.00
200.40.3	200	43.09	55.08	55.08	27.82	1.00	300.82	45.95	45.95	6.63	26.60	300.01	43.09	43.09	0.00	151.60	300.00
200.40.4	200	43.24	60.37	60.37	39.61	1.00	302.45	44.27	44.27	2.39	38.60	300.01	43.24	43.24	0.00	154.00	300.00

Table 12: Detailed results of three configurations for the VRPD-M

Instance	n	Obj*	HVNS-EDP					HVNS-NosubHDP					HVNS				
			Obj	$\overline{\text{Obj}}$	$\overline{\text{Gap}}$ (%)	Ite	Time (s)	Obj	$\overline{\text{Obj}}$	$\overline{\text{Gap}}$ (%)	Ite	Time (s)	Obj	$\overline{\text{Obj}}$	$\overline{\text{Gap}}$ (%)	Ite	Time (s)
singlecenter-61-n20	19	361.10	361.10	361.10	0.00	10000.00	54.20	361.10	361.10	0.00	10000.00	29.32	361.10	361.10	0.00	10000.00	19.94
singlecenter-62-n20	19	288.97	288.97	288.97	0.00	10000.00	50.89	288.97	288.97	0.00	10000.00	47.87	288.97	288.97	0.00	10000.00	34.76
singlecenter-63-n20	19	401.07	401.07	401.07	0.00	10000.00	52.76	401.07	401.07	0.00	10000.00	26.73	401.07	401.07	0.00	10000.00	16.67
singlecenter-64-n20	19	331.81	331.81	331.81	0.00	10000.00	93.30	331.81	331.81	0.00	10000.00	40.08	331.81	331.81	0.00	10000.00	33.78
singlecenter-65-n20	19	335.58	335.58	335.58	0.00	10000.00	50.94	335.58	335.58	0.00	10000.00	25.40	335.58	335.58	0.00	10000.00	19.94
singlecenter-66-n20	19	331.64	331.64	331.64	0.00	10000.00	38.81	331.64	331.64	0.00	10000.00	21.71	331.64	331.64	0.00	10000.00	16.38
singlecenter-67-n20	19	341.43	341.43	341.43	0.00	10000.00	51.49	341.43	341.43	0.00	10000.00	19.72	341.43	341.43	0.00	10000.00	17.02
singlecenter-68-n20	19	394.28	394.28	394.28	0.00	10000.00	71.39	394.28	394.28	0.00	10000.00	29.65	394.28	394.28	0.00	10000.00	13.90
singlecenter-69-n20	19	403.61	403.61	403.61	0.00	10000.00	31.03	403.61	403.61	0.00	10000.00	29.03	403.61	403.61	0.00	10000.00	14.16
singlecenter-70-n20	19	297.87	297.87	297.87	0.00	10000.00	103.76	297.87	297.87	0.00	10000.00	41.14	297.87	297.87	0.00	10000.00	20.19
doublecenter-61-n20	19	678.53	678.53	678.53	0.00	10000.00	31.57	678.53	678.53	0.00	10000.00	15.06	678.53	678.53	0.00	10000.00	11.15
doublecenter-62-n20	19	656.74	656.74	656.91	0.02	10000.00	52.98	656.74	656.74	0.00	10000.00	43.52	656.74	657.07	0.05	10000.00	20.87
doublecenter-63-n20	19	537.09	537.09	537.09	0.00	10000.00	12.06	537.09	537.09	0.00	10000.00	10.98	537.09	537.09	0.00	10000.00	8.88
doublecenter-64-n20	19	867.47	867.47	867.47	0.00	10000.00	59.57	867.47	867.47	0.00	10000.00	23.89	867.47	867.47	0.00	10000.00	14.97
doublecenter-65-n20	19	456.69	456.69	456.69	0.00	10000.00	23.36	456.69	456.69	0.00	10000.00	15.17	456.69	456.69	0.00	10000.00	11.46
doublecenter-66-n20	19	626.85	626.85	626.86	0.00	10000.00	40.76	626.85	626.85	0.00	10000.00	28.31	626.85	626.85	0.00	10000.00	14.00
doublecenter-67-n20	19	496.38	496.38	496.38	0.00	10000.00	23.19	496.38	496.38	0.00	10000.00	18.38	496.38	496.38	0.00	10000.00	17.15
doublecenter-68-n20	19	546.79	546.79	546.79	0.00	10000.00	34.38	546.79	546.79	0.00	10000.00	16.23	546.79	546.79	0.00	10000.00	13.75
doublecenter-69-n20	19	611.58	611.58	611.58	0.00	10000.00	34.76	611.58	611.58	0.00	10000.00	25.03	611.58	611.58	0.00	10000.00	12.79
doublecenter-70-n20	19	580.05	580.05	580.05	0.00	10000.00	25.73	580.05	580.05	0.00	10000.00	21.21	580.05	580.05	0.00	10000.00	11.43
uniform-61-n20	19	232.59	232.59	232.59	0.00	10000.00	62.06	232.59	232.59	0.00	10000.00	38.18	232.59	232.59	0.00	10000.00	17.14
uniform-62-n20	19	222.52	222.52	222.52	0.00	10000.00	32.79	222.52	222.52	0.00	10000.00	19.05	222.52	222.52	0.00	10000.00	14.03
uniform-63-n20	19	221.17	221.17	221.17	0.00	10000.00	31.57	221.17	221.17	0.00	10000.00	19.44	221.17	221.17	0.00	10000.00	10.60
uniform-64-n20	19	231.94	231.94	231.94	0.00	10000.00	60.15	231.94	232.07	0.06	10000.00	41.17	231.94	231.94	0.00	10000.00	19.90
uniform-65-n20	19	269.33	269.33	269.33	0.00	10000.00	37.50	269.33	269.40	0.02	10000.00	20.64	269.33	269.44	0.04	10000.00	12.97
uniform-66-n20	19	284.67	284.67	284.67	0.00	10000.00	29.19	284.67	284.67	0.00	10000.00	16.99	284.67	284.67	0.00	10000.00	10.10
uniform-67-n20	19	261.49	261.49	261.49	0.00	10000.00	27.54	261.49	261.82	0.13	10000.00	16.16	261.49	262.48	0.38	10000.00	15.64
uniform-68-n20	19	277.40	277.40	277.40	0.00	10000.00	22.21	277.40	277.40	0.00	10000.00	13.47	277.40	277.40	0.00	10000.00	9.66
uniform-69-n20	19	230.91	230.91	230.91	0.00	10000.00	28.92	230.91	230.91	0.00	10000.00	18.65	230.91	230.91	0.00	10000.00	11.71
uniform-70-n20	19	251.01	251.01	251.01	0.00	10000.00	35.25	251.01	251.01	0.00	10000.00	22.28	251.01	251.01	0.00	10000.00	17.95
singlecenter-71-n50	49	279.86	279.86	281.23	0.49	372.40	300.00	279.86	279.86	0.00	2414.80	300.00	279.86	280.96	0.40	7498.00	300.00
singlecenter-72-n50	49	356.93	356.93	356.93	0.00	343.40	300.00	356.93	356.93	0.00	1848.80	300.00	356.93	356.93	0.00	6062.80	300.00

Table 12 – continued from previous page

Instance	n	Obj*	HVNS-EDP					HVNS-NosubHDP					HVNS				
			Obj	$\overline{\text{Obj}}$	$\overline{\text{Gap}}$ (%)	Ite	Time (s)	Obj	$\overline{\text{Obj}}$	$\overline{\text{Gap}}$ (%)	Ite	Time (s)	Obj	$\overline{\text{Obj}}$	$\overline{\text{Gap}}$ (%)	Ite	Time (s)
singlecenter-73-n50	49	231.62	231.62	232.53	0.39	216.60	300.01	231.62	231.62	0.00	1324.60	300.00	231.62	231.88	0.11	5753.80	300.00
singlecenter-74-n50	49	390.59	390.59	390.90	0.08	486.20	300.00	390.59	390.59	0.00	1531.00	300.00	390.59	390.77	0.05	7236.80	299.62
singlecenter-75-n50	49	450.89	450.89	451.41	0.12	331.00	300.00	450.89	450.89	0.00	1241.80	300.00	450.89	451.00	0.03	4458.40	300.00
singlecenter-76-n50	49	398.82	398.82	398.86	0.01	437.80	300.00	398.82	398.82	0.00	2086.20	300.00	398.82	398.86	0.01	8341.80	261.01
singlecenter-77-n50	49	351.19	351.19	352.30	0.32	209.40	300.00	351.19	351.27	0.03	770.80	300.00	351.19	351.19	0.00	4468.40	300.00
singlecenter-78-n50	49	427.82	427.82	428.82	0.23	318.20	300.00	427.82	428.89	0.25	1589.40	300.00	427.82	427.82	0.00	4508.00	300.00
singlecenter-79-n50	49	349.10	349.10	349.18	0.02	247.40	300.00	349.10	349.10	0.00	1686.80	300.00	349.10	349.10	0.00	6865.00	300.00
singlecenter-80-n50	49	459.90	459.90	460.49	0.13	476.40	300.01	459.90	459.93	0.01	2118.20	300.00	459.90	459.90	0.00	7370.20	263.51
doublecenter-71-n50	49	809.95	809.95	809.95	0.00	503.00	300.00	809.95	809.95	0.00	1964.80	300.00	809.95	809.95	0.00	9977.80	290.27
doublecenter-72-n50	49	729.16	729.16	731.03	0.26	776.00	300.00	729.16	729.76	0.08	3927.60	300.00	729.16	729.16	0.00	7356.80	280.49
doublecenter-73-n50	49	675.50	675.50	675.50	0.00	386.80	300.01	675.50	675.98	0.07	3522.00	300.00	675.50	675.73	0.03	8764.20	274.34
doublecenter-74-n50	49	657.37	657.37	660.96	0.55	474.20	300.00	657.37	657.37	0.00	3119.60	300.00	657.37	658.23	0.13	10000.00	248.57
doublecenter-75-n50	49	771.37	771.37	775.19	0.50	800.00	300.00	771.37	771.37	0.00	3960.20	300.00	771.37	771.37	0.00	8297.00	238.35
doublecenter-76-n50	49	758.38	758.38	759.53	0.15	488.20	300.00	758.38	758.38	0.00	4411.40	300.00	758.38	759.41	0.14	7432.00	251.86
doublecenter-77-n50	49	715.30	715.30	716.45	0.16	503.00	300.00	715.30	715.30	0.00	2055.40	300.00	715.30	715.55	0.03	7002.20	300.00
doublecenter-78-n50	49	701.40	701.40	701.53	0.02	981.20	300.01	701.40	701.40	0.00	2837.00	300.00	701.40	701.47	0.01	7422.00	263.55
doublecenter-79-n50	49	667.02	667.02	667.04	0.00	1048.60	300.00	667.02	667.02	0.00	3159.00	300.00	667.02	667.02	0.00	10000.00	258.34
doublecenter-80-n50	49	794.81	794.81	795.50	0.09	1449.60	300.00	794.81	794.81	0.00	3976.60	300.00	794.81	794.81	0.00	7812.60	203.59
uniform-71-n50	49	274.92	274.92	276.26	0.49	648.40	300.00	274.92	275.37	0.16	2413.60	300.00	274.92	274.92	0.00	5782.60	300.00
uniform-72-n50	49	286.38	286.38	286.42	0.02	536.60	300.00	286.38	286.38	0.00	2972.40	300.00	286.38	286.41	0.01	9628.20	294.54
uniform-73-n50	49	283.60	283.60	284.24	0.23	900.40	300.00	283.60	283.60	0.00	2373.00	300.00	283.60	283.60	0.00	9438.20	277.27
uniform-74-n50	49	289.81	289.81	290.50	0.24	485.80	300.00	289.81	290.07	0.09	2275.60	300.00	289.81	289.81	0.00	6790.20	300.00
uniform-75-n50	49	282.46	282.46	282.95	0.18	492.40	300.00	282.46	282.46	0.00	3187.80	300.00	282.46	283.09	0.22	8807.00	267.35
uniform-76-n50	49	260.05	260.05	260.58	0.21	752.20	300.00	260.05	260.05	0.00	2879.60	300.00	260.05	262.69	1.02	10000.00	234.79
uniform-77-n50	49	285.22	285.22	287.11	0.66	730.80	300.00	285.22	285.58	0.13	2946.20	300.00	285.22	285.22	0.00	8121.20	300.00
uniform-78-n50	49	280.18	280.18	280.92	0.27	913.20	300.00	280.18	280.18	0.00	3879.60	300.00	280.18	281.07	0.32	9007.80	283.26
uniform-79-n50	49	277.56	277.56	279.15	0.57	390.80	300.02	277.56	278.70	0.41	3409.60	300.00	277.56	277.56	0.00	5865.80	300.00
uniform-80-n50	49	252.27	252.27	252.27	0.00	617.60	300.00	252.27	252.27	0.00	3045.20	300.00	252.27	252.31	0.02	9605.00	291.20
singlecenter-81-n75	74	549.00	549.00	668.56	21.78	22.60	300.05	549.00	549.00	0.00	308.00	300.00	549.00	553.77	0.87	1406.00	300.00
singlecenter-82-n75	74	391.46	391.46	413.31	5.58	38.20	300.02	391.46	391.46	0.00	273.60	300.00	391.46	391.48	0.01	1686.60	300.00
singlecenter-83-n75	74	430.37	430.37	437.12	1.57	17.60	300.08	430.37	430.37	0.00	206.80	300.02	430.37	430.66	0.07	1332.80	300.00
singlecenter-84-n75	74	451.47	451.47	565.01	25.15	30.80	300.02	451.47	451.47	0.00	261.40	300.00	451.47	452.69	0.27	1577.80	300.00
singlecenter-85-n75	74	390.61	390.61	417.59	6.91	25.60	300.05	390.61	390.61	0.00	108.60	300.01	390.61	394.08	0.89	939.00	300.00
singlecenter-86-n75	74	552.49	552.49	771.08	39.57	22.20	300.08	552.49	555.68	0.58	247.00	300.00	552.49	552.49	0.00	1521.00	300.00

Table 12 – continued from previous page

Instance	n	Obj*	HVNS-EDP					HVNS-NosubHDP					HVNS				
			Obj	$\overline{\text{Obj}}$	$\overline{\text{Gap}}$ (%)	Ite	Time (s)	Obj	$\overline{\text{Obj}}$	$\overline{\text{Gap}}$ (%)	Ite	Time (s)	Obj	$\overline{\text{Obj}}$	$\overline{\text{Gap}}$ (%)	Ite	Time (s)
singlecenter-87-n75	74	502.61	502.61	708.03	40.87	29.80	300.07	502.61	502.61	0.00	234.20	300.00	502.61	503.63	0.20	1014.60	300.00
singlecenter-88-n75	74	565.73	565.73	776.81	37.31	15.00	300.04	565.73	565.76	0.00	121.40	300.01	565.73	565.73	0.00	1373.60	300.00
singlecenter-89-n75	74	440.58	440.58	620.12	40.75	30.80	300.05	440.58	444.65	0.93	264.60	300.00	440.58	440.58	0.00	1317.00	300.00
singlecenter-90-n75	74	490.44	490.44	507.49	3.48	23.60	300.05	490.44	491.29	0.17	226.40	300.00	490.44	490.44	0.00	2326.20	300.00
doublecenter-81-n75	74	676.19	676.19	889.35	31.52	34.60	300.04	676.19	678.41	0.33	248.60	300.00	676.19	676.19	0.00	2023.00	300.00
doublecenter-82-n75	74	768.98	768.98	778.17	1.20	61.20	300.05	768.98	768.98	0.00	288.40	300.00	768.98	770.39	0.18	2283.20	300.00
doublecenter-83-n75	74	790.42	790.42	805.72	1.94	54.80	300.03	790.42	795.61	0.66	380.60	300.00	790.42	790.42	0.00	1375.00	300.00
doublecenter-84-n75	74	928.31	928.31	935.87	0.81	70.00	300.01	928.31	928.31	0.00	408.80	300.00	928.31	933.39	0.55	2715.00	300.00
doublecenter-85-n75	74	955.27	955.27	973.14	1.87	87.00	300.01	955.27	955.27	0.00	441.80	300.00	955.27	955.57	0.03	2371.40	300.00
doublecenter-86-n75	74	749.16	749.16	752.29	0.42	49.40	300.05	749.16	749.16	0.00	591.20	300.00	749.16	749.40	0.03	1863.40	300.00
doublecenter-87-n75	74	798.30	798.30	807.75	1.18	41.00	300.01	798.30	798.30	0.00	336.40	300.00	798.30	798.46	0.02	1275.20	300.00
doublecenter-88-n75	74	953.06	953.06	1109.68	16.43	29.60	300.04	953.06	953.06	0.00	403.80	300.00	953.06	956.18	0.33	1908.80	300.00
doublecenter-89-n75	74	776.12	776.12	807.98	4.10	42.80	300.05	776.12	778.72	0.33	436.00	300.00	776.12	776.12	0.00	1908.80	300.00
doublecenter-90-n75	74	759.29	759.29	771.93	1.67	78.60	300.01	759.29	759.29	0.00	404.80	300.00	759.29	760.85	0.21	2195.80	300.00
uniform-81-n75	74	296.77	296.77	305.40	2.91	54.80	300.01	296.77	296.77	0.00	454.60	300.00	296.77	297.04	0.09	2386.60	300.00
uniform-82-n75	74	276.40	276.40	280.45	1.47	43.40	300.02	276.40	276.40	0.00	352.00	300.00	276.40	277.09	0.25	1409.60	300.00
uniform-83-n75	74	281.72	281.72	293.85	4.31	42.20	300.03	281.72	283.36	0.58	314.60	300.00	281.72	281.72	0.00	1541.40	300.00
uniform-84-n75	74	302.55	302.55	344.53	13.87	41.40	300.03	302.55	305.29	0.90	245.20	300.01	302.55	302.55	0.00	1551.80	300.00
uniform-85-n75	74	310.47	310.47	317.88	2.39	57.80	300.03	310.47	310.47	0.00	468.80	300.00	310.47	310.54	0.02	2317.80	300.00
uniform-86-n75	74	291.20	291.20	300.17	3.08	40.40	300.05	291.20	292.86	0.57	210.60	300.00	291.20	291.20	0.00	1544.40	300.00
uniform-87-n75	74	300.53	300.53	345.02	14.80	36.00	300.03	300.53	302.21	0.56	338.80	300.01	300.53	300.53	0.00	2079.40	300.00
uniform-88-n75	74	298.58	298.58	304.22	1.89	45.00	300.02	298.58	298.98	0.13	426.60	300.00	298.58	298.58	0.00	1878.60	300.00
uniform-89-n75	74	286.79	286.79	291.25	1.56	49.00	300.03	286.79	286.79	0.00	427.00	300.00	286.79	287.34	0.19	1765.60	300.00
uniform-90-n75	74	298.98	298.98	304.25	1.76	31.40	300.04	298.98	299.82	0.28	369.60	300.00	298.98	298.98	0.00	1659.60	300.00
singlecenter-91-n100	99	537.15	537.15	1129.10	110.20	1.00	301.17	537.15	541.41	0.79	47.40	300.02	537.15	537.15	0.00	270.00	300.00
singlecenter-92-n100	99	603.04	603.04	1022.09	69.49	1.00	302.37	603.04	612.11	1.50	63.20	300.02	603.04	603.04	0.00	406.60	300.00
singlecenter-93-n100	99	635.56	635.56	873.73	37.47	1.00	301.22	635.56	648.95	2.11	68.20	300.04	635.56	635.56	0.00	385.00	300.00
singlecenter-94-n100	99	654.40	654.40	1200.01	83.38	1.00	301.92	654.40	663.08	1.33	24.00	300.02	654.40	654.40	0.00	643.20	300.00
singlecenter-95-n100	99	454.55	454.55	868.11	90.98	1.00	300.49	454.55	454.55	0.00	86.60	300.02	454.55	455.53	0.22	615.00	300.00
singlecenter-96-n100	99	575.16	575.16	745.09	29.55	1.00	300.58	575.16	581.54	1.11	66.80	300.01	575.16	575.16	0.00	702.60	300.00
singlecenter-97-n100	99	608.38	608.38	1134.46	86.47	1.00	300.51	608.38	611.40	0.50	38.20	300.04	608.38	608.38	0.00	493.40	300.00
singlecenter-98-n100	99	614.03	614.03	1063.20	73.15	1.00	301.86	614.03	621.66	1.24	46.00	300.01	614.03	614.03	0.00	347.20	300.00
singlecenter-99-n100	99	427.06	427.06	644.76	50.98	1.00	301.18	427.06	444.83	4.16	47.00	300.02	427.06	427.06	0.00	440.60	300.00
singlecenter-100-n100	99	518.55	518.55	958.76	84.89	1.00	301.54	518.55	529.95	2.20	83.00	300.01	518.55	518.55	0.00	617.80	300.00

Table 12 – continued from previous page

Instance	n	Obj*	HVNS-EDP					HVNS-NosubHDP					HVNS				
			Obj	$\overline{\text{Obj}}$	$\overline{\text{Gap}}$ (%)	Ite	Time (s)	Obj	$\overline{\text{Obj}}$	$\overline{\text{Gap}}$ (%)	Ite	Time (s)	Obj	$\overline{\text{Obj}}$	$\overline{\text{Gap}}$ (%)	Ite	Time (s)
doublecenter-91-n100	99	791.47	791.47	1409.36	78.07	1.00	301.24	791.47	804.32	1.62	45.60	300.02	791.47	791.47	0.00	405.80	300.00
doublecenter-92-n100	99	840.28	840.28	1464.01	74.23	1.00	300.89	840.28	853.11	1.53	70.80	300.02	840.28	840.28	0.00	326.60	300.00
doublecenter-93-n100	99	825.86	825.86	1102.38	33.48	1.60	300.22	825.86	825.86	0.00	104.80	300.01	825.86	827.18	0.16	641.00	300.00
doublecenter-94-n100	99	868.18	868.18	1361.43	56.81	1.00	302.24	868.18	875.19	0.81	171.80	300.00	868.18	868.18	0.00	939.60	300.00
doublecenter-95-n100	99	873.36	873.36	1471.66	68.50	1.80	300.35	873.36	883.91	1.21	61.20	300.06	873.36	873.36	0.00	887.00	300.00
doublecenter-96-n100	99	918.98	918.98	1409.17	53.34	1.40	301.28	918.98	921.91	0.32	89.20	300.00	918.98	918.98	0.00	453.60	300.00
doublecenter-97-n100	99	1004.51	1004.51	1290.07	28.43	3.60	300.76	1004.51	1013.63	0.91	94.80	300.00	1004.51	1004.51	0.00	1170.00	300.00
doublecenter-98-n100	99	846.10	846.10	1196.01	41.36	1.00	300.86	846.10	863.41	2.05	138.20	300.01	846.10	846.10	0.00	479.00	300.00
doublecenter-99-n100	99	836.25	836.25	1265.10	51.28	1.00	300.75	836.25	848.38	1.45	63.40	300.01	836.25	836.25	0.00	436.80	300.00
doublecenter-100-n100	99	920.02	920.02	1277.94	38.90	8.00	300.18	920.02	923.79	0.41	176.60	300.01	920.02	920.02	0.00	968.40	300.00
uniform-91-n100	99	325.90	325.90	508.74	56.10	1.00	301.37	325.90	327.60	0.52	108.20	300.00	325.90	325.90	0.00	504.60	300.00
uniform-92-n100	99	301.57	301.57	497.79	65.07	1.40	302.25	301.57	303.69	0.70	74.20	300.01	301.57	301.57	0.00	1106.20	300.00
uniform-93-n100	99	302.88	302.88	466.65	54.07	1.00	301.10	302.88	307.58	1.55	168.80	300.01	302.88	302.88	0.00	802.20	300.00
uniform-94-n100	99	327.15	327.15	490.03	49.79	1.00	300.69	327.15	330.30	0.96	67.00	300.01	327.15	327.15	0.00	500.80	300.00
uniform-95-n100	99	330.99	330.99	521.32	57.50	1.00	304.94	330.99	333.47	0.75	88.40	300.03	330.99	330.99	0.00	1018.20	300.00
uniform-96-n100	99	326.89	326.89	582.38	78.16	1.00	301.47	326.89	329.26	0.72	110.60	300.01	326.89	326.89	0.00	793.20	300.00
uniform-97-n100	99	339.52	339.52	544.41	60.35	2.00	302.03	339.52	341.39	0.55	116.40	300.02	339.52	339.52	0.00	778.60	300.00
uniform-98-n100	99	321.93	321.93	442.56	37.47	1.00	300.89	321.93	322.59	0.20	108.40	300.01	321.93	321.93	0.00	658.40	300.00
uniform-99-n100	99	339.14	339.14	448.82	32.34	2.40	300.60	339.14	341.87	0.81	143.00	300.00	339.14	339.14	0.00	903.60	300.00
uniform-100-n100	99	318.46	318.46	585.27	83.78	1.00	301.12	318.46	318.46	0.00	115.60	300.01	318.46	322.49	1.27	892.00	300.00
singlecenter-101-n175	174	712.21	712.21	1235.96	73.54	1.00	305.65	712.21	1044.47	46.65	1.00	300.57	712.21	712.21	0.00	39.80	300.00
singlecenter-102-n175	174	754.98	754.98	1184.30	56.86	1.00	305.31	754.98	1156.17	53.14	1.00	300.66	754.98	754.98	0.00	53.00	300.01
singlecenter-103-n175	174	678.41	678.41	1353.31	99.48	1.00	306.81	678.41	1107.80	63.29	1.00	300.88	678.41	678.41	0.00	42.40	300.01
singlecenter-104-n175	174	740.50	740.50	1311.79	77.15	1.00	301.31	740.50	1056.48	42.67	1.00	300.48	740.50	740.50	0.00	62.80	300.01
singlecenter-105-n175	174	769.95	769.95	1280.68	66.33	1.00	309.01	769.95	1171.36	52.14	1.00	300.68	769.95	769.95	0.00	39.60	300.01
singlecenter-106-n175	174	808.61	808.61	1485.11	83.66	1.00	308.75	808.61	1016.68	25.73	1.00	300.33	808.61	808.61	0.00	34.80	300.00
singlecenter-107-n175	174	771.88	771.88	1703.50	120.69	1.00	309.03	771.88	958.70	24.20	1.00	300.27	771.88	771.88	0.00	48.20	300.02
singlecenter-108-n175	174	763.36	763.36	1253.63	64.23	1.00	303.10	763.36	1121.63	46.93	1.00	300.32	763.36	763.36	0.00	50.20	300.01
singlecenter-109-n175	174	710.04	710.04	1183.52	66.68	1.00	304.31	710.04	1090.30	53.55	1.00	300.46	710.04	710.04	0.00	67.00	300.01
singlecenter-110-n175	174	707.57	707.57	1085.23	53.37	1.00	305.52	707.57	1110.29	56.92	1.00	300.63	707.57	707.57	0.00	49.60	300.00
doublecenter-101-n175	174	961.54	961.54	1419.39	47.62	1.00	302.28	961.54	1423.86	48.08	1.00	300.56	961.54	961.54	0.00	69.60	300.01
doublecenter-102-n175	174	1018.01	1018.01	1574.95	54.71	1.00	303.68	1018.01	1445.56	42.00	1.00	300.28	1018.01	1018.01	0.00	159.20	300.00
doublecenter-103-n175	174	1094.74	1094.74	1615.58	47.58	1.00	306.40	1094.74	1484.62	35.61	1.00	300.32	1094.74	1094.74	0.00	91.00	300.00
doublecenter-104-n175	174	1088.03	1088.03	1883.32	73.09	1.00	307.27	1088.03	1579.13	45.14	1.00	300.52	1088.03	1088.03	0.00	112.00	300.00

Table 12 – continued from previous page

Instance	n	Obj*	HVNS-EDP					HVNS-NosubHDP					HVNS				
			Obj	$\overline{\text{Obj}}$	$\overline{\text{Gap}}$ (%)	Ite	Time (s)	Obj	$\overline{\text{Obj}}$	$\overline{\text{Gap}}$ (%)	Ite	Time (s)	Obj	$\overline{\text{Obj}}$	$\overline{\text{Gap}}$ (%)	Ite	Time (s)
doublecenter-105-n175	174	1132.88	1132.88	2342.41	106.77	1.00	308.09	1132.88	1562.71	37.94	1.00	300.28	1132.88	1132.88	0.00	109.40	300.01
doublecenter-106-n175	174	1127.92	1127.92	1702.05	50.90	1.00	309.16	1127.92	1432.83	27.03	1.00	300.50	1127.92	1127.92	0.00	72.60	300.00
doublecenter-107-n175	174	1005.04	1005.04	1594.21	58.62	1.00	308.61	1005.04	1407.43	40.04	1.00	300.31	1005.04	1005.04	0.00	66.80	300.01
doublecenter-108-n175	174	1114.80	1114.80	2142.47	92.18	1.00	305.82	1114.80	1600.12	43.54	1.00	300.98	1114.80	1114.80	0.00	49.20	300.01
doublecenter-109-n175	174	1060.22	1060.22	1647.81	55.42	1.00	303.41	1060.22	1307.52	23.33	1.00	300.25	1060.22	1060.22	0.00	44.80	300.01
doublecenter-110-n175	174	1119.43	1119.43	1892.11	69.02	1.00	303.67	1119.43	1574.85	40.68	1.00	300.27	1119.43	1119.43	0.00	77.00	300.01
uniform-101-n175	174	389.26	389.26	699.90	79.80	1.00	305.91	389.26	571.91	46.92	1.00	300.60	389.26	389.26	0.00	54.00	300.00
uniform-102-n175	174	391.86	391.86	848.00	116.40	1.00	314.92	391.86	582.41	48.63	1.00	300.39	391.86	391.86	0.00	110.20	300.01
uniform-103-n175	174	393.51	393.51	728.70	85.18	1.00	305.03	393.51	639.05	62.40	1.00	300.67	393.51	393.51	0.00	116.60	300.01
uniform-104-n175	174	390.79	390.79	842.95	115.70	1.00	305.93	390.79	575.02	47.14	1.00	300.53	390.79	390.79	0.00	90.60	300.01
uniform-105-n175	174	391.04	391.04	750.78	92.00	1.00	306.20	391.04	606.57	55.12	1.00	300.34	391.04	391.04	0.00	107.80	300.00
uniform-106-n175	174	384.30	384.30	711.55	85.16	1.00	307.60	384.30	507.97	32.18	1.00	300.35	384.30	384.30	0.00	129.80	300.01
uniform-107-n175	174	384.38	384.38	708.05	84.20	1.00	305.97	384.38	507.55	32.04	1.00	300.41	384.38	384.38	0.00	123.80	300.00
uniform-108-n175	174	398.47	398.47	632.90	58.83	1.00	310.31	398.47	633.98	59.10	1.00	300.71	398.47	398.47	0.00	84.40	300.01
uniform-109-n175	174	388.07	388.07	749.78	93.21	1.00	306.73	388.07	529.69	36.49	1.00	300.49	388.07	388.07	0.00	74.60	300.01
uniform-110-n175	174	381.66	381.66	708.15	85.54	1.00	310.47	381.66	468.37	22.72	1.00	300.66	381.66	381.66	0.00	107.80	300.00

3. Detailed results on benchmarks for VRPD-C in Section 6.3.1

Table 13 presents detailed results of our HVNS in five runs and results from Sacramento et al. (2019) and Rave et al. (2022) for the VRPD-C. The notations in the table are defined as follows.

Instance: The name of the instance.

n: The number of customers in the instance.

Obj^{best}: The best objective function value obtained from ten runs of SPR and RFK, and the best objective function value obtained from five runs of our HVNS.

$\overline{\text{Obj}}^{10}$: The average objective function value obtained from ten runs of SPR and RFK.

$\overline{\text{Obj}}^{5}$: The average objective function value obtained from five runs of our HVNS.

Gap^{SPR} (%): The gap between best objective function values obtained by the HVNS and by SPR.

Gap^{RFK} (%): The gap between best objective function values obtained by the HVNS and by RFK.

$\overline{\text{Gap}}^{\text{SPR}}$ (%): The gap between average objective function values obtained by the HVNS and by SPR.

$\overline{\text{Gap}}^{\text{RFK}}$ (%): The gap between average objective function values obtained by the HVNS and by RFK.

Time (s): The average computational time.

Ite: The average number of iterations.

Table 13: Detailed results of our HVNS compared with benchmarks on SPR and RFK

Instance	n	SPR		RFK		HVNS							
		Obj^{best}	$\overline{\text{Obj}}^{10}$	Obj^{best}	$\overline{\text{Obj}}^{10}$	Obj^{best}	$\overline{\text{Obj}}^{5}$	Gap^{SPR} (%)	Gap^{RFK} (%)	$\overline{\text{Gap}}^{\text{SPR}}$ (%)	$\overline{\text{Gap}}^{\text{RFK}}$ (%)	Time (s)	Ite
6.5.1	6	1.0982	1.0982	1.0982	1.0982	1.0982	1.0982	0.00	0.00	0.00	0.00	2.71	10000.00
6.5.2	6	0.8422	0.8422	0.8422	0.8422	0.8422	0.8422	0.00	0.00	0.00	0.00	2.28	10000.00
6.5.3	6	1.2114	1.2114	1.2114	1.2114	1.2114	1.2114	0.00	0.00	0.00	0.00	1.15	10000.00
6.5.4	6	0.9460	0.9460	0.9460	0.9460	0.9460	0.9460	0.00	0.00	0.00	0.00	2.30	10000.00
6.10.1	6	2.4061	2.4061	2.4061	2.4061	2.4061	2.4061	0.00	0.00	0.00	0.00	2.20	10000.00
6.10.2	6	1.6793	1.6793	1.6793	1.6793	1.6793	1.6793	0.00	0.00	0.00	0.00	1.69	10000.00
6.10.3	6	1.3255	1.3255	1.3255	1.3255	1.3255	1.3255	0.00	0.00	0.00	0.00	2.44	10000.00
6.10.4	6	1.4431	1.4431	1.4431	1.4431	1.4431	1.4431	0.00	0.00	0.00	0.00	1.70	10000.00
6.20.1	6	2.6776	2.6776	2.6776	2.6776	2.6776	2.6776	0.00	0.00	0.00	0.00	1.80	10000.00
6.20.2	6	4.3196	4.3196	4.3196	4.3196	4.3196	4.3196	0.00	0.00	0.00	0.00	1.12	10000.00
6.20.3	6	3.8248	3.8248	3.8248	3.8247	3.8248	3.8248	0.00	0.00	0.00	0.00	1.11	10000.00
6.20.4	6	3.6787	3.6787	3.6787	3.6787	3.6787	3.6787	0.00	0.00	0.00	0.00	1.06	10000.00
10.5.1	10	1.6556	1.6556	1.6556	1.6556	1.6556	1.6556	0.00	0.00	0.00	0.00	1.76	10000.00
10.5.2	10	1.4519	1.4519	1.4519	1.4519	1.4519	1.4519	0.00	0.00	0.00	0.00	4.91	10000.00
10.5.3	10	1.4736	1.4736	1.4736	1.4736	1.4736	1.4736	0.00	0.00	0.00	0.00	3.61	10000.00
10.5.4	10	1.2849	1.2849	1.2849	1.2849	1.2849	1.2849	0.00	0.00	0.00	0.00	6.91	10000.00
10.10.1	10	2.3265	2.3265	2.3265	2.3265	2.3265	2.3265	0.00	0.00	0.00	0.00	4.87	10000.00
10.10.2	10	3.1586	3.1586	3.1586	3.1586	3.1586	3.1586	0.00	0.00	0.00	0.00	4.15	10000.00
10.10.3	10	2.5527	2.5527	2.5527	2.5527	2.5527	2.5527	0.00	0.00	0.00	0.00	6.03	10000.00
10.10.4	10	2.5393	2.5393	2.5393	2.5393	2.5393	2.5393	0.00	0.00	0.00	0.00	3.56	10000.00
10.20.1	10	4.4524	4.4524	4.4524	4.4524	4.4524	4.4524	0.00	0.00	0.00	0.00	2.06	10000.00

Table 13 – continued from previous page

Instance	n	SPR		RFK		HVNS							
		Obj^{best}	$\overline{\text{Obj}}^{10}$	Obj^{best}	$\overline{\text{Obj}}^{10}$	Obj^{best}	$\overline{\text{Obj}}^{5}$	Gap^{SPR} (%)	Gap^{RFK} (%)	$\overline{\text{Gap}}^{\text{SPR}}$ (%)	$\overline{\text{Gap}}^{\text{RFK}}$ (%)	Time (s)	Ite
10.20.2	10	6.1678	6.1678	6.1678	6.1678	6.1678	6.1678	0.00	0.00	0.00	0.00	1.41	10000.00
10.20.3	10	4.5463	4.5463	4.5463	4.5463	4.5463	4.5463	0.00	0.00	0.00	0.00	2.19	10000.00
10.20.4	10	6.1536	6.1536	6.1536	6.1668	6.1536	6.1536	0.00	0.00	0.00	-0.21	3.90	10000.00
12.5.1	12	1.3738	1.3738	1.3738	1.3738	1.3738	1.3738	0.00	0.00	0.00	0.00	8.24	10000.00
12.5.2	12	1.0590	1.0590	1.0590	1.0590	1.0590	1.0590	0.00	0.00	0.00	0.00	19.27	10000.00
12.5.3	12	1.4477	1.4477	1.4477	1.4477	1.4477	1.4477	0.00	0.00	0.00	0.00	8.25	10000.00
12.5.4	12	1.5810	1.5810	1.5810	1.5810	1.5810	1.5810	0.00	0.00	0.00	0.00	4.29	10000.00
12.10.1	12	2.6810	2.6810	2.6810	2.6810	2.6810	2.6810	0.00	0.00	0.00	0.00	13.79	10000.00
12.10.2	12	2.6842	2.6842	2.6842	2.6842	2.6842	2.6842	0.00	0.00	0.00	0.00	9.31	10000.00
12.10.3	12	2.8805	2.8805	2.8805	2.8805	2.8805	2.8805	0.00	0.00	0.00	0.00	7.36	10000.00
12.10.4	12	2.3142	2.3142	2.3142	2.3142	2.3142	2.3142	0.00	0.00	0.00	0.00	10.87	10000.00
12.20.1	12	5.7776	5.7776	5.7776	5.7776	5.7776	5.7776	0.00	0.00	0.00	0.00	6.96	10000.00
12.20.2	12	8.2725	8.2725	8.2725	8.2725	8.2725	8.2725	0.00	0.00	0.00	0.00	2.74	10000.00
12.20.3	12	4.1669	4.1669	4.1669	4.1669	4.1669	4.1669	0.00	0.00	0.00	0.00	4.69	10000.00
12.20.4	12	6.0886	6.0886	6.0886	6.0886	6.0886	6.1409	0.00	0.00	0.86	0.86	5.10	10000.00
20.5.1	20	1.7935	1.7935	1.7935	1.7935	1.7935	1.7935	0.00	0.00	0.00	0.00	44.10	10000.00
20.5.2	20	1.9540	1.9540	1.8221	1.8221	1.8221	1.8221	-6.75	0.00	-6.75	0.00	19.45	10000.00
20.5.3	20	1.4866	1.4866	1.4866	1.4866	1.4866	1.4866	0.00	0.00	0.00	0.00	32.06	10000.00
20.5.4	20	1.3789	1.3789	1.3789	1.3789	1.3789	1.3789	0.00	0.00	0.00	0.00	62.14	10000.00
20.10.1	20	3.2525	3.2525	3.2525	3.2525	3.2525	3.2525	0.00	0.00	0.00	0.00	30.16	10000.00
20.10.2	20	3.0894	3.0894	3.0894	3.0894	3.0894	3.0894	0.00	0.00	0.00	0.00	52.99	10000.00
20.10.3	20	3.7023	3.7258	3.7023	3.7023	3.7023	3.7023	0.00	0.00	-0.63	0.00	47.54	10000.00
20.10.4	20	3.3089	3.3137	3.1966	3.1966	3.1966	3.1966	-3.39	0.00	-3.53	0.00	59.57	10000.00
20.20.1	20	7.3445	7.3512	7.3230	7.3291	7.3230	7.3230	-0.29	0.00	-0.38	-0.08	40.22	10000.00
20.20.2	20	7.5489	7.5489	7.5489	7.5607	7.5489	7.5489	0.00	0.00	0.00	-0.16	26.90	10000.00
20.20.3	20	7.4610	7.4746	7.4610	7.4610	7.4610	7.4610	0.00	0.00	-0.18	0.00	20.30	10000.00
20.20.4	20	7.0133	7.0133	7.0133	7.0133	7.0133	7.0133	0.00	0.00	0.00	0.00	36.94	10000.00
50.10.1	50	5.8613	5.8613	5.8614	5.9408	5.8613	5.8613	0.00	0.00	0.00	-1.34	300.00	5905.80
50.10.2	50	5.5849	5.6210	5.5849	5.5849	5.5849	5.5849	0.00	0.00	-0.64	0.00	300.00	7605.80
50.10.3	50	5.4224	5.4255	5.4888	5.7062	5.4058	5.4140	-0.31	-1.51	-0.21	-5.12	300.00	3905.60
50.10.4	50	5.2083	5.3526	5.1405	5.4827	5.1405	5.1405	-1.30	0.00	-3.96	-6.24	300.00	5340.60
50.20.1	50	10.4553	10.4564	10.4566	10.6110	10.2349	10.2349	-2.11	-2.12	-2.12	-3.54	300.00	6139.80
50.20.2	50	10.0561	10.0561	10.0561	10.0820	10.0561	10.0561	0.00	0.00	0.00	-0.26	279.28	10000.00
50.20.3	50	10.5425	10.6570	10.5425	10.7049	10.5018	10.5018	-0.39	-0.39	-1.46	-1.90	300.00	6130.60
50.20.4	50	10.6642	11.0008	11.0395	11.1409	10.6642	10.6649	0.00	-3.40	-3.05	-4.27	300.00	4458.40
50.30.1	50	15.8179	15.8179	15.8179	15.9497	15.7714	15.7714	-0.29	-0.29	-0.29	-1.12	266.48	10000.00
50.30.2	50	15.0148	15.4636	14.9795	15.0286	15.0148	15.0148	0.00	0.24	-2.90	-0.09	300.00	6099.00
50.30.3	50	16.7690	16.7713	16.7796	16.8633	16.3865	16.3865	-2.28	-2.34	-2.29	-2.83	300.00	9032.60
50.30.4	50	18.2875	18.2875	18.2875	18.3780	18.3028	18.4265	0.08	0.08	0.76	0.26	237.47	10000.00
50.40.1	50	20.3751	21.1771	20.0882	21.2848	20.1210	20.1210	-1.25	0.16	-4.99	-5.47	187.15	10000.00
50.40.2	50	20.6262	20.6262	20.6262	20.6790	20.4210	20.4210	-0.99	-0.99	-0.99	-1.25	245.99	10000.00
50.40.3	50	22.6452	22.7053	22.6657	22.9102	22.6452	22.6452	0.00	-0.09	-0.26	-1.16	300.00	8202.80
50.40.4	50	22.3371	22.7891	22.3371	22.3371	22.3371	22.3371	0.00	0.00	-1.98	0.00	255.82	10000.00
100.10.1	100	6.8574	6.8902	6.8931	7.0288	6.6924	6.7238	-2.41	-2.91	-2.42	-4.34	300.01	291.00
100.10.2	100	7.5851	7.6781	7.5547	7.6083	7.4805	7.4992	-1.38	-0.98	-2.33	-1.43	300.00	686.80
100.10.3	100	7.1835	7.3055	7.2405	7.3730	7.1098	7.1340	-1.03	-1.81	-2.35	-3.24	300.00	363.40
100.10.4	100	7.4568	7.5459	7.4689	7.5310	7.3445	7.3740	-1.51	-1.67	-2.28	-2.08	300.00	1027.60
100.20.1	100	13.6067	13.7946	13.9798	13.9986	13.5915	13.5969	-0.11	-2.78	-1.43	-2.87	300.00	886.20
100.20.2	100	14.1340	14.5375	14.1667	14.4054	14.0253	14.0253	-0.77	-1.00	-3.52	-2.64	300.00	755.80
100.20.3	100	13.7099	13.7672	14.0065	14.4508	13.6072	13.6163	-0.75	-2.85	-1.10	-5.77	300.00	738.00

Table 13 – continued from previous page

Instance	n	SPR		RFK		HVNS							
		Obj^{best}	$\overline{Obj}^{10}$	Obj^{best}	$\overline{Obj}^{10}$	Obj^{best}	$\overline{Obj}^{5}$	Gap^{SPR} (%)	Gap^{RFK} (%)	$\overline{Gap}^{SPR}$ (%)	$\overline{Gap}^{RFK}$ (%)	Time (s)	Ite
100.20.4	100	13.8494	14.1976	13.6085	13.8257	13.8325	13.8518	-0.12	1.65	-2.44	0.19	300.01	552.60
100.30.1	100	22.5882	23.6364	22.1278	22.3138	21.9473	21.9800	-2.84	-0.82	-7.01	-1.50	300.00	1037.60
100.30.2	100	22.3143	22.3846	22.6947	22.8905	22.1745	22.2298	-0.63	-2.29	-0.69	-2.89	300.00	1383.80
100.30.3	100	23.7195	23.9094	23.3769	23.5578	23.1536	23.3703	-2.39	-0.96	-2.25	-0.80	300.00	1351.60
100.30.4	100	22.3701	22.6585	22.7022	22.9554	22.3727	22.4140	0.01	-1.45	-1.08	-2.36	300.00	1417.60
100.40.1	100	29.1397	30.1807	28.9907	29.3766	28.7108	28.7592	-1.47	-0.97	-4.71	-2.10	300.00	957.20
100.40.2	100	30.9900	31.2092	31.1576	31.3523	29.6584	29.8602	-4.30	-4.81	-4.32	-4.76	300.00	1421.40
100.40.3	100	29.0248	29.6653	29.3583	30.1569	28.2243	28.2404	-2.76	-3.86	-4.80	-6.36	300.00	1135.80
100.40.4	100	28.9735	29.2049	29.2673	29.4952	28.7045	28.8048	-0.93	-1.92	-1.37	-2.34	300.00	1368.40
150.10.1	150	8.7903	8.9351	8.8329	9.0109	8.5945	8.7403	-2.23	-2.70	-2.18	-3.00	300.01	148.60
150.10.2	150	8.2591	8.4160	8.3217	8.4821	8.1480	8.2414	-1.35	-2.09	-2.07	-2.84	300.01	151.40
150.10.3	150	8.4960	9.0207	8.4138	8.6962	8.3258	8.4436	-2.00	-1.05	-6.40	-2.90	300.02	174.00
150.10.4	150	8.8373	9.0398	8.8469	8.9152	8.7656	8.8463	-0.81	-0.92	-2.14	-0.77	300.04	93.40
150.20.1	150	17.3194	17.5964	17.4518	17.7115	17.2619	17.3363	-0.33	-1.09	-1.48	-2.12	300.01	157.80
150.20.2	150	16.6341	17.4507	16.6581	16.7896	16.6925	16.8407	0.35	0.21	-3.50	0.30	300.00	192.60
150.20.3	150	17.4058	18.3447	17.6484	18.2769	17.5381	17.7227	0.76	-0.62	-3.39	-3.03	300.01	130.20
150.20.4	150	16.8752	17.4774	16.8430	17.0358	16.8373	16.8824	-0.22	-0.03	-3.40	-0.90	300.01	136.80
150.30.1	150	25.9854	26.5488	25.5617	25.7346	25.4347	25.5261	-2.12	-0.50	-3.85	-0.81	300.00	234.40
150.30.2	150	26.2055	26.7411	27.0083	27.4973	26.0791	26.2995	-0.48	-3.44	-1.65	-4.36	300.00	353.60
150.30.3	150	25.3164	26.1137	25.5945	26.2195	25.2426	25.5849	-0.29	-1.37	-2.02	-2.42	300.00	302.00
150.30.4	150	26.1027	27.2923	25.9322	26.1393	25.8843	26.2667	-0.84	-0.18	-3.76	0.49	300.00	303.20
150.40.1	150	34.0121	35.4534	33.8560	34.1849	33.4893	34.2282	-1.54	-1.08	-3.46	0.13	300.00	336.40
150.40.2	150	36.5616	38.2965	37.3489	39.7175	37.1529	37.3013	1.62	-0.52	-2.60	-6.08	300.00	326.40
150.40.3	150	36.6574	38.2955	36.2182	36.4779	36.2764	36.5367	-1.04	0.16	-4.59	0.16	300.00	393.40
150.40.4	150	35.0156	36.0662	34.8401	35.3078	34.4310	35.0148	-1.67	-1.17	-2.92	-0.83	300.00	353.20
200.10.1	200	10.0945	10.4050	9.8962	9.9743	9.9323	10.0683	-1.61	0.36	-3.24	0.94	300.01	108.20
200.10.2	200	10.4226	10.6149	10.0557	10.1145	9.7236	9.8792	-6.71	-3.30	-6.93	-2.33	300.01	49.00
200.10.3	200	9.7990	9.9235	9.7359	9.8236	9.8819	10.0374	0.85	1.50	1.15	2.18	300.01	53.60
200.10.4	200	10.3553	10.6400	10.3061	10.3850	10.0630	10.2724	-2.82	-2.36	-3.45	-1.08	300.01	72.40
200.20.1	200	21.2151	21.4601	20.9326	21.2115	20.7129	21.0154	-2.37	-1.05	-2.07	-0.92	300.01	85.00
200.20.2	200	21.4585	22.0461	21.6359	21.7961	21.6408	21.7891	0.85	0.02	-1.17	-0.03	300.01	161.80
200.20.3	200	20.8522	21.0604	20.8347	20.9688	20.3784	20.5302	-2.27	-2.19	-2.52	-2.09	300.01	81.80
200.20.4	200	19.2350	20.1804	19.2561	19.6779	19.1865	19.5861	-0.25	-0.36	-2.94	-0.47	300.02	79.60
200.30.1	200	30.3602	31.7826	29.9292	30.2124	30.0107	30.4036	-1.15	0.27	-4.34	0.63	300.00	124.20
200.30.2	200	32.8128	33.2164	31.5970	31.8373	30.5677	30.9224	-6.84	-3.26	-6.91	-2.87	300.01	119.40
200.30.3	200	32.2535	32.7373	31.1024	31.3947	31.2074	31.6370	-3.24	0.34	-3.36	0.77	300.01	106.80
200.30.4	200	32.0931	32.7638	31.7090	33.3396	31.6439	32.0454	-1.40	-0.21	-2.19	-3.88	300.01	133.80
200.40.1	200	41.4980	42.3048	41.9058	44.9005	40.9395	41.4848	-1.35	-2.31	-1.94	-7.61	300.00	153.00
200.40.2	200	43.2502	44.2211	42.9621	43.5546	42.2601	42.6241	-2.29	-1.63	-3.61	-2.14	300.00	154.80
200.40.3	200	43.3375	44.2613	43.6542	44.2726	42.3375	43.0889	-2.31	-3.02	-2.65	-2.67	300.00	151.60
200.40.4	200	42.0579	43.3370	39.7972	40.1223	42.7886	43.2406	1.74	7.52	-0.22	7.77	300.00	154.00

4. Detailed results on benchmarks for VRPD-M in Section 6.3.2

Tables 14–18 present detailed results of our HVNS in five runs and results from El-Adle et al. (2021), Tamke and Buscher (2021) and Roberti and Ruthmair (2021) for the VRPD-M. The notations in these tables are defined as follows.

Instance: The name of the instance.

n: The number of customers in the instance.

Status: The solving status of each exact method. "O", optimal; "L", otherwise.

BKS: The objective function value obtained by each exact method.

Time (s): The computational time of each exact method, and the average computational time of five runs of our HVNS.

Obj: The best objective function value obtained from five runs of our HVNS.

Gap (%): The gap between Obj and BKS computed by $100(\text{Obj} - \text{BKS})/\text{BKS}$.

$\overline{\text{Obj}}$: The average objective function value obtained from five runs of our HVNS.

$\overline{\text{Gap}}$ (%): The gap between $\overline{\text{Obj}}$ and BKS computed by $100(\overline{\text{Obj}} - \text{BKS})/\text{BKS}$.

Ite: The average number of iterations of five runs of our HVNS.

Table 14: Detailed results of our HVNS compared with benchmark EGH

Instance	n	EGH			HVNS					
		Status	BKS	Time (s)	Obj	Gap (%)	$\overline{\text{Obj}}$	$\overline{\text{Gap}}$ (%)	Ite	Time (s)
SingleCenter-61-n16	15	O	415.75	17.60	415.75	0.00	415.75	0.00	10000.00	6.37
SingleCenter-62-n16	15	O	459.02	30.20	459.02	0.00	459.02	0.00	10000.00	14.95
SingleCenter-63-n16	15	O	604.81	7.30	604.81	0.00	604.81	0.00	10000.00	11.67
SingleCenter-64-n16	15	O	499.07	18.10	499.07	0.00	499.07	0.00	10000.00	6.01
SingleCenter-65-n16	15	O	505.20	7.10	505.20	0.00	505.20	0.00	10000.00	6.14
SingleCenter-66-n16	15	O	341.53	38.00	341.52	0.00	341.52	0.00	10000.00	6.93
SingleCenter-67-n16	15	O	448.20	13.10	448.20	0.00	448.20	0.00	10000.00	4.28
SingleCenter-68-n16	15	O	516.89	22.90	516.89	0.00	516.89	0.00	10000.00	7.41
SingleCenter-69-n16	15	O	597.03	52.80	597.03	0.00	597.03	0.00	10000.00	4.29
SingleCenter-70-n16	15	O	395.48	35.60	395.48	0.00	395.48	0.00	10000.00	4.40
DoubleCenter-61-n16	15	O	846.53	8.70	846.53	0.00	846.53	0.00	10000.00	1.98
DoubleCenter-62-n16	15	O	785.61	10.90	785.61	0.00	785.61	0.00	10000.00	4.09
DoubleCenter-63-n16	15	O	917.14	4.60	917.14	0.00	917.14	0.00	10000.00	1.91
DoubleCenter-64-n16	15	O	991.58	8.20	991.57	0.00	991.57	0.00	10000.00	2.90
DoubleCenter-65-n16	15	O	662.94	25.40	662.94	0.00	662.94	0.00	10000.00	5.65
DoubleCenter-66-n16	15	O	698.70	12.10	698.70	0.00	698.70	0.00	10000.00	3.69
DoubleCenter-67-n16	15	O	643.99	25.00	643.99	0.00	643.99	0.00	10000.00	2.97
DoubleCenter-68-n16	15	O	608.55	10.10	608.55	0.00	608.55	0.00	10000.00	3.30
DoubleCenter-69-n16	15	O	683.01	30.60	683.01	0.00	683.01	0.00	10000.00	3.45
DoubleCenter-70-n16	15	O	755.10	143.50	755.10	0.00	755.10	0.00	10000.00	5.42
Uniform-61-n16	15	O	292.16	48.30	292.16	0.00	292.16	0.00	10000.00	5.06
Uniform-62-n16	15	O	280.14	184.90	280.14	0.00	280.14	0.00	10000.00	5.56
Uniform-63-n16	15	O	265.49	17.90	265.49	0.00	265.49	0.00	10000.00	2.57
Uniform-64-n16	15	O	307.38	138.80	307.38	0.00	307.38	0.00	10000.00	9.17
Uniform-65-n16	15	O	305.31	658.70	305.31	0.00	305.31	0.00	10000.00	7.05
Uniform-66-n16	15	O	368.17	91.80	368.17	0.00	368.17	0.00	10000.00	4.36
Uniform-67-n16	15	O	325.36	24.90	325.35	0.00	325.35	0.00	10000.00	4.03
Uniform-68-n16	15	O	344.50	124.30	344.50	0.00	344.50	0.00	10000.00	4.83
Uniform-69-n16	15	O	284.12	62.60	284.12	0.00	284.12	0.00	10000.00	6.47
Uniform-70-n16	15	O	328.75	71.50	328.75	0.00	328.75	0.00	10000.00	4.49
SingleCenter-61-n20	19	O	523.73	288.90	523.73	0.00	523.73	0.00	10000.00	16.19
SingleCenter-62-n20	19	O	466.55	124.40	466.55	0.00	466.55	0.00	10000.00	14.97
SingleCenter-63-n20	19	O	673.06	80.00	673.06	0.00	673.54	0.07	10000.00	6.33

Table 14 – continued from previous page

Instance	n	EGH			HVNS					
		Status	BKS	Time (s)	Obj	Gap (%)	$\overline{\text{Obj}}$	$\overline{\text{Gap}}$ (%)	Ite	Time (s)
SingleCenter-64-n20	19	O	548.98	3185.70	548.98	0.00	548.98	0.00	10000.00	10.44
SingleCenter-65-n20	19	O	570.25	138.40	570.25	0.00	570.25	0.00	10000.00	7.18
SingleCenter-66-n20	19	O	448.77	65.90	448.77	0.00	448.77	0.00	10000.00	10.02
SingleCenter-67-n20	19	O	524.77	185.10	524.77	0.00	524.77	0.00	10000.00	12.16
SingleCenter-68-n20	19	O	535.79	6687.80	535.78	0.00	535.78	0.00	10000.00	12.58
SingleCenter-69-n20	19	O	639.26	914.60	639.26	0.00	639.26	0.00	10000.00	18.20
SingleCenter-70-n20	19	O	442.04	539.10	442.04	0.00	442.04	0.00	10000.00	15.36
DoubleCenter-61-n20	19	O	866.96	19.00	866.95	0.00	866.95	0.00	10000.00	4.42
DoubleCenter-62-n20	19	O	808.66	34.10	808.66	0.00	808.66	0.00	10000.00	9.22
DoubleCenter-63-n20	19	O	964.34	27.50	964.34	0.00	964.34	0.00	10000.00	3.86
DoubleCenter-64-n20	19	O	1033.51	2306.40	1033.51	0.00	1033.51	0.00	10000.00	6.87
DoubleCenter-65-n20	19	O	696.40	2271.90	696.40	0.00	696.40	0.00	10000.00	10.44
DoubleCenter-66-n20	19	O	708.01	126.60	708.01	0.00	708.01	0.00	10000.00	10.27
DoubleCenter-67-n20	19	O	731.90	63.30	731.90	0.00	731.90	0.00	10000.00	8.35
DoubleCenter-68-n20	19	O	709.52	45.80	709.52	0.00	709.52	0.00	10000.00	12.26
DoubleCenter-69-n20	19	O	686.74	2613.60	686.74	0.00	686.74	0.00	10000.00	9.39
DoubleCenter-70-n20	19	O	794.15	1121.50	794.15	0.00	794.15	0.00	10000.00	8.12
Uniform-61-n20	19	O	296.19	1861.00	296.19	0.00	296.19	0.00	10000.00	17.05
Uniform-62-n20	19	L	293.84	12004.00	293.84	0.00	293.84	0.00	10000.00	22.29
Uniform-63-n20	19	O	274.05	2215.60	274.05	0.00	274.05	0.00	10000.00	13.20
Uniform-64-n20	19	O	280.82	3828.80	280.82	0.00	280.82	0.00	10000.00	11.47
Uniform-65-n20	19	L	319.05	11491.90	319.05	0.00	319.05	0.00	10000.00	9.87
Uniform-66-n20	19	O	360.04	305.10	360.04	0.00	360.04	0.00	10000.00	9.08
Uniform-67-n20	19	O	326.08	2067.70	326.08	0.00	326.08	0.00	10000.00	9.51
Uniform-68-n20	19	O	347.18	1580.60	347.18	0.00	347.18	0.00	10000.00	10.77
Uniform-69-n20	19	O	286.00	2680.60	286.00	0.00	286.00	0.00	10000.00	16.50
Uniform-70-n20	19	O	331.13	503.50	331.13	0.00	331.13	0.00	10000.00	10.37
SingleCenter-71-n24	23	L	380.79	11696.60	380.70	-0.02	380.70	-0.02	10000.00	24.68
SingleCenter-72-n24	23	O	479.18	47903.20	479.18	0.00	479.18	0.00	10000.00	63.14
SingleCenter-73-n24	23	O	358.25	8346.80	358.25	0.00	358.25	0.00	10000.00	62.72
SingleCenter-74-n24	23	O	468.90	1470.90	468.90	0.00	468.90	0.00	10000.00	26.62
SingleCenter-75-n24	23	O	780.79	826.70	780.79	0.00	780.79	0.00	10000.00	28.09
SingleCenter-76-n24	23	O	467.36	2369.00	467.36	0.00	467.36	0.00	10000.00	17.60
SingleCenter-77-n24	23	L	395.23	11045.90	388.49	-1.71	388.49	-1.71	10000.00	53.92
SingleCenter-78-n24	23	L	446.05	11814.40	441.44	-1.03	441.44	-1.03	10000.00	43.59
SingleCenter-79-n24	23	O	422.00	7677.80	422.00	0.00	422.00	0.00	10000.00	50.48
SingleCenter-80-n24	23	O	551.51	3350.90	551.51	0.00	551.51	0.00	10000.00	21.18
DoubleCenter-71-n24	23	O	931.95	602.50	931.95	0.00	931.95	0.00	10000.00	25.74
DoubleCenter-72-n24	23	O	755.95	672.20	755.95	0.00	755.95	0.00	10000.00	20.52
DoubleCenter-73-n24	23	O	731.86	5472.50	731.86	0.00	731.86	0.00	10000.00	18.31
DoubleCenter-74-n24	23	L	787.33	10462.80	787.33	0.00	787.33	0.00	10000.00	24.15
DoubleCenter-75-n24	23	O	854.13	4498.70	854.13	0.00	854.13	0.00	10000.00	15.77
DoubleCenter-76-n24	23	O	760.88	487.70	760.88	0.00	760.88	0.00	10000.00	9.81
DoubleCenter-77-n24	23	L	867.99	10584.10	867.99	0.00	867.99	0.00	10000.00	25.62
DoubleCenter-78-n24	23	O	1102.14	133.70	1102.14	0.00	1102.14	0.00	10000.00	10.77
DoubleCenter-79-n24	23	O	899.42	2176.00	899.42	0.00	899.42	0.00	10000.00	20.84
DoubleCenter-80-n24	23	O	791.45	1752.10	791.45	0.00	791.45	0.00	10000.00	14.54
Uniform-71-n24	23	L	308.92	12008.10	308.92	0.00	308.92	0.00	10000.00	23.85
Uniform-72-n24	23	L	323.93	12008.60	323.93	0.00	323.93	0.00	10000.00	15.90
Uniform-73-n24	23	L	315.99	12008.30	315.99	0.00	315.99	0.00	10000.00	9.39

Table 14 – continued from previous page

Instance	n	EGH			HVNS					
		Status	BKS	Time (s)	Obj	Gap (%)	$\overline{\text{Obj}}$	$\overline{\text{Gap}}$ (%)	Ite	Time (s)
Uniform-74-n24	23	L	368.90	11191.30	368.90	0.00	368.90	0.00	10000.00	20.44
Uniform-75-n24	23	L	378.00	12005.80	378.00	0.00	378.00	0.00	10000.00	25.18
Uniform-76-n24	23	L	269.23	11465.00	268.59	-0.24	268.59	-0.24	10000.00	25.82
Uniform-77-n24	23	O	362.22	3998.80	362.22	0.00	362.22	0.00	10000.00	20.31
Uniform-78-n24	23	L	317.43	11568.30	315.44	-0.63	315.44	-0.63	10000.00	30.62
Uniform-79-n24	23	O	310.49	5624.10	310.49	0.00	310.49	0.00	10000.00	21.05
Uniform-80-n24	23	L	321.37	12008.10	312.34	-2.81	312.34	-2.81	10000.00	18.93
SingleCenter-71-n28	27	L	407.12	12089.20	401.26	-1.44	401.26	-1.44	10000.00	41.56
SingleCenter-72-n28	27	L	486.43	10264.30	486.43	0.00	486.43	0.00	10000.00	37.26
SingleCenter-73-n28	27	L	373.15	11228.00	360.68	-3.34	360.68	-3.34	10000.00	50.14
SingleCenter-74-n28	27	O	435.94	6770.10	435.94	0.00	435.94	0.00	10000.00	27.30
SingleCenter-75-n28	27	L	779.96	10471.70	779.93	0.00	779.93	0.00	10000.00	43.50
SingleCenter-76-n28	27	L	520.92	11587.00	520.92	0.00	520.92	0.00	10000.00	35.11
SingleCenter-77-n28	27	L	507.55	12033.00	500.00	-1.49	500.00	-1.49	10000.00	51.07
SingleCenter-78-n28	27	L	589.65	11008.70	581.74	-1.34	581.74	-1.34	10000.00	47.07
SingleCenter-79-n28	27	L	440.16	11638.10	433.48	-1.52	433.48	-1.52	10000.00	75.55
SingleCenter-80-n28	27	L	704.01	10856.00	698.65	-0.76	698.65	-0.76	10000.00	30.46
DoubleCenter-71-n28	27	L	941.01	10390.60	934.48	-0.69	934.48	-0.69	10000.00	38.63
DoubleCenter-72-n28	27	L	774.21	10279.10	771.62	-0.33	771.62	-0.33	10000.00	30.43
DoubleCenter-73-n28	27	L	823.80	10471.40	823.79	0.00	823.79	0.00	10000.00	33.18
DoubleCenter-74-n28	27	L	795.73	11369.50	795.73	0.00	795.73	0.00	10000.00	30.87
DoubleCenter-75-n28	27	L	994.42	10945.80	992.39	-0.20	992.39	-0.20	10000.00	24.14
DoubleCenter-76-n28	27	O	785.93	449.10	785.93	0.00	785.93	0.00	10000.00	16.55
DoubleCenter-77-n28	27	L	889.97	11100.50	884.30	-0.64	884.30	-0.64	10000.00	28.91
DoubleCenter-78-n28	27	O	1140.45	2610.60	1140.45	0.00	1140.45	0.00	10000.00	20.89
DoubleCenter-79-n28	27	O	892.82	3872.90	892.82	0.00	892.82	0.00	10000.00	34.38
DoubleCenter-80-n28	27	O	813.17	5890.20	813.17	0.00	813.17	0.00	10000.00	21.01
Uniform-71-n28	27	L	315.06	12014.00	315.06	0.00	315.06	0.00	10000.00	69.67
Uniform-72-n28	27	L	327.61	11404.60	327.61	0.00	327.61	0.00	10000.00	33.48
Uniform-73-n28	27	L	318.01	12012.10	318.01	0.00	318.01	0.00	10000.00	27.40
Uniform-74-n28	27	L	363.77	12013.10	360.71	-0.84	360.71	-0.84	10000.00	36.39
Uniform-75-n28	27	L	355.00	11124.40	353.58	-0.40	353.58	-0.40	10000.00	40.53
Uniform-76-n28	27	L	300.65	11148.10	284.51	-5.37	284.51	-5.37	10000.00	45.73
Uniform-77-n28	27	L	347.78	11675.70	347.78	0.00	347.78	0.00	10000.00	35.73
Uniform-78-n28	27	L	361.71	12013.90	357.34	-1.21	357.34	-1.21	10000.00	42.20
Uniform-79-n28	27	L	320.50	11388.70	320.50	0.00	320.50	0.00	10000.00	36.87
Uniform-80-n28	27	L	339.61	12012.60	339.61	0.00	339.61	0.00	10000.00	62.86
SingleCenter-71-n32	31	L	434.14	11381.00	412.53	-4.98	412.53	-4.98	10000.00	133.53
SingleCenter-72-n32	31	L	504.58	10628.30	499.84	-0.94	499.84	-0.94	10000.00	70.77
SingleCenter-73-n32	31	L	369.13	11358.80	369.13	0.00	369.13	0.00	10000.00	127.63
SingleCenter-74-n32	31	L	490.48	11491.00	490.48	0.00	490.48	0.00	10000.00	88.21
SingleCenter-75-n32	31	L	783.28	11092.90	783.28	0.00	783.28	0.00	10000.00	73.18
SingleCenter-76-n32	31	L	581.98	11497.60	534.60	-8.14	534.60	-8.14	10000.00	71.84
SingleCenter-77-n32	31	L	521.75	10611.00	513.30	-1.62	513.30	-1.62	10000.00	98.51
SingleCenter-78-n32	31	L	634.48	10764.50	622.22	-1.93	622.22	-1.93	10000.00	52.87
SingleCenter-79-n32	31	L	425.98	11491.90	423.95	-0.48	423.95	-0.48	10000.00	90.01
SingleCenter-80-n32	31	L	783.57	11146.20	779.82	-0.48	779.82	-0.48	10000.00	28.95
DoubleCenter-71-n32	31	L	1177.80	10572.70	1162.89	-1.27	1162.89	-1.27	10000.00	53.84
DoubleCenter-72-n32	31	L	858.87	10236.30	840.45	-2.14	840.45	-2.14	10000.00	79.21
DoubleCenter-73-n32	31	L	875.38	11658.20	849.90	-2.91	849.90	-2.91	10000.00	40.51

Table 14 – continued from previous page

Instance	n	EGH			HVNS					
		Status	BKS	Time (s)	Obj	Gap (%)	$\overline{\text{Obj}}$	$\overline{\text{Gap}}$ (%)	Ite	Time (s)
DoubleCenter-74-n32	31	L	877.20	10820.80	805.49	-8.17	805.49	-8.17	10000.00	52.47
DoubleCenter-75-n32	31	L	1008.95	10153.10	1008.95	0.00	1008.95	0.00	10000.00	34.68
DoubleCenter-76-n32	31	O	985.70	805.30	985.70	0.00	985.70	0.00	10000.00	28.39
DoubleCenter-77-n32	31	L	1005.04	11147.80	935.01	-6.97	935.01	-6.97	10000.00	86.22
DoubleCenter-78-n32	31	L	1101.60	11219.80	1101.60	0.00	1101.60	0.00	10000.00	40.49
DoubleCenter-79-n32	31	L	905.13	11048.30	902.62	-0.28	902.62	-0.28	10000.00	37.70
DoubleCenter-80-n32	31	O	825.82	6852.00	825.83	0.00	825.83	0.00	10000.00	24.69
Uniform-71-n32	31	L	352.68	11426.10	330.57	-6.27	330.57	-6.27	10000.00	55.69
Uniform-72-n32	31	L	357.14	11537.50	349.27	-2.20	349.27	-2.20	10000.00	45.09
Uniform-73-n32	31	L	340.10	12012.30	340.01	-0.03	340.01	-0.03	10000.00	98.52
Uniform-74-n32	31	L	370.89	11630.60	365.62	-1.42	365.62	-1.42	10000.00	61.79
Uniform-75-n32	31	L	364.21	11765.60	364.21	0.00	364.21	0.00	10000.00	83.17
Uniform-76-n32	31	L	363.39	12033.50	359.29	-1.13	359.29	-1.13	10000.00	54.39
Uniform-77-n32	31	L	401.17	11430.10	372.30	-7.20	372.30	-7.20	10000.00	51.26
Uniform-78-n32	31	L	403.04	12012.20	362.79	-9.99	362.79	-9.99	10000.00	82.53
Uniform-79-n32	31	L	499.11	12012.80	318.75	-36.14	318.75	-36.14	10000.00	61.79
Uniform-80-n32	31	L	359.80	12010.30	342.29	-4.87	342.29	-4.87	10000.00	102.17

Table 15: Detailed results of our HVNS compared with benchmark TB1

Instance	n	TB1			HVNS					
		Status	BKS	Time (s)	Obj	Gap (%)	$\overline{\text{Obj}}$	$\overline{\text{Gap}}$ (%)	Ite	Time (s)
kroA100_15	14	O	7107.87	234.65	7107.87	0.00	7107.87	0.00	10000.00	11.47
kroB100_15	14	O	6688.84	124.87	6688.84	0.00	6688.84	0.00	10000.00	13.89
kroC100_15	14	O	6699.96	119.18	6699.96	0.00	6699.96	0.00	10000.00	11.26
kroA100_15	14	O	6869.38	110.60	6869.38	0.00	6869.38	0.00	10000.00	10.96
kroB100_15	14	O	6645.69	116.22	6645.69	0.00	6645.69	0.00	10000.00	12.68
kroC100_15	14	O	6699.96	119.63	6699.96	0.00	6699.96	0.00	10000.00	10.91
kroA100_20	19	O	7944.35	22665.64	7944.35	0.00	7944.35	0.00	10000.00	23.16
kroB100_20	19	O	7953.69	26773.19	7953.69	0.00	7953.69	0.00	10000.00	30.55
kroC100_20	19	O	7347.12	5407.77	7347.12	0.00	7347.12	0.00	10000.00	25.46
kroA100_20	19	O	7679.08	7496.77	7679.08	0.00	7679.08	0.00	10000.00	22.38
kroB100_20	19	O	7812.77	22925.38	7812.77	0.00	7812.77	0.00	10000.00	40.89
kroC100_20	19	O	7347.12	6245.03	7347.12	0.00	7347.12	0.00	10000.00	25.74
kroA100_25	24	O	9408.19	5793.66	9408.19	0.00	9408.19	0.00	10000.00	45.20
kroB100_25	24	O	8941.29	5674.39	8941.29	0.00	8941.29	0.00	10000.00	32.77
kroC100_25	24	O	8908.64	727.70	8908.64	0.00	8908.64	0.00	10000.00	23.44
kroA100_25	24	L	8874.13	43200.39	8874.13	0.00	8874.13	0.00	10000.00	28.79
kroB100_25	24	L	8178.12	43200.56	8178.12	0.00	8178.12	0.00	10000.00	42.42
kroC100_25	24	L	8274.64	43200.59	8274.64	0.00	8274.64	0.00	10000.00	35.81
kroA100_30	29	O	10248.40	29334.23	10248.43	0.00	10248.43	0.00	10000.00	67.00
kroB100_30	29	L	9406.15	43200.33	9406.15	0.00	9406.15	0.00	10000.00	42.01
kroC100_30	29	O	9923.72	1662.53	9923.72	0.00	9923.72	0.00	10000.00	32.95
kroA100_30	29	L	9639.77	43200.49	9639.77	0.00	9639.77	0.00	10000.00	56.05
kroB100_30	29	L	8950.26	43200.96	8950.26	0.00	8950.26	0.00	10000.00	36.87
kroC100_30	29	L	9027.36	43200.67	9027.36	0.00	9027.36	0.00	10000.00	47.64

Table 16: Detailed results of our HVNS compared with benchmark TB2

Instance	n	TB2			HVNS					
		Status	BKS	Time (s)	Obj	Gap (%)	$\overline{\text{Obj}}$	$\overline{\text{Gap}}$ (%)	Ite	Time (s)
kroA100_15	14	O	7107.87	234.65	7107.87	0.00	7107.87	0.00	10000.00	11.47
kroB100_15	14	O	6688.84	124.87	6688.84	0.00	6688.84	0.00	10000.00	13.89
kroC100_15	14	O	6699.96	119.18	6699.96	0.00	6699.96	0.00	10000.00	11.26
kroA100_15	14	O	6869.38	110.60	6869.38	0.00	6869.38	0.00	10000.00	10.96
kroB100_15	14	O	6645.69	116.22	6645.69	0.00	6645.69	0.00	10000.00	12.68
kroC100_15	14	O	6699.96	119.63	6699.96	0.00	6699.96	0.00	10000.00	10.91
kroA100_20	19	O	7944.35	22665.64	7944.35	0.00	7944.35	0.00	10000.00	23.16
kroB100_20	19	O	7953.69	26773.19	7953.69	0.00	7953.69	0.00	10000.00	30.55
kroC100_20	19	O	7347.12	5407.77	7347.12	0.00	7347.12	0.00	10000.00	25.46
kroA100_20	19	O	7679.08	7496.77	7679.08	0.00	7679.08	0.00	10000.00	22.38
kroB100_20	19	O	7812.77	22925.38	7812.77	0.00	7812.77	0.00	10000.00	40.89
kroC100_20	19	O	7347.12	6245.03	7347.12	0.00	7347.12	0.00	10000.00	25.74
kroA100_25	24	O	9408.19	5793.66	9408.19	0.00	9408.19	0.00	10000.00	45.20
kroB100_25	24	O	8941.29	5674.39	8941.29	0.00	8941.29	0.00	10000.00	32.77
kroC100_25	24	O	8908.64	727.70	8908.64	0.00	8908.64	0.00	10000.00	23.44
kroA100_25	24	L	8874.13	43200.39	8874.13	0.00	8874.13	0.00	10000.00	28.79
kroB100_25	24	L	8178.12	43200.56	8178.12	0.00	8178.12	0.00	10000.00	42.42
kroC100_25	24	L	8274.64	43200.59	8274.64	0.00	8274.64	0.00	10000.00	35.81
kroA100_30	29	O	10248.40	29334.23	10248.43	0.00	10248.43	0.00	10000.00	67.00
kroB100_30	29	L	9406.15	43200.33	9406.15	0.00	9406.15	0.00	10000.00	42.01
kroC100_30	29	O	9923.72	1662.53	9923.72	0.00	9923.72	0.00	10000.00	32.95
kroA100_30	29	L	9639.77	43200.49	9639.77	0.00	9639.77	0.00	10000.00	56.05
kroB100_30	29	L	8950.26	43200.96	8950.26	0.00	8950.26	0.00	10000.00	36.87
kroC100_30	29	L	9027.36	43200.67	9027.36	0.00	9027.36	0.00	10000.00	47.64

Table 17: Detailed results of our HVNS compared with benchmark RR-RANGE30

Instance	n	RR-RANGE30			HVNS					
		Status	BKS	Time (s)	Obj	Gap (%)	$\overline{\text{Obj}}$	$\overline{\text{Gap}}$ (%)	Ite	Time (s)
poi-10-1	9	O	167.00	0.13	167.00	0.00	167.00	0.00	10000.00	1.84
poi-10-1	9	O	141.00	0.74	141.00	0.00	141.00	0.00	10000.00	4.13
poi-10-1	9	O	113.00	0.24	113.00	0.00	113.00	0.00	10000.00	5.86
poi-10-10	9	O	160.00	0.15	160.00	0.00	160.00	0.00	10000.00	2.86
poi-10-10	9	O	88.00	0.49	88.00	0.00	88.00	0.00	10000.00	3.93
poi-10-10	9	O	67.00	0.43	67.00	0.00	67.00	0.00	10000.00	4.37
poi-10-11	9	O	155.00	0.23	155.00	0.00	155.00	0.00	10000.00	1.09
poi-10-11	9	O	125.00	0.42	125.00	0.00	125.00	0.00	10000.00	3.22
poi-10-11	9	O	81.00	0.17	81.00	0.00	81.00	0.00	10000.00	4.51
poi-10-12	9	O	170.00	0.13	170.00	0.00	170.00	0.00	10000.00	1.34
poi-10-12	9	O	146.00	0.17	146.00	0.00	146.00	0.00	10000.00	3.16
poi-10-12	9	O	74.00	0.25	74.00	0.00	74.00	0.00	10000.00	4.57
poi-10-13	9	O	142.00	0.12	142.00	0.00	142.00	0.00	10000.00	1.21
poi-10-13	9	O	93.00	0.19	93.00	0.00	93.00	0.00	10000.00	2.51
poi-10-13	9	O	82.00	0.52	82.00	0.00	82.00	0.00	10000.00	3.23
poi-10-14	9	O	135.00	0.14	135.00	0.00	135.00	0.00	10000.00	1.26
poi-10-14	9	O	90.00	0.19	90.00	0.00	90.00	0.00	10000.00	1.64
poi-10-14	9	O	87.00	0.21	87.00	0.00	87.00	0.00	10000.00	1.42
poi-10-15	9	O	177.00	0.15	177.00	0.00	177.00	0.00	10000.00	1.81

Table 17 – continued from previous page

Instance	n	RR-RANGE30			HVNS					
		Status	BKS	Time (s)	Obj	Gap (%)	$\overline{\text{Obj}}$	$\overline{\text{Gap}}$ (%)	Ite	Time (s)
poi-10-15	9	O	130.00	0.41	130.00	0.00	130.00	0.00	10000.00	2.51
poi-10-15	9	O	97.00	0.22	97.00	0.00	97.00	0.00	10000.00	3.13
poi-10-16	9	O	166.00	0.25	166.00	0.00	166.00	0.00	10000.00	1.58
poi-10-16	9	O	103.00	0.14	103.00	0.00	103.00	0.00	10000.00	3.01
poi-10-16	9	O	84.00	0.20	84.00	0.00	84.00	0.00	10000.00	3.82
poi-10-17	9	O	175.00	0.11	175.00	0.00	175.00	0.00	10000.00	0.59
poi-10-17	9	O	111.00	0.19	111.00	0.00	111.00	0.00	10000.00	2.58
poi-10-17	9	O	92.00	0.17	92.00	0.00	92.00	0.00	10000.00	3.15
poi-10-18	9	O	142.00	0.13	142.00	0.00	142.00	0.00	10000.00	0.73
poi-10-18	9	O	101.00	0.17	101.00	0.00	101.00	0.00	10000.00	1.49
poi-10-18	9	O	100.00	0.30	100.00	0.00	100.00	0.00	10000.00	1.94
poi-10-19	9	O	164.00	0.13	164.00	0.00	164.00	0.00	10000.00	0.80
poi-10-19	9	O	129.00	0.15	129.00	0.00	129.00	0.00	10000.00	1.38
poi-10-19	9	O	118.00	0.30	118.00	0.00	118.00	0.00	10000.00	2.02
poi-10-2	9	O	163.00	0.12	163.00	0.00	163.00	0.00	10000.00	1.66
poi-10-2	9	O	111.00	0.19	111.00	0.00	111.00	0.00	10000.00	2.96
poi-10-2	9	O	109.00	0.53	109.00	0.00	109.00	0.00	10000.00	3.01
poi-10-20	9	O	145.00	0.12	145.00	0.00	145.00	0.00	10000.00	0.81
poi-10-20	9	O	114.00	0.13	114.00	0.00	114.00	0.00	10000.00	2.46
poi-10-20	9	O	105.00	0.13	105.00	0.00	105.00	0.00	10000.00	3.60
poi-10-21	9	O	105.00	0.17	105.00	0.00	105.00	0.00	10000.00	1.34
poi-10-21	9	O	71.00	0.21	71.00	0.00	71.00	0.00	10000.00	2.32
poi-10-21	9	O	67.00	0.19	67.00	0.00	67.00	0.00	10000.00	3.33
poi-10-22	9	O	145.00	0.19	145.00	0.00	145.00	0.00	10000.00	1.69
poi-10-22	9	O	87.00	0.17	87.00	0.00	87.00	0.00	10000.00	2.76
poi-10-22	9	O	67.00	0.23	67.00	0.00	67.00	0.00	10000.00	3.70
poi-10-23	9	O	179.00	0.13	179.00	0.00	179.00	0.00	10000.00	0.56
poi-10-23	9	O	162.00	1.35	162.00	0.00	162.00	0.00	10000.00	1.54
poi-10-23	9	O	127.00	0.42	127.00	0.00	127.00	0.00	10000.00	2.45
poi-10-24	9	O	156.00	0.11	156.00	0.00	156.00	0.00	10000.00	1.95
poi-10-24	9	O	97.00	0.63	97.00	0.00	97.00	0.00	10000.00	2.82
poi-10-24	9	O	81.00	0.19	81.00	0.00	81.00	0.00	10000.00	3.36
poi-10-25	9	O	169.00	0.14	169.00	0.00	169.00	0.00	10000.00	0.59
poi-10-25	9	O	134.00	0.60	134.00	0.00	134.00	0.00	10000.00	1.91
poi-10-25	9	O	125.00	0.19	125.00	0.00	125.00	0.00	10000.00	2.48
poi-10-3	9	O	172.00	0.08	172.00	0.00	172.00	0.00	10000.00	0.62
poi-10-3	9	O	135.00	0.32	135.00	0.00	135.00	0.00	10000.00	2.61
poi-10-3	9	O	98.00	0.10	98.00	0.00	98.00	0.00	10000.00	3.02
poi-10-4	9	O	156.00	0.14	156.00	0.00	156.00	0.00	10000.00	1.37
poi-10-4	9	O	135.00	0.83	135.00	0.00	135.00	0.00	10000.00	1.84
poi-10-4	9	O	94.00	0.22	94.00	0.00	94.00	0.00	10000.00	3.07
poi-10-5	9	O	145.00	0.13	145.00	0.00	145.00	0.00	10000.00	0.84
poi-10-5	9	O	128.00	0.65	128.00	0.00	128.00	0.00	10000.00	1.75
poi-10-5	9	O	85.00	0.18	85.00	0.00	85.00	0.00	10000.00	2.29
poi-10-6	9	O	158.00	0.25	158.00	0.00	158.00	0.00	10000.00	0.65
poi-10-6	9	O	119.00	0.19	119.00	0.00	119.00	0.00	10000.00	3.29
poi-10-6	9	O	113.00	0.39	113.00	0.00	113.00	0.00	10000.00	3.31
poi-10-7	9	O	135.00	0.11	135.00	0.00	135.00	0.00	10000.00	1.84
poi-10-7	9	O	87.00	0.17	87.00	0.00	87.00	0.00	10000.00	2.19
poi-10-7	9	O	79.00	0.17	79.00	0.00	79.00	0.00	10000.00	3.34

Table 17 – continued from previous page

Instance	n	RR-RANGE30			HVNS					
		Status	BKS	Time (s)	Obj	Gap (%)	$\overline{\text{Obj}}$	$\overline{\text{Gap}}$ (%)	Ite	Time (s)
poi-10-8	9	O	123.00	0.19	123.00	0.00	123.00	0.00	10000.00	0.98
poi-10-8	9	O	80.00	0.24	80.00	0.00	80.00	0.00	10000.00	1.86
poi-10-8	9	O	66.00	0.17	66.00	0.00	66.00	0.00	10000.00	3.91
poi-10-9	9	O	169.00	0.10	169.00	0.00	169.00	0.00	10000.00	0.67
poi-10-9	9	O	142.00	0.18	142.00	0.00	142.00	0.00	10000.00	1.07
poi-10-9	9	O	139.00	0.21	139.00	0.00	139.00	0.00	10000.00	1.64
poi-20-1	19	O	196.00	2.20	196.00	0.00	196.00	0.00	10000.00	13.71
poi-20-1	19	O	153.00	9.48	153.00	0.00	153.00	0.00	10000.00	24.12
poi-20-1	19	O	132.00	4.77	132.00	0.00	132.20	0.15	10000.00	33.33
poi-20-10	19	O	179.00	1.20	179.00	0.00	179.00	0.00	10000.00	10.15
poi-20-10	19	O	144.00	5.88	144.00	0.00	144.00	0.00	10000.00	15.75
poi-20-10	19	O	130.00	1.85	130.00	0.00	130.00	0.00	10000.00	30.59
poi-20-11	19	O	177.00	4.80	177.00	0.00	177.00	0.00	10000.00	13.59
poi-20-11	19	O	150.00	16.32	150.00	0.00	150.00	0.00	10000.00	18.17
poi-20-11	19	O	148.00	39.89	148.00	0.00	148.00	0.00	10000.00	25.63
poi-20-12	19	O	186.00	9.17	186.00	0.00	186.00	0.00	10000.00	17.01
poi-20-12	19	O	136.00	13.88	136.00	0.00	136.20	0.15	10000.00	24.18
poi-20-12	19	O	123.00	40.63	123.00	0.00	123.00	0.00	10000.00	40.75
poi-20-13	19	O	178.00	23.63	178.00	0.00	178.00	0.00	10000.00	9.85
poi-20-13	19	O	157.00	242.03	157.00	0.00	157.20	0.13	10000.00	23.39
poi-20-13	19	O	129.00	29.77	129.00	0.00	129.40	0.31	10000.00	41.53
poi-20-14	19	O	169.00	1.63	169.00	0.00	169.00	0.00	10000.00	15.68
poi-20-14	19	O	145.00	18.58	145.00	0.00	145.00	0.00	10000.00	25.94
poi-20-14	19	O	134.00	8.94	134.00	0.00	134.80	0.60	10000.00	32.91
poi-20-15	19	O	199.00	12.27	199.00	0.00	199.00	0.00	10000.00	11.19
poi-20-15	19	O	139.00	6.02	139.00	0.00	139.00	0.00	10000.00	29.90
poi-20-15	19	O	121.00	5.40	121.00	0.00	121.00	0.00	10000.00	42.48
poi-20-16	19	O	174.00	11.72	174.00	0.00	174.00	0.00	10000.00	15.07
poi-20-16	19	O	129.00	7.20	129.00	0.00	129.00	0.00	10000.00	19.35
poi-20-16	19	O	118.00	2.97	118.00	0.00	118.00	0.00	10000.00	39.57
poi-20-17	19	O	158.00	16.09	158.00	0.00	158.00	0.00	10000.00	14.13
poi-20-17	19	O	108.00	2.63	108.00	0.00	108.00	0.00	10000.00	17.95
poi-20-17	19	O	101.00	2.06	101.00	0.00	101.00	0.00	10000.00	23.41
poi-20-18	19	O	197.00	7.66	197.00	0.00	197.00	0.00	10000.00	9.55
poi-20-18	19	O	152.00	56.20	152.00	0.00	152.00	0.00	10000.00	11.35
poi-20-18	19	O	135.00	7.77	135.00	0.00	135.00	0.00	10000.00	28.99
poi-20-19	19	O	168.00	6.80	168.00	0.00	168.00	0.00	10000.00	9.61
poi-20-19	19	O	122.00	1.60	122.00	0.00	122.00	0.00	10000.00	25.22
poi-20-19	19	O	114.00	13.51	114.00	0.00	114.00	0.00	10000.00	31.00
poi-20-2	19	O	194.00	24.93	194.00	0.00	194.00	0.00	10000.00	10.96
poi-20-2	19	O	151.00	23.03	151.00	0.00	151.20	0.13	10000.00	28.29
poi-20-2	19	O	130.00	2.64	130.00	0.00	130.00	0.00	10000.00	34.53
poi-20-20	19	O	193.00	2.08	193.00	0.00	193.00	0.00	10000.00	6.74
poi-20-20	19	O	154.00	24.29	154.00	0.00	154.00	0.00	10000.00	13.69
poi-20-20	19	O	148.00	63.70	148.00	0.00	148.00	0.00	10000.00	26.60
poi-20-21	19	O	171.00	3.54	171.00	0.00	171.00	0.00	10000.00	9.21
poi-20-21	19	O	137.00	1.74	137.00	0.00	137.00	0.00	10000.00	16.85
poi-20-21	19	O	129.00	10.62	129.00	0.00	129.00	0.00	10000.00	19.91
poi-20-22	19	O	203.00	35.13	203.00	0.00	203.00	0.00	10000.00	10.35
poi-20-22	19	O	136.00	4.61	136.00	0.00	136.00	0.00	10000.00	26.94

Table 17 – continued from previous page

Instance	n	RR-RANGE30			HVNS					
		Status	BKS	Time (s)	Obj	Gap (%)	$\overline{\text{Obj}}$	$\overline{\text{Gap}}$ (%)	Ite	Time (s)
poi-20-22	19	O	114.00	12.11	114.00	0.00	114.00	0.00	10000.00	36.85
poi-20-23	19	O	190.00	46.16	190.00	0.00	190.00	0.00	10000.00	14.62
poi-20-23	19	O	134.00	2.66	134.00	0.00	134.00	0.00	10000.00	33.63
poi-20-23	19	O	123.00	3.05	123.00	0.00	123.00	0.00	10000.00	52.22
poi-20-24	19	O	198.00	23.89	198.00	0.00	198.00	0.00	10000.00	14.88
poi-20-24	19	O	125.00	2.21	125.00	0.00	125.00	0.00	10000.00	26.56
poi-20-24	19	O	111.00	4.50	111.00	0.00	111.00	0.00	10000.00	37.77
poi-20-25	19	O	203.00	34.49	203.00	0.00	203.00	0.00	10000.00	9.27
poi-20-25	19	O	141.00	11.01	141.00	0.00	141.00	0.00	10000.00	26.30
poi-20-25	19	O	122.00	26.13	122.00	0.00	122.00	0.00	10000.00	35.65
poi-20-3	19	O	218.00	29.40	218.00	0.00	218.00	0.00	10000.00	10.02
poi-20-3	19	O	172.00	25.42	172.00	0.00	172.00	0.00	10000.00	21.73
poi-20-3	19	O	154.00	10.03	154.00	0.00	154.00	0.00	10000.00	32.68
poi-20-4	19	O	203.00	78.81	203.00	0.00	203.00	0.00	10000.00	10.65
poi-20-4	19	O	140.00	6.43	140.00	0.00	140.00	0.00	10000.00	24.37
poi-20-4	19	O	125.00	11.01	125.00	0.00	125.00	0.00	10000.00	37.27
poi-20-5	19	O	179.00	38.76	179.00	0.00	179.00	0.00	10000.00	12.25
poi-20-5	19	O	138.00	24.60	138.00	0.00	138.00	0.00	10000.00	24.84
poi-20-5	19	O	129.00	53.20	129.00	0.00	129.00	0.00	10000.00	28.17
poi-20-6	19	O	170.00	2.43	170.00	0.00	170.00	0.00	10000.00	15.32
poi-20-6	19	O	121.00	2.48	121.00	0.00	121.00	0.00	10000.00	29.33
poi-20-6	19	O	110.00	18.90	110.00	0.00	110.00	0.00	10000.00	36.94
poi-20-7	19	O	201.00	2.91	201.00	0.00	201.00	0.00	10000.00	12.67
poi-20-7	19	O	161.00	50.39	161.00	0.00	161.00	0.00	10000.00	30.46
poi-20-7	19	O	124.00	19.06	124.00	0.00	124.00	0.00	10000.00	40.88
poi-20-8	19	O	190.00	62.50	190.00	0.00	190.00	0.00	10000.00	12.86
poi-20-8	19	O	161.00	24.03	161.00	0.00	161.00	0.00	10000.00	25.31
poi-20-8	19	O	131.00	2.31	131.00	0.00	131.00	0.00	10000.00	33.89
poi-20-9	19	O	161.00	1.19	161.00	0.00	161.00	0.00	10000.00	11.34
poi-20-9	19	O	136.00	23.04	137.00	0.74	137.80	1.32	10000.00	13.21
poi-20-9	19	O	130.00	34.35	130.00	0.00	130.00	0.00	10000.00	28.99
poi-30-1	29	O	211.00	1815.04	211.00	0.00	211.00	0.00	10000.00	27.65
poi-30-1	29	O	165.00	425.19	165.00	0.00	165.00	0.00	10000.00	86.40
poi-30-1	29	O	139.00	29.26	140.00	0.72	140.00	0.72	10000.00	113.02
poi-30-10	29	O	199.00	225.56	199.00	0.00	199.00	0.00	10000.00	78.89
poi-30-10	29	O	159.00	642.42	159.00	0.00	159.00	0.00	10000.00	99.54
poi-30-10	29	O	139.00	215.40	139.00	0.00	139.00	0.00	10000.00	134.45
poi-30-11	29	O	205.00	106.68	205.00	0.00	205.00	0.00	10000.00	49.41
poi-30-11	29	O	162.00	295.10	162.00	0.00	162.00	0.00	10000.00	112.09
poi-30-11	29	O	144.00	1604.51	145.00	0.69	145.00	0.69	10000.00	134.91
poi-30-12	29	O	218.00	186.63	218.00	0.00	218.00	0.00	10000.00	32.67
poi-30-12	29	O	160.00	27.38	160.00	0.00	160.00	0.00	10000.00	55.45
poi-30-12	29	O	150.00	173.52	150.00	0.00	150.80	0.53	10000.00	85.79
poi-30-13	29	O	209.00	138.18	209.00	0.00	209.00	0.00	10000.00	39.19
poi-30-13	29	O	157.00	68.90	157.00	0.00	157.00	0.00	10000.00	77.67
poi-30-13	29	O	147.00	1467.26	147.00	0.00	147.00	0.00	10000.00	104.56
poi-30-14	29	O	191.00	241.93	191.00	0.00	191.00	0.00	10000.00	53.97
poi-30-14	29	O	161.00	531.09	161.00	0.00	161.00	0.00	10000.00	66.86
poi-30-14	29	O	148.00	275.72	149.00	0.68	149.40	0.95	10000.00	102.01
poi-30-15	29	O	188.00	1789.83	188.00	0.00	188.00	0.00	10000.00	81.68

Table 17 – continued from previous page

Instance	n	RR-RANGE30			HVNS					
		Status	BKS	Time (s)	Obj	Gap (%)	$\overline{\text{Obj}}$	$\overline{\text{Gap}}$ (%)	Ite	Time (s)
poi-30-15	29	O	144.00	100.78	144.00	0.00	144.00	0.00	10000.00	78.97
poi-30-15	29	O	137.00	634.41	137.00	0.00	137.00	0.00	10000.00	133.02
poi-30-16	29	O	197.00	66.25	197.00	0.00	197.00	0.00	10000.00	45.86
poi-30-16	29	O	156.00	148.26	156.00	0.00	156.00	0.00	10000.00	59.42
poi-30-16	29	O	143.00	368.61	146.00	2.10	146.40	2.38	10000.00	100.03
poi-30-17	29	L	222.00	3600.00	221.00	-0.45	221.00	-0.45	10000.00	45.66
poi-30-17	29	O	162.00	215.78	162.00	0.00	162.00	0.00	10000.00	94.22
poi-30-17	29	O	147.00	255.68	147.00	0.00	148.20	0.82	10000.00	111.55
poi-30-18	29	L	212.00	3600.00	212.00	0.00	212.00	0.00	10000.00	38.25
poi-30-18	29	O	160.00	132.84	160.00	0.00	160.00	0.00	10000.00	90.02
poi-30-18	29	O	136.00	274.40	136.00	0.00	136.20	0.15	10000.00	118.84
poi-30-19	29	O	198.00	1606.31	198.00	0.00	198.00	0.00	10000.00	33.47
poi-30-19	29	O	165.00	586.48	165.00	0.00	165.00	0.00	10000.00	57.89
poi-30-19	29	O	155.00	985.03	156.00	0.65	156.40	0.90	10000.00	108.15
poi-30-2	29	O	210.00	178.56	210.00	0.00	210.00	0.00	10000.00	44.85
poi-30-2	29	O	160.00	315.34	160.00	0.00	160.00	0.00	10000.00	103.83
poi-30-2	29	O	142.00	621.15	142.00	0.00	142.60	0.42	10000.00	133.87
poi-30-20	29	O	191.00	378.31	191.00	0.00	191.00	0.00	10000.00	42.70
poi-30-20	29	O	148.00	714.56	148.00	0.00	148.00	0.00	10000.00	116.81
poi-30-20	29	L	270.00	3600.00	138.00	-48.89	138.40	-48.74	10000.00	122.85
poi-30-21	29	O	205.00	673.75	205.00	0.00	205.00	0.00	10000.00	43.27
poi-30-21	29	O	164.00	990.67	164.00	0.00	164.80	0.49	10000.00	84.40
poi-30-21	29	O	142.00	733.21	143.00	0.70	143.00	0.70	10000.00	127.08
poi-30-22	29	O	211.00	34.75	211.00	0.00	211.00	0.00	10000.00	44.36
poi-30-22	29	O	173.00	95.23	173.00	0.00	173.00	0.00	10000.00	47.82
poi-30-22	29	O	162.00	463.12	162.00	0.00	162.00	0.00	10000.00	94.98
poi-30-23	29	L	200.00	3600.00	200.00	0.00	200.00	0.00	10000.00	59.18
poi-30-23	29	L	341.00	3600.00	151.00	-55.72	151.60	-55.54	10000.00	109.81
poi-30-23	29	L	341.00	3600.00	137.00	-59.82	137.60	-59.65	10000.00	173.00
poi-30-24	29	O	184.00	1599.63	184.00	0.00	184.00	0.00	10000.00	57.16
poi-30-24	29	O	146.00	134.55	146.00	0.00	146.40	0.27	10000.00	110.03
poi-30-24	29	O	132.00	406.92	132.00	0.00	132.00	0.00	10000.00	119.25
poi-30-25	29	L	239.00	3600.00	235.00	-1.67	235.00	-1.67	10000.00	37.60
poi-30-25	29	O	183.00	120.08	183.00	0.00	183.00	0.00	10000.00	72.68
poi-30-25	29	O	164.00	72.54	164.00	0.00	164.00	0.00	10000.00	120.97
poi-30-3	29	O	185.00	65.83	185.00	0.00	185.00	0.00	10000.00	52.66
poi-30-3	29	O	153.00	189.52	153.00	0.00	153.00	0.00	10000.00	97.75
poi-30-3	29	O	143.00	217.48	143.00	0.00	145.00	1.40	10000.00	120.86
poi-30-4	29	O	224.00	2187.55	224.00	0.00	224.00	0.00	10000.00	43.40
poi-30-4	29	O	150.00	32.01	150.00	0.00	150.00	0.00	10000.00	94.97
poi-30-4	29	O	129.00	1040.64	129.00	0.00	129.20	0.16	10000.00	142.88
poi-30-5	29	O	197.00	255.85	197.00	0.00	197.00	0.00	10000.00	69.24
poi-30-5	29	O	164.00	561.09	164.00	0.00	164.80	0.49	10000.00	59.92
poi-30-5	29	O	144.00	185.35	144.00	0.00	144.00	0.00	10000.00	94.66
poi-30-6	29	O	214.00	410.48	214.00	0.00	214.00	0.00	10000.00	43.77
poi-30-6	29	O	156.00	144.97	156.00	0.00	156.00	0.00	10000.00	44.24
poi-30-6	29	O	146.00	571.90	146.00	0.00	146.60	0.41	10000.00	109.89
poi-30-7	29	O	182.00	189.27	182.00	0.00	182.00	0.00	10000.00	32.18
poi-30-7	29	O	147.00	114.04	147.00	0.00	147.00	0.00	10000.00	121.23
poi-30-7	29	O	131.00	112.78	131.00	0.00	131.00	0.00	10000.00	113.49

Table 17 – continued from previous page

Instance	n	RR-RANGE30			HVNS					
		Status	BKS	Time (s)	Obj	Gap (%)	$\overline{\text{Obj}}$	$\overline{\text{Gap}}$ (%)	Ite	Time (s)
poi-30-8	29	O	199.00	36.14	199.00	0.00	199.00	0.00	10000.00	46.75
poi-30-8	29	O	164.00	195.58	164.00	0.00	164.20	0.12	10000.00	55.75
poi-30-8	29	O	155.00	652.24	155.00	0.00	155.00	0.00	10000.00	77.58
poi-30-9	29	O	197.00	122.27	197.00	0.00	197.00	0.00	10000.00	50.86
poi-30-9	29	O	157.00	206.17	157.00	0.00	157.00	0.00	10000.00	79.45
poi-30-9	29	O	143.00	782.22	143.00	0.00	143.00	0.00	10000.00	105.78
poi-40-1	39	L	390.00	3600.00	226.00	-42.05	226.60	-41.90	10000.00	236.29
poi-40-1	39	L	390.00	3600.00	172.00	-55.90	172.00	-55.90	10000.00	239.63
poi-40-1	39	L	390.00	3600.00	154.00	-60.51	154.80	-60.31	10000.00	267.60
poi-40-10	39	L	216.00	3600.00	215.00	-0.46	215.00	-0.46	10000.00	117.36
poi-40-10	39	L	404.00	3600.00	177.00	-56.19	177.40	-56.09	10000.00	240.65
poi-40-10	39	L	404.00	3600.00	166.00	-58.91	166.20	-58.86	9715.40	298.92
poi-40-11	39	L	384.00	3600.00	221.00	-42.45	221.00	-42.45	10000.00	153.71
poi-40-11	39	O	175.00	1126.27	175.00	0.00	175.20	0.11	10000.00	240.39
poi-40-11	39	O	159.00	1788.03	159.00	0.00	159.40	0.25	10000.00	280.11
poi-40-12	39	O	207.00	242.61	207.00	0.00	207.00	0.00	10000.00	106.71
poi-40-12	39	O	168.00	2787.80	168.00	0.00	168.00	0.00	10000.00	238.45
poi-40-12	39	O	147.00	1142.27	147.00	0.00	147.00	0.00	10000.00	273.63
poi-40-13	39	L	363.00	3600.00	228.00	-37.19	228.00	-37.19	10000.00	100.25
poi-40-13	39	L	363.00	3600.00	179.00	-50.69	179.00	-50.69	9892.00	293.48
poi-40-13	39	L	363.00	3600.00	163.00	-55.10	163.60	-54.93	9071.80	300.00
poi-40-14	39	L	387.00	3600.00	234.00	-39.53	234.20	-39.48	10000.00	159.51
poi-40-14	39	L	387.00	3600.00	177.00	-54.26	177.00	-54.26	10000.00	230.47
poi-40-14	39	L	387.00	3600.00	159.00	-58.91	159.80	-58.71	9933.00	296.18
poi-40-15	39	L	346.00	3600.00	229.00	-33.82	229.00	-33.82	10000.00	80.41
poi-40-15	39	O	174.00	991.88	174.00	0.00	174.00	0.00	10000.00	177.27
poi-40-15	39	L	346.00	3600.00	162.00	-53.18	162.00	-53.18	10000.00	203.79
poi-40-16	39	O	211.00	508.17	211.00	0.00	211.00	0.00	10000.00	128.55
poi-40-16	39	L	377.00	3600.00	171.00	-54.64	172.00	-54.38	10000.00	236.23
poi-40-16	39	O	149.00	634.13	149.00	0.00	150.40	0.94	9540.40	300.00
poi-40-17	39	O	232.00	1903.11	232.00	0.00	232.00	0.00	10000.00	130.96
poi-40-17	39	L	359.00	3600.00	180.00	-49.86	180.00	-49.86	10000.00	136.17
poi-40-17	39	O	162.00	3464.50	162.00	0.00	162.40	0.25	10000.00	183.32
poi-40-18	39	L	391.00	3600.00	236.00	-39.64	236.00	-39.64	10000.00	95.36
poi-40-18	39	L	391.00	3600.00	185.00	-52.69	185.00	-52.69	10000.00	227.27
poi-40-18	39	L	391.00	3600.00	166.00	-57.54	166.00	-57.54	8834.80	300.00
poi-40-19	39	L	368.00	3600.00	196.00	-46.74	196.00	-46.74	10000.00	132.78
poi-40-19	39	L	368.00	3600.00	157.00	-57.34	157.20	-57.28	10000.00	213.62
poi-40-19	39	L	368.00	3600.00	140.00	-61.96	140.80	-61.74	9978.60	285.75
poi-40-2	39	L	348.00	3600.00	225.00	-35.34	225.00	-35.34	10000.00	108.78
poi-40-2	39	O	173.00	844.36	173.00	0.00	173.20	0.12	10000.00	200.00
poi-40-2	39	O	152.00	592.72	152.00	0.00	152.60	0.39	10000.00	281.98
poi-40-20	39	L	328.00	3600.00	219.00	-33.23	219.00	-33.23	10000.00	140.38
poi-40-20	39	L	328.00	3600.00	180.00	-45.12	180.00	-45.12	10000.00	259.14
poi-40-20	39	O	160.00	854.12	160.00	0.00	161.20	0.75	10000.00	286.17
poi-40-21	39	L	329.00	3600.00	233.00	-29.18	233.00	-29.18	10000.00	132.35
poi-40-21	39	O	169.00	327.51	169.00	0.00	169.00	0.00	10000.00	247.49
poi-40-21	39	O	154.00	1882.09	155.00	0.65	155.20	0.78	9978.60	283.10
poi-40-22	39	L	339.00	3600.00	249.00	-26.55	249.00	-26.55	10000.00	173.28
poi-40-22	39	L	339.00	3600.00	201.00	-40.71	204.00	-39.82	10000.00	120.42

Table 17 – continued from previous page

Instance	n	RR-RANGE30			HVNS					
		Status	BKS	Time (s)	Obj	Gap (%)	$\overline{\text{Obj}}$	$\overline{\text{Gap}}$ (%)	Ite	Time (s)
poi-40-22	39	L	339.00	3600.00	181.00	-46.61	184.00	-45.72	10000.00	150.77
poi-40-23	39	L	395.00	3600.00	248.00	-37.22	248.00	-37.22	10000.00	146.88
poi-40-23	39	L	395.00	3600.00	193.00	-51.14	193.40	-51.04	9858.20	293.70
poi-40-23	39	L	395.00	3600.00	173.00	-56.20	173.20	-56.15	8718.40	300.00
poi-40-24	39	O	206.00	1623.44	206.00	0.00	206.00	0.00	10000.00	100.03
poi-40-24	39	O	171.00	2320.92	171.00	0.00	171.00	0.00	10000.00	230.33
poi-40-24	39	L	340.00	3600.00	159.00	-53.24	159.20	-53.18	10000.00	238.32
poi-40-25	39	L	417.00	3600.00	233.00	-44.12	233.00	-44.12	10000.00	90.03
poi-40-25	39	L	417.00	3600.00	180.00	-56.83	180.80	-56.64	10000.00	192.21
poi-40-25	39	L	417.00	3600.00	153.00	-63.31	153.80	-63.12	9098.80	300.00
poi-40-3	39	L	416.00	3600.00	233.00	-43.99	233.00	-43.99	10000.00	136.07
poi-40-3	39	L	416.00	3600.00	192.00	-53.85	192.60	-53.70	10000.00	243.43
poi-40-3	39	L	416.00	3600.00	178.00	-57.21	178.20	-57.16	9979.20	295.07
poi-40-4	39	O	231.00	2966.49	231.00	0.00	231.00	0.00	10000.00	142.64
poi-40-4	39	O	193.00	2029.52	193.00	0.00	193.20	0.10	10000.00	246.75
poi-40-4	39	O	167.00	1208.02	167.00	0.00	167.60	0.36	10000.00	272.75
poi-40-5	39	L	354.00	3600.00	237.00	-33.05	238.60	-32.60	10000.00	134.09
poi-40-5	39	L	354.00	3600.00	188.00	-46.89	188.00	-46.89	10000.00	125.23
poi-40-5	39	L	354.00	3600.00	159.00	-55.08	159.00	-55.08	9648.60	299.73
poi-40-6	39	O	186.00	1246.71	186.00	0.00	186.00	0.00	10000.00	144.28
poi-40-6	39	O	149.00	2279.35	149.00	0.00	149.40	0.27	10000.00	237.17
poi-40-6	39	L	335.00	3600.00	140.00	-58.21	140.00	-58.21	9885.60	278.09
poi-40-7	39	O	225.00	416.48	225.00	0.00	225.00	0.00	10000.00	132.56
poi-40-7	39	L	396.00	3600.00	162.00	-59.09	162.40	-58.99	10000.00	187.00
poi-40-7	39	L	396.00	3600.00	144.00	-63.64	144.60	-63.48	10000.00	170.53
poi-40-8	39	L	351.00	3600.00	239.00	-31.91	239.00	-31.91	10000.00	70.99
poi-40-8	39	L	351.00	3600.00	187.00	-46.72	187.60	-46.55	10000.00	154.61
poi-40-8	39	L	351.00	3600.00	170.00	-51.57	170.60	-51.40	10000.00	276.76
poi-40-9	39	O	228.00	625.96	228.00	0.00	228.00	0.00	10000.00	104.56
poi-40-9	39	L	387.00	3600.00	184.00	-52.45	184.20	-52.40	10000.00	211.92
poi-40-9	39	O	161.00	3444.58	161.00	0.00	161.80	0.50	10000.00	199.30

Table 18: Detailed results of our HVNS compared with benchmark RR-MHD

Instance	n	RR-MHD			HVNS					
		Status	BKS	Time (s)	Obj	Gap (%)	$\overline{\text{Obj}}$	$\overline{\text{Gap}}$ (%)	Ite	Time (s)
poi-10-1	9	O	173.00	0.07	173.00	0.00	173.00	0.00	10000.00	1.66
poi-10-1	9	O	166.00	0.07	166.00	0.00	166.00	0.00	10000.00	1.42
poi-10-1	9	O	166.00	0.10	166.00	0.00	166.00	0.00	10000.00	2.83
poi-10-10	9	O	175.00	0.12	175.00	0.00	175.00	0.00	10000.00	1.65
poi-10-10	9	O	138.00	0.16	138.00	0.00	138.00	0.00	10000.00	4.25
poi-10-10	9	O	110.00	0.30	110.00	0.00	110.00	0.00	10000.00	4.83
poi-10-11	9	O	169.00	0.09	169.00	0.00	169.00	0.00	10000.00	1.09
poi-10-11	9	O	154.00	0.09	154.00	0.00	154.00	0.00	10000.00	2.12
poi-10-11	9	O	140.00	0.15	140.00	0.00	140.00	0.00	10000.00	3.19
poi-10-12	9	O	182.00	0.10	182.00	0.00	182.00	0.00	10000.00	0.93
poi-10-12	9	O	171.00	0.13	171.00	0.00	171.00	0.00	10000.00	1.92
poi-10-12	9	O	169.00	0.12	169.00	0.00	169.00	0.00	10000.00	2.45
poi-10-13	9	O	170.00	0.10	170.00	0.00	170.00	0.00	10000.00	0.63

Table 18 – continued from previous page

Instance	n	RR-MHD			HVNS					
		Status	BKS	Time (s)	Obj	Gap (%)	$\overline{\text{Obj}}$	$\overline{\text{Gap}}$ (%)	Ite	Time (s)
poi-10-13	9	O	149.00	0.10	149.00	0.00	149.00	0.00	10000.00	0.97
poi-10-13	9	O	100.00	0.19	100.00	0.00	100.00	0.00	10000.00	1.45
poi-10-14	9	O	162.00	0.12	162.00	0.00	162.00	0.00	10000.00	0.59
poi-10-14	9	O	138.00	0.14	138.00	0.00	138.00	0.00	10000.00	1.05
poi-10-14	9	O	106.00	0.17	106.00	0.00	106.00	0.00	10000.00	2.04
poi-10-15	9	O	195.00	0.13	195.00	0.00	195.00	0.00	10000.00	0.57
poi-10-15	9	O	179.00	0.15	179.00	0.00	179.00	0.00	10000.00	0.99
poi-10-15	9	O	143.00	0.14	143.00	0.00	143.00	0.00	10000.00	1.60
poi-10-16	9	O	174.00	0.11	174.00	0.00	174.00	0.00	10000.00	0.43
poi-10-16	9	O	151.00	0.10	151.00	0.00	151.00	0.00	10000.00	1.57
poi-10-16	9	O	113.00	0.12	113.00	0.00	113.00	0.00	10000.00	2.00
poi-10-17	9	O	201.00	0.10	201.00	0.00	201.00	0.00	10000.00	0.61
poi-10-17	9	O	185.00	0.10	185.00	0.00	185.00	0.00	10000.00	0.72
poi-10-17	9	O	129.00	0.13	129.00	0.00	129.00	0.00	10000.00	1.35
poi-10-18	9	O	166.00	0.10	166.00	0.00	166.00	0.00	10000.00	0.33
poi-10-18	9	O	141.00	0.11	141.00	0.00	141.00	0.00	10000.00	0.87
poi-10-18	9	O	135.00	0.24	135.00	0.00	135.00	0.00	10000.00	1.16
poi-10-19	9	O	174.00	0.12	174.00	0.00	174.00	0.00	10000.00	0.53
poi-10-19	9	O	163.00	0.10	163.00	0.00	163.00	0.00	10000.00	0.87
poi-10-19	9	O	159.00	0.10	159.00	0.00	159.00	0.00	10000.00	1.38
poi-10-2	9	O	175.00	0.10	175.00	0.00	175.00	0.00	10000.00	0.39
poi-10-2	9	O	162.00	0.10	162.00	0.00	162.00	0.00	10000.00	0.92
poi-10-2	9	O	162.00	0.14	162.00	0.00	162.00	0.00	10000.00	0.90
poi-10-20	9	O	155.00	0.07	155.00	0.00	155.00	0.00	10000.00	0.33
poi-10-20	9	O	140.00	0.10	140.00	0.00	140.00	0.00	10000.00	0.67
poi-10-20	9	O	128.00	0.10	128.00	0.00	128.00	0.00	10000.00	1.37
poi-10-21	9	O	132.00	0.12	132.00	0.00	132.00	0.00	10000.00	0.53
poi-10-21	9	O	79.00	0.22	79.00	0.00	79.00	0.00	10000.00	2.09
poi-10-21	9	O	78.00	0.24	78.00	0.00	78.00	0.00	10000.00	2.65
poi-10-22	9	O	153.00	0.12	153.00	0.00	153.00	0.00	10000.00	0.41
poi-10-22	9	O	150.00	0.14	150.00	0.00	150.00	0.00	10000.00	0.99
poi-10-22	9	O	147.00	0.15	147.00	0.00	147.00	0.00	10000.00	1.63
poi-10-23	9	O	182.00	0.12	182.00	0.00	182.00	0.00	10000.00	0.34
poi-10-23	9	O	182.00	0.13	182.00	0.00	182.00	0.00	10000.00	0.35
poi-10-23	9	O	182.00	0.15	182.00	0.00	182.00	0.00	10000.00	0.53
poi-10-24	9	O	168.00	0.09	168.00	0.00	168.00	0.00	10000.00	0.37
poi-10-24	9	O	122.00	0.12	122.00	0.00	122.00	0.00	10000.00	1.45
poi-10-24	9	O	118.00	0.12	118.00	0.00	118.00	0.00	10000.00	1.44
poi-10-25	9	O	169.00	0.13	169.00	0.00	169.00	0.00	10000.00	0.33
poi-10-25	9	O	164.00	0.11	164.00	0.00	164.00	0.00	10000.00	0.77
poi-10-25	9	O	148.00	0.10	148.00	0.00	148.00	0.00	10000.00	1.37
poi-10-3	9	O	178.00	0.14	178.00	0.00	178.00	0.00	10000.00	0.45
poi-10-3	9	O	177.00	0.10	177.00	0.00	177.00	0.00	10000.00	0.48
poi-10-3	9	O	165.00	0.08	165.00	0.00	165.00	0.00	10000.00	1.28
poi-10-4	9	O	178.00	0.13	178.00	0.00	178.00	0.00	10000.00	0.45
poi-10-4	9	O	149.00	0.09	149.00	0.00	149.00	0.00	10000.00	1.08
poi-10-4	9	O	145.00	0.29	145.00	0.00	145.00	0.00	10000.00	1.61
poi-10-5	9	O	150.00	0.09	150.00	0.00	150.00	0.00	10000.00	0.56
poi-10-5	9	O	147.00	0.09	147.00	0.00	147.00	0.00	10000.00	0.62
poi-10-5	9	O	147.00	0.14	147.00	0.00	147.00	0.00	10000.00	0.66

Table 18 – continued from previous page

Instance	n	RR-MHD			HVNS					
		Status	BKS	Time (s)	Obj	Gap (%)	$\overline{\text{Obj}}$	$\overline{\text{Gap}}$ (%)	Ite	Time (s)
poi-10-6	9	O	178.00	0.11	178.00	0.00	178.00	0.00	10000.00	0.41
poi-10-6	9	O	153.00	0.11	153.00	0.00	153.00	0.00	10000.00	1.03
poi-10-6	9	O	148.00	0.21	148.00	0.00	148.00	0.00	10000.00	2.00
poi-10-7	9	O	158.00	0.12	158.00	0.00	158.00	0.00	10000.00	0.64
poi-10-7	9	O	131.00	0.12	131.00	0.00	131.00	0.00	10000.00	1.16
poi-10-7	9	O	123.00	0.26	123.00	0.00	123.00	0.00	10000.00	1.31
poi-10-8	9	O	133.00	0.10	133.00	0.00	133.00	0.00	10000.00	0.64
poi-10-8	9	O	113.00	0.12	113.00	0.00	113.00	0.00	10000.00	1.44
poi-10-8	9	O	97.00	0.37	97.00	0.00	97.00	0.00	10000.00	2.22
poi-10-9	9	O	189.00	0.10	189.00	0.00	189.00	0.00	10000.00	0.65
poi-10-9	9	O	168.00	0.11	168.00	0.00	168.00	0.00	10000.00	0.86
poi-10-9	9	O	159.00	0.17	159.00	0.00	159.00	0.00	10000.00	1.09
poi-20-1	19	O	226.00	0.40	226.00	0.00	226.00	0.00	10000.00	5.79
poi-20-1	19	O	212.00	0.71	212.00	0.00	212.00	0.00	10000.00	9.35
poi-20-1	19	O	185.00	3.67	187.00	1.08	187.00	1.08	10000.00	16.40
poi-20-10	19	O	213.00	0.23	213.00	0.00	213.00	0.00	10000.00	3.24
poi-20-10	19	O	188.00	2.05	188.00	0.00	188.00	0.00	10000.00	7.68
poi-20-10	19	O	178.00	1.27	178.00	0.00	179.00	0.56	10000.00	9.64
poi-20-11	19	O	205.00	0.32	205.00	0.00	205.00	0.00	10000.00	4.45
poi-20-11	19	O	180.00	1.08	180.00	0.00	180.00	0.00	10000.00	9.62
poi-20-11	19	O	175.00	3.17	175.00	0.00	175.00	0.00	10000.00	11.24
poi-20-12	19	O	225.00	15.03	225.00	0.00	225.00	0.00	10000.00	4.52
poi-20-12	19	O	172.00	7.96	172.00	0.00	172.00	0.00	10000.00	12.95
poi-20-12	19	O	158.00	3.46	158.00	0.00	158.00	0.00	10000.00	16.90
poi-20-13	19	O	208.00	0.41	208.00	0.00	208.00	0.00	10000.00	6.09
poi-20-13	19	O	200.00	3.51	200.00	0.00	200.00	0.00	10000.00	6.32
poi-20-13	19	O	162.00	11.00	162.00	0.00	169.80	4.81	10000.00	9.53
poi-20-14	19	O	189.00	1.12	189.00	0.00	189.00	0.00	10000.00	5.04
poi-20-14	19	O	174.00	16.54	174.00	0.00	174.00	0.00	10000.00	13.04
poi-20-14	19	O	159.00	8.84	160.00	0.63	160.00	0.63	10000.00	20.17
poi-20-15	19	O	251.00	1.12	251.00	0.00	251.00	0.00	10000.00	3.65
poi-20-15	19	O	170.00	1.67	170.00	0.00	170.00	0.00	10000.00	15.63
poi-20-15	19	O	157.00	7.30	157.00	0.00	157.00	0.00	10000.00	13.78
poi-20-16	19	O	212.00	0.49	212.00	0.00	212.00	0.00	10000.00	4.48
poi-20-16	19	O	172.00	1.10	172.00	0.00	172.00	0.00	10000.00	7.26
poi-20-16	19	O	171.00	3.22	171.00	0.00	171.00	0.00	10000.00	16.29
poi-20-17	19	O	192.00	2.23	192.00	0.00	192.00	0.00	10000.00	3.80
poi-20-17	19	O	137.00	1.34	137.00	0.00	137.00	0.00	10000.00	12.42
poi-20-17	19	O	134.00	6.41	134.00	0.00	134.00	0.00	10000.00	21.05
poi-20-18	19	O	223.00	0.57	223.00	0.00	223.00	0.00	10000.00	4.19
poi-20-18	19	O	201.00	1.05	201.00	0.00	201.00	0.00	10000.00	6.60
poi-20-18	19	O	178.00	2.82	178.00	0.00	178.00	0.00	10000.00	12.50
poi-20-19	19	O	215.00	1.12	215.00	0.00	215.00	0.00	10000.00	4.41
poi-20-19	19	O	155.00	0.92	155.00	0.00	155.00	0.00	10000.00	16.12
poi-20-19	19	O	146.00	1.80	146.00	0.00	146.00	0.00	10000.00	22.75
poi-20-2	19	O	233.00	0.75	233.00	0.00	233.00	0.00	10000.00	3.33
poi-20-2	19	O	195.00	2.27	196.00	0.51	196.00	0.51	10000.00	7.24
poi-20-2	19	O	172.00	3.93	172.00	0.00	172.00	0.00	10000.00	18.70
poi-20-20	19	O	208.00	0.65	208.00	0.00	208.00	0.00	10000.00	5.79
poi-20-20	19	O	186.00	2.25	186.00	0.00	186.00	0.00	10000.00	8.37

Table 18 – continued from previous page

Instance	n	RR-MHD			HVNS					
		Status	BKS	Time (s)	Obj	Gap (%)	$\overline{\text{Obj}}$	$\overline{\text{Gap}}$ (%)	Ite	Time (s)
poi-20-20	19	O	184.00	2.02	184.00	0.00	184.00	0.00	10000.00	11.23
poi-20-21	19	O	205.00	0.27	205.00	0.00	205.00	0.00	10000.00	2.62
poi-20-21	19	O	179.00	0.99	179.00	0.00	179.00	0.00	10000.00	10.01
poi-20-21	19	O	166.00	5.93	166.00	0.00	166.00	0.00	10000.00	12.97
poi-20-22	19	O	235.00	0.68	235.00	0.00	235.00	0.00	10000.00	3.74
poi-20-22	19	O	198.00	7.09	198.00	0.00	198.00	0.00	10000.00	12.58
poi-20-22	19	O	167.00	2.91	167.00	0.00	167.00	0.00	10000.00	19.31
poi-20-23	19	O	227.00	1.11	227.00	0.00	227.00	0.00	10000.00	4.03
poi-20-23	19	O	207.00	3.08	207.00	0.00	207.20	0.10	10000.00	8.30
poi-20-23	19	O	169.00	10.15	169.00	0.00	169.00	0.00	10000.00	17.35
poi-20-24	19	O	234.00	1.20	234.00	0.00	234.00	0.00	10000.00	4.84
poi-20-24	19	O	154.00	0.94	154.00	0.00	154.00	0.00	10000.00	13.04
poi-20-24	19	O	128.00	3.89	128.00	0.00	128.00	0.00	10000.00	24.26
poi-20-25	19	O	230.00	0.55	230.00	0.00	230.00	0.00	10000.00	3.44
poi-20-25	19	O	185.00	2.43	185.00	0.00	185.00	0.00	10000.00	8.64
poi-20-25	19	O	170.00	4.71	170.00	0.00	170.80	0.47	10000.00	12.41
poi-20-3	19	O	255.00	0.60	255.00	0.00	255.00	0.00	10000.00	3.24
poi-20-3	19	O	221.00	1.41	221.00	0.00	221.00	0.00	10000.00	5.78
poi-20-3	19	O	198.00	0.80	198.00	0.00	198.00	0.00	10000.00	9.93
poi-20-4	19	O	228.00	0.78	228.00	0.00	228.00	0.00	10000.00	4.75
poi-20-4	19	O	166.00	5.24	167.00	0.60	168.00	1.20	10000.00	11.24
poi-20-4	19	O	146.00	8.66	146.00	0.00	146.00	0.00	10000.00	22.97
poi-20-5	19	O	217.00	2.10	217.00	0.00	217.00	0.00	10000.00	2.94
poi-20-5	19	O	166.00	5.91	166.00	0.00	166.00	0.00	10000.00	11.22
poi-20-5	19	O	153.00	10.33	153.00	0.00	153.00	0.00	10000.00	17.27
poi-20-6	19	O	208.00	0.86	208.00	0.00	208.00	0.00	10000.00	4.54
poi-20-6	19	O	144.00	1.19	144.00	0.00	144.00	0.00	10000.00	14.25
poi-20-6	19	O	130.00	3.46	130.00	0.00	130.00	0.00	10000.00	25.40
poi-20-7	19	O	220.00	0.76	220.00	0.00	220.00	0.00	10000.00	4.65
poi-20-7	19	O	200.00	1.07	200.00	0.00	200.00	0.00	10000.00	12.33
poi-20-7	19	O	200.00	4.27	200.00	0.00	200.00	0.00	10000.00	13.77
poi-20-8	19	O	217.00	1.56	217.00	0.00	217.00	0.00	10000.00	6.25
poi-20-8	19	O	196.00	3.19	196.00	0.00	196.00	0.00	10000.00	6.86
poi-20-8	19	O	178.00	4.05	178.00	0.00	178.00	0.00	10000.00	16.03
poi-20-9	19	O	188.00	0.30	188.00	0.00	188.00	0.00	10000.00	3.67
poi-20-9	19	O	167.00	2.79	167.00	0.00	167.00	0.00	10000.00	9.58
poi-20-9	19	O	158.00	7.12	158.00	0.00	158.00	0.00	10000.00	10.38
poi-30-1	29	O	246.00	21.16	246.00	0.00	246.00	0.00	10000.00	10.73
poi-30-1	29	O	204.00	110.71	204.00	0.00	204.00	0.00	10000.00	32.19
poi-30-1	29	O	185.00	21.82	185.00	0.00	185.00	0.00	10000.00	52.53
poi-30-10	29	O	248.00	47.25	248.00	0.00	248.00	0.00	10000.00	18.58
poi-30-10	29	O	204.00	74.63	204.00	0.00	205.20	0.59	10000.00	38.81
poi-30-10	29	O	189.00	175.50	189.00	0.00	189.00	0.00	10000.00	75.30
poi-30-11	29	O	249.00	60.31	250.00	0.40	250.00	0.40	10000.00	23.81
poi-30-11	29	O	200.00	73.34	200.00	0.00	200.80	0.40	10000.00	58.16
poi-30-11	29	O	189.00	139.91	189.00	0.00	189.00	0.00	10000.00	74.42
poi-30-12	29	O	258.00	1.88	258.00	0.00	258.00	0.00	10000.00	19.96
poi-30-12	29	O	190.00	16.21	190.00	0.00	190.00	0.00	10000.00	55.49
poi-30-12	29	O	180.00	73.77	183.00	1.67	183.20	1.78	10000.00	71.62
poi-30-13	29	O	256.00	21.42	256.00	0.00	256.00	0.00	10000.00	14.16

Table 18 – continued from previous page

Instance	n	RR-MHD			HVNS					
		Status	BKS	Time (s)	Obj	Gap (%)	$\overline{\text{Obj}}$	$\overline{\text{Gap}}$ (%)	Ite	Time (s)
poi-30-13	29	O	205.00	52.99	205.00	0.00	205.00	0.00	10000.00	34.51
poi-30-13	29	O	199.00	181.04	199.00	0.00	199.00	0.00	10000.00	68.40
poi-30-14	29	O	229.00	7.17	229.00	0.00	229.00	0.00	10000.00	13.26
poi-30-14	29	O	186.00	117.55	186.00	0.00	186.00	0.00	10000.00	35.88
poi-30-14	29	O	177.00	200.46	178.00	0.56	178.00	0.56	10000.00	64.85
poi-30-15	29	O	214.00	57.29	214.00	0.00	214.00	0.00	10000.00	18.02
poi-30-15	29	O	189.00	73.75	189.00	0.00	189.00	0.00	10000.00	41.38
poi-30-15	29	O	184.00	44.88	184.00	0.00	184.00	0.00	10000.00	92.32
poi-30-16	29	O	246.00	4.99	246.00	0.00	246.00	0.00	10000.00	14.79
poi-30-16	29	O	202.00	50.72	202.00	0.00	202.00	0.00	10000.00	46.83
poi-30-16	29	O	196.00	83.64	196.00	0.00	196.00	0.00	10000.00	64.95
poi-30-17	29	O	255.00	33.82	255.00	0.00	255.00	0.00	10000.00	15.39
poi-30-17	29	O	192.00	26.28	192.00	0.00	192.00	0.00	10000.00	38.20
poi-30-17	29	O	174.00	32.11	174.00	0.00	179.60	3.22	10000.00	56.56
poi-30-18	29	O	257.00	28.80	257.00	0.00	257.00	0.00	10000.00	30.96
poi-30-18	29	O	219.00	159.40	219.00	0.00	219.40	0.18	10000.00	33.10
poi-30-18	29	O	179.00	53.90	185.00	3.35	185.00	3.35	10000.00	40.62
poi-30-19	29	O	232.00	6.59	232.00	0.00	232.00	0.00	10000.00	16.38
poi-30-19	29	O	203.00	9.20	203.00	0.00	203.00	0.00	10000.00	27.78
poi-30-19	29	O	202.00	53.92	202.00	0.00	202.00	0.00	10000.00	40.76
poi-30-2	29	O	263.00	55.31	263.00	0.00	263.00	0.00	10000.00	12.47
poi-30-2	29	O	200.00	78.26	200.00	0.00	200.40	0.20	10000.00	47.09
poi-30-2	29	O	180.00	120.08	180.00	0.00	181.00	0.56	10000.00	80.40
poi-30-20	29	O	228.00	16.14	228.00	0.00	228.00	0.00	10000.00	19.00
poi-30-20	29	O	178.00	158.56	178.00	0.00	178.00	0.00	10000.00	65.81
poi-30-20	29	O	168.00	482.93	171.00	1.79	171.00	1.79	10000.00	88.62
poi-30-21	29	O	233.00	6.53	233.00	0.00	233.00	0.00	10000.00	18.34
poi-30-21	29	O	213.00	90.81	214.00	0.47	214.00	0.47	10000.00	32.01
poi-30-21	29	O	201.00	28.63	201.00	0.00	201.00	0.00	10000.00	52.87
poi-30-22	29	O	255.00	5.38	255.00	0.00	255.00	0.00	10000.00	23.37
poi-30-22	29	O	217.00	101.55	217.00	0.00	217.00	0.00	10000.00	39.78
poi-30-22	29	O	209.00	160.06	209.00	0.00	209.00	0.00	10000.00	67.58
poi-30-23	29	O	232.00	181.92	232.00	0.00	232.00	0.00	10000.00	32.01
poi-30-23	29	O	197.00	709.05	197.00	0.00	197.00	0.00	10000.00	85.06
poi-30-23	29	O	180.00	39.12	180.00	0.00	180.00	0.00	10000.00	92.98
poi-30-24	29	O	219.00	21.66	219.00	0.00	219.00	0.00	10000.00	18.55
poi-30-24	29	O	185.00	37.68	185.00	0.00	185.00	0.00	10000.00	68.43
poi-30-24	29	O	177.00	63.39	177.00	0.00	177.20	0.11	10000.00	80.76
poi-30-25	29	O	259.00	2.39	259.00	0.00	259.00	0.00	10000.00	18.63
poi-30-25	29	O	234.00	46.16	235.00	0.43	235.00	0.43	10000.00	31.12
poi-30-25	29	O	227.00	197.12	227.00	0.00	228.60	0.70	10000.00	56.04
poi-30-3	29	O	224.00	75.84	224.00	0.00	224.00	0.00	10000.00	18.32
poi-30-3	29	O	192.00	39.39	192.00	0.00	192.00	0.00	10000.00	66.04
poi-30-3	29	O	192.00	245.50	192.00	0.00	192.00	0.00	10000.00	76.80
poi-30-4	29	O	260.00	6.67	260.00	0.00	260.00	0.00	10000.00	18.06
poi-30-4	29	O	206.00	25.13	206.00	0.00	206.00	0.00	10000.00	70.85
poi-30-4	29	O	158.00	25.69	158.00	0.00	158.00	0.00	10000.00	89.87
poi-30-5	29	O	230.00	9.56	230.00	0.00	230.00	0.00	10000.00	18.15
poi-30-5	29	O	193.00	54.89	193.00	0.00	193.00	0.00	10000.00	46.65
poi-30-5	29	O	188.00	80.25	188.00	0.00	188.00	0.00	10000.00	59.10

Table 18 – continued from previous page

Instance	n	RR-MHD			HVNS					
		Status	BKS	Time (s)	Obj	Gap (%)	$\overline{\text{Obj}}$	$\overline{\text{Gap}}$ (%)	Ite	Time (s)
poi-30-6	29	O	251.00	101.66	251.00	0.00	251.00	0.00	10000.00	10.58
poi-30-6	29	O	208.00	76.10	208.00	0.00	208.00	0.00	10000.00	20.84
poi-30-6	29	O	194.00	125.45	194.00	0.00	194.00	0.00	10000.00	57.55
poi-30-7	29	O	211.00	12.19	211.00	0.00	211.00	0.00	10000.00	14.34
poi-30-7	29	O	190.00	14.73	190.00	0.00	190.00	0.00	10000.00	53.76
poi-30-7	29	O	182.00	72.03	182.00	0.00	182.60	0.33	10000.00	92.78
poi-30-8	29	O	239.00	5.93	239.00	0.00	239.00	0.00	10000.00	12.56
poi-30-8	29	O	200.00	14.55	200.00	0.00	200.00	0.00	10000.00	29.63
poi-30-8	29	O	195.00	109.96	195.00	0.00	195.00	0.00	10000.00	54.41
poi-30-9	29	O	259.00	66.90	259.00	0.00	259.00	0.00	10000.00	22.87
poi-30-9	29	O	210.00	154.03	210.00	0.00	210.40	0.19	10000.00	33.84
poi-30-9	29	O	193.00	886.05	193.00	0.00	193.40	0.21	10000.00	42.30
poi-40-1	39	O	283.00	1364.79	283.00	0.00	283.00	0.00	10000.00	34.85
poi-40-1	39	O	213.00	563.64	213.00	0.00	213.00	0.00	10000.00	195.81
poi-40-1	39	O	194.00	3267.08	194.00	0.00	194.00	0.00	10000.00	187.20
poi-40-10	39	O	259.00	403.45	259.00	0.00	259.00	0.00	10000.00	48.51
poi-40-10	39	O	220.00	74.69	220.00	0.00	220.00	0.00	10000.00	68.14
poi-40-10	39	O	218.00	696.90	218.00	0.00	218.40	0.18	10000.00	121.97
poi-40-11	39	L	266.00	3600.00	266.00	0.00	266.00	0.00	10000.00	36.64
poi-40-11	39	O	222.00	527.99	222.00	0.00	222.00	0.00	10000.00	124.33
poi-40-11	39	O	210.00	378.64	210.00	0.00	210.00	0.00	10000.00	176.36
poi-40-12	39	O	262.00	35.93	262.00	0.00	262.00	0.00	10000.00	29.92
poi-40-12	39	O	222.00	1405.59	222.00	0.00	222.00	0.00	10000.00	87.04
poi-40-12	39	O	209.00	2534.00	209.00	0.00	209.00	0.00	10000.00	115.08
poi-40-13	39	O	266.00	988.14	266.00	0.00	266.00	0.00	10000.00	64.15
poi-40-13	39	O	222.00	326.15	222.00	0.00	222.00	0.00	10000.00	160.97
poi-40-13	39	L	363.00	3600.00	210.00	-42.15	210.00	-42.15	10000.00	172.08
poi-40-14	39	O	287.00	64.94	287.00	0.00	287.00	0.00	10000.00	33.39
poi-40-14	39	O	229.00	673.80	229.00	0.00	229.00	0.00	10000.00	148.28
poi-40-14	39	O	210.00	254.43	212.00	0.95	212.00	0.95	10000.00	220.63
poi-40-15	39	O	279.00	215.33	279.00	0.00	279.00	0.00	10000.00	34.52
poi-40-15	39	O	234.00	302.24	234.00	0.00	234.00	0.00	10000.00	75.02
poi-40-15	39	L	346.00	3600.00	233.00	-32.66	233.00	-32.66	10000.00	162.36
poi-40-16	39	O	270.00	1918.15	270.00	0.00	270.00	0.00	10000.00	47.13
poi-40-16	39	O	210.00	952.09	212.00	0.95	212.00	0.95	10000.00	132.93
poi-40-16	39	O	201.00	229.68	201.00	0.00	201.00	0.00	10000.00	198.99
poi-40-17	39	O	285.00	187.93	285.00	0.00	285.00	0.00	10000.00	38.04
poi-40-17	39	O	246.00	79.75	247.00	0.41	247.60	0.65	10000.00	82.64
poi-40-17	39	L	359.00	3600.00	242.00	-32.59	242.00	-32.59	10000.00	165.30
poi-40-18	39	L	391.00	3600.00	296.00	-24.30	296.00	-24.30	10000.00	36.20
poi-40-18	39	O	239.00	487.04	239.00	0.00	239.00	0.00	10000.00	107.05
poi-40-18	39	O	221.00	68.90	223.00	0.90	223.20	1.00	10000.00	253.85
poi-40-19	39	O	236.00	560.59	236.00	0.00	236.00	0.00	10000.00	43.01
poi-40-19	39	O	204.00	2748.63	204.00	0.00	204.00	0.00	10000.00	137.32
poi-40-19	39	O	204.00	2452.33	204.00	0.00	204.00	0.00	10000.00	136.50
poi-40-2	39	O	269.00	60.64	269.00	0.00	269.00	0.00	10000.00	46.25
poi-40-2	39	O	218.00	1092.70	218.00	0.00	218.20	0.09	10000.00	173.89
poi-40-2	39	O	204.00	834.17	204.00	0.00	204.00	0.00	10000.00	172.63
poi-40-20	39	O	262.00	2285.60	262.00	0.00	262.00	0.00	10000.00	26.25
poi-40-20	39	O	220.00	1332.06	220.00	0.00	220.00	0.00	10000.00	129.35

Table 18 – continued from previous page

Instance	n	RR-MHD			HVNS					
		Status	BKS	Time (s)	Obj	Gap (%)	$\overline{\text{Obj}}$	$\overline{\text{Gap}}$ (%)	Ite	Time (s)
poi-40-20	39	O	216.00	2545.92	216.00	0.00	216.00	0.00	10000.00	136.36
poi-40-21	39	O	269.00	2148.13	269.00	0.00	269.00	0.00	10000.00	66.99
poi-40-21	39	O	227.00	309.95	227.00	0.00	227.80	0.35	10000.00	177.26
poi-40-21	39	O	218.00	802.95	218.00	0.00	218.00	0.00	10000.00	188.00
poi-40-22	39	O	286.00	50.98	286.00	0.00	286.00	0.00	10000.00	33.44
poi-40-22	39	O	243.00	413.37	243.00	0.00	243.00	0.00	10000.00	81.68
poi-40-22	39	L	339.00	3600.00	223.00	-34.22	225.40	-33.51	10000.00	95.80
poi-40-23	39	L	395.00	3600.00	302.00	-23.54	302.00	-23.54	10000.00	37.84
poi-40-23	39	L	395.00	3600.00	244.00	-38.23	244.00	-38.23	10000.00	206.87
poi-40-23	39	O	230.00	1297.49	230.00	0.00	231.20	0.52	10000.00	182.95
poi-40-24	39	O	244.00	3227.38	244.00	0.00	244.00	0.00	10000.00	57.24
poi-40-24	39	O	215.00	125.84	215.00	0.00	215.40	0.19	10000.00	125.68
poi-40-24	39	O	212.00	1537.43	212.00	0.00	212.00	0.00	10000.00	143.40
poi-40-25	39	L	417.00	3600.00	281.00	-32.61	281.00	-32.61	10000.00	47.83
poi-40-25	39	O	210.00	361.20	210.00	0.00	210.00	0.00	10000.00	69.72
poi-40-25	39	O	190.00	2450.66	193.00	1.58	193.00	1.58	10000.00	92.92
poi-40-3	39	O	282.00	438.14	282.00	0.00	282.00	0.00	10000.00	33.24
poi-40-3	39	L	416.00	3600.00	235.00	-43.51	235.40	-43.41	10000.00	182.88
poi-40-3	39	L	416.00	3600.00	222.00	-46.63	222.80	-46.44	10000.00	119.89
poi-40-4	39	L	284.00	3600.00	284.00	0.00	284.00	0.00	10000.00	42.07
poi-40-4	39	O	234.00	933.35	234.00	0.00	235.20	0.51	10000.00	146.42
poi-40-4	39	O	210.00	565.64	210.00	0.00	210.00	0.00	10000.00	143.44
poi-40-5	39	O	285.00	810.61	285.00	0.00	285.00	0.00	10000.00	31.78
poi-40-5	39	O	231.00	2302.31	235.00	1.73	235.00	1.73	10000.00	72.83
poi-40-5	39	O	203.00	450.09	205.00	0.99	205.60	1.28	10000.00	117.08
poi-40-6	39	O	240.00	2325.71	240.00	0.00	240.00	0.00	10000.00	53.28
poi-40-6	39	O	192.00	1270.80	192.00	0.00	192.00	0.00	10000.00	106.66
poi-40-6	39	O	181.00	1351.85	181.00	0.00	181.80	0.44	10000.00	173.35
poi-40-7	39	L	271.00	3600.00	271.00	0.00	271.00	0.00	10000.00	72.95
poi-40-7	39	O	206.00	506.34	206.00	0.00	206.40	0.19	10000.00	155.45
poi-40-7	39	L	396.00	3600.00	194.00	-51.01	194.60	-50.86	10000.00	161.45
poi-40-8	39	O	277.00	494.89	277.00	0.00	277.00	0.00	10000.00	41.38
poi-40-8	39	O	228.00	628.96	230.00	0.88	231.40	1.49	10000.00	56.96
poi-40-8	39	O	220.00	972.64	220.00	0.00	220.80	0.36	10000.00	188.80
poi-40-9	39	O	289.00	422.85	289.00	0.00	289.00	0.00	10000.00	59.84
poi-40-9	39	O	226.00	924.52	226.00	0.00	226.00	0.00	10000.00	117.52
poi-40-9	39	O	208.00	1252.64	209.00	0.48	209.00	0.48	10000.00	199.48